DISS. ETH NO. 21526

A hybrid graft of silk-based artificial ligament and TCP/PEEK anchorage for ACL reconstruction

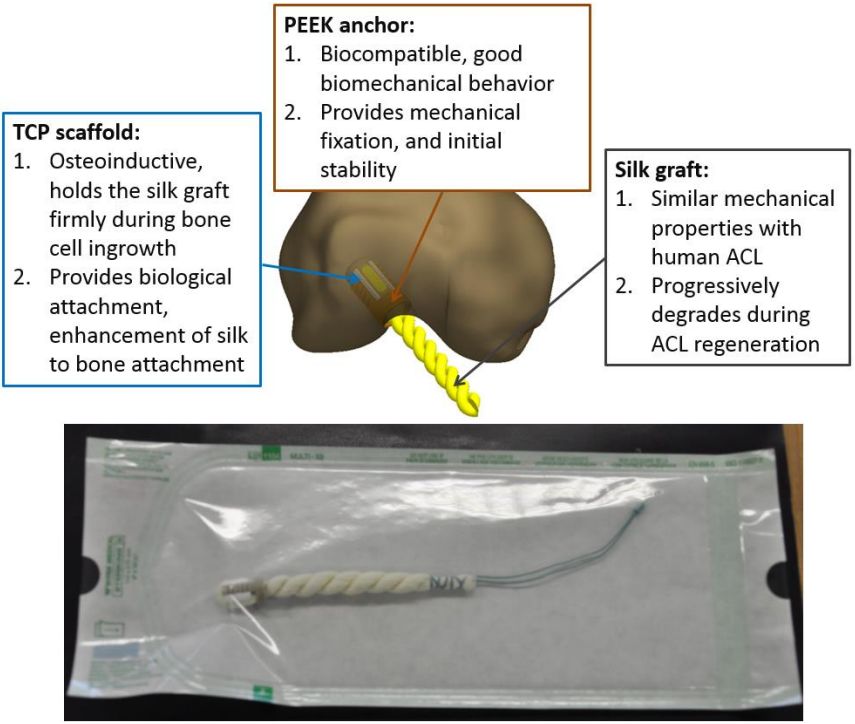

Xiang Li

2013

DISS. ETH NO. 21526

A hybrid graft of silk-based artificial ligament and TCP/PEEK anchorage for ACL reconstruction

A thesis submitted to attain the degree of
DOCTOR OF SCIENCES of ETH ZURICH
(Dr. sc. ETH Zürich)

presented by

XIANG LI

M.Sc., Xi'an Jiaotong University
born on 28 December 1983
citizen of China

accepted on the recommendation of
Prof. Dr. Jess G. Snedeker, examiner
Prof. Dr. Stephen J. Ferguson, co-examiner
Prof. Dr. Marc Bohner, co-examiner

2013

Dedicated to my beloved wife – Nan Shi

TABLE OF CONTENTS

SUMMARY

Anterior cruciate ligament (ACL) ruptures are among the most frequent and severe ligament injuries, with the number of ACL reconstruction performed increasing year by year. Current 'gold standard' treatment for ACL repair is to use a bone patella tendon bone (BPTB) autograft reconstruction. However substantial donor site morbidity accompanies use of this graft, restricting clinical application with a BPTB reconstruction in favor of less effective approaches. Solutions such as allograft, xenograft, or synthetic grafts have been employed toward avoiding donor site morbidity, but outcomes have been viewed as inferior on account of immune response, material and mechanical mismatch, and numerous other reasons. Some successful and promising preclinical results indicate that tissue engineering approaches may yield a superior solution to the dilemma of graft choice in ACL reconstruction, and more generally address what is regarded as the largest challenge to ACL reconstruction, namely achieving robust integration of an ACL graft to host bone. The present work develops and describes a strategy of using a silk-based artificial ligament with bone-like ends (TCP/PEEK anchor) for ACL reconstruction, a design that is biomimetic with a BPTB autograft. A silk-based artificial ACL with mechanical properties similar to the human ACL was developed and verified by cyclic mechanical loading. An optimized geometric design of a complementary TCP/PEEK anchor was similarly derived from biomechanical testing. The efficacy of this combined (hybrid) graft with a silk ligament scaffold anchored by a TCP/PEEK device was tested and evaluated in large animal preclinical model of ACL reconstruction. The results showed that the concept of combination TCP and PEEK for ACL graft fixation is both feasible and effective. The present study thus lays a solid foundation for translation of these concepts to clinical application in veterinary and eventually human medicine.

ZUSAMMENFASSUNG

Rupturen des vorderen Kreuzbandes (Anterior cruciate ligament, ACL) gehören zu den häufigsten und schwersten Bandverletzungen. Damit verbunden ist eine steigende Zahl durchgeführter ACL Rekonstruktionen Jahr für Jahr. Aktueller „Goldstandard" der Behandlung einer ACL Ruptur ist die Rekonstruktion mit einem Knochen-Patellasehnen-Knochen-Transplantat (bone patella tendon bone, BPTB). Allerdings ist die Verwendung dieses Transplantats mit beträchtlichen Komplikationen vor allem der Entnahmestelle verbunden, dadurch beschränkt sich die klinische Anwendung einer BPTB Rekonstruktion zugunsten weniger wirksamer Techniken. Andere Lösungen wie z.B. Allograft, Xenograft oder synthetische Transplantate können zwar die Morbidität an der Entnahmestelle verhindern, jedoch sind die Resultate bezüglich Immunsystemreaktion, materiellen und mechanischen Eigenschaften sowie einer Vielzahl anderer Gründe deutlich schlechter. Einige präklinisch erfolgreiche und vielversprechende Resultate zeigen, dass Ansätze der Gewebezüchtung (tissue engineering) zu einer Lösung des Dilemmas der Transplantatwahl in der ACL-Rekonstruktion führen können. Damit wird auch eine der grössten Herausforderungen der ACL-Rekonstruktion nämlich eine robuste knöcherne Integration des ACL-Transplantats angegangen. Die vorliegende Arbeit entwickelt und beschreibt die Strategie zum Verwenden eines Seide-basierenden künstlichen Bandes mit knochenähnlichen Ankern (TCP/PEEK) für die VKB-Rekonstruktion, ein Design das biologisch identische Eigenschaften wie ein BPTB-Transplantat vorweist. Ein seide-basiertes künstliches ACL mit ähnlichen mechanischen Eigenschaften wie ein menschliches ACL wurde entwickelt und mit zyklischen mechanischen Belastungstest überprüft. Ebenso wurde ein optimiertes geometrisches Design eines komplementären TCP/PEEK-Anker von biomechanischen Tests abgeleitet. Die Wirksamkeit dieses kombinierten Transplantats bestehend aus einem Seidebandgerüst verankert mit einer TCP/PEEK Vorrichtung wurde in einem präklinischen Tiermodel für ACL-Rekonstruktionen getestet und evaluiert. Die Resultate zeigen, dass dieses Konzept der Kombination von TCP und PEEK für die Fixation eines ACL-Transplantats realisierbar und effektiv ist. Die vorliegende Studie legt dadurch ein solides Fundament für die Weiterentwicklung dieses Konzepts zu einem klinischen Verwendungszweck in der Veterinär- und eventuell der Humanmedizin.

CHAPTER I

Introduction

1.1 BACKGROUND

ACL injuries

The anterior cruciate ligament (ACL), because of its anatomical location, is occasionally subjected to tremendous force during sports or traumatic loading. Ruptures of the ACL are regarded as the most frequent and severe ligament injuries in the knee[1], with around 250,000 to 400,000 patients per year diagnosed with ACL disruption in the United States[2-4]. Surgery for ACL reconstruction is increasingly common, with approximately 75,000 to 100,000 patients undergoing surgical reconstruction annually in the United States, in comparison with 120,000 patients undergoing hip replacement surgery [5, 6]. A rising number of adolescents or young people have been reported to suffer from ACL tear, possibly due to higher sport and activity intensity in this age group [7]. Since the ACL plays a significant role in guaranteeing knee normal motion and joint stability, the loss of the ACL can lead to joint instability and secondary damage of the menisci and articular cartilage, often leading to the ultimate result of early onset osteoarthritis[8, 9]. Unfortunately, the ACL has a very limited capacity for self-regeneration[10]. Thus reconstruction surgery is often recommended and employed for the treatment of ACL rupture.

Philosophies of ACL repair

Generally, there are two broad classes of surgical approach to treatment of the injured ACL: to enhance primary repair, or to reconstruct with a graft [11]. The first philosophy aims to guide and support primary repair with a suture or other scaffold along the axis of the ACL. Here the insertion of the native ligament to bone, as well as related proprioceptive nerves, is preserved. Although it is believed that human fibroblasts remain viable in the ACL stump, and many bio-enhanced approaches[12-14] for primary repair have been tried aiming to promote cellular proliferation and migration into the scaffold, the healing and regeneration of the native ACL is apparently limited regarding long-term outcome, with often non-vascular and a cellular nature of the resulting ligament [15-19]. Therefore, most orthopaedic surgeons have embraced the second philosophy of ACL reconstruction using a graft. This approach removes the stumps of the ruptured ACL, drilling tunnels into the bone through the original ACL footprints. The graft will then fixed

into the bone tunnel, aiming to entirely replace the ACL. The biggest advantage of this approach is that the mechanical function of ACL can be restored immediately. However, the problem of this approach is also obvious, which is that the biological connection of the ACL to the bone is completely absent, and must be regenerated for the ligament to achieve adequate stability. The graft to bone healing thus represents the largest challenge to success of a reconstruction method [20].

Graft choices

There are a number of currently available graft choices for ACL reconstruction, including autografts, allografts, xenografts, and a variety of synthetic grafts[18, 21-23]. Hamstring tendon autografts have emerged as the most widespread clinical choice, normally employed using either the semitendinosus tendon and/or gracilis tendon [24-27]. Despite the excellent mechanical characteristics of these ligament grafts, hamstring graft to bone healing is typically poor, with tendon graft elongation (or even pullout) and bone tunnel expansion emerging as common failure modes for hamstring graft reconstructions [28-32]. To mitigate this poor graft-bone integration, many surgeons favor a bone patellar tendon bone (BPTB) autograft extracted from the middle third of the middle of patellar tendon along with bone blocks in continuity at each end of the graft (blocks from tibial tubercle and the outer surface of the patella, respectively). Because the native bone-tendon interface in these grafts is quite strong, and bone-bone healing is rapid, clinical outcomes using these grafts are widely viewed as superior. The BPTB graft has for decades thus been regarded as a 'Gold Standard' graft choice for ACL reconstruction, among some controversy [6, 33-36]. Still the BTPB autograft is severly limited by graft source site morbidity, with occasionally severe pain lasting up to 12 months after surgery – a fact that has drastically limited the use of BPTB autograft in the clinic [37, 38]. Allograft or xenografts have thus been employed as alternatives to avoid donor site morbidity, although concerns of disease transmission and immune response also limit their favor in clinical application [39-41]. Avoiding both issues of comorbidity and disease transmission, synthetic grafts for ACL reconstruction are theoretically very appealing, also allowing surgeons shorten operating time over autografts [18]. A variety of commercially available synthetic ACL grafts or artificial ACL such as Lars, Leeds-Keio, Teflon, Dacron, Carbon fiber, Gore-Tex, and others have been used in clinics [42-47], mimicking characteristics of the native ACL in terms of strength, compliance, and elasticity.

However, the long-term clinical outcomes after use of a synthetic ACL graft have been generally poor [45, 48, 49]. Thus the use of synthetic ACL graft materials has decreased dramatically over the past decades, and continues mostly as an experimental endeavor [18], or forming the basis of "next generation" tissue engineering approaches [11, 50].

ACL tissue engineering

Among the various aspects that can be considered in a tissue engineering approach to ACL reconstruction (cells, bioactive factors, and scaffolds), the scaffold represents a powerful element in its ability to drive local and recruited cell behavior and guide tissue regeneration. An ideal scaffold for ACL reconstruction should be biodegradable, biocompatible, with suitable porosity for cell ingrowth, and yet provide sufficient mechanical stability[51, 52]. Numerous classes of biomaterials have been studied and used to fabricate tissue engineering scaffolds for ACL reconstruction, including collagen, poly (lactic acid) (PLA), Polylactic-co-glycolic acid (PLGA), poly(ε-caprolactone) (PCL), silk fibroin, and various hybrid combinations of them [53-57]. Of these biomaterials, silk fibroin has been increasingly investigated as a potential ligament or tendon graft, due to advantageous biocompatibility and biomechanical properties [50, 58-62]. Silkworm silk fibroin, a naturally derived biopolymer obtained after removal of hyper-allergenic sericin from raw silk[63, 64], has been used as clinical suture material for centuries [65]. Silk fibroin provides an excellent combination of outstanding and customizable mechanical properties (up to 4.8 GPa ultimate stress), remarkable toughness and elasticity (up to 35% failure strain), and environmental stability [56, 66, 67]. As a structural template, silk fibroin has been shown to be similar to collagen scaffolds in supporting cell attachment, inducing appropriate cell morphology, and promoting cell growth [68, 69]. Silk also presents a relatively slow in vivo degradation rate characterized by a gradual loss of tensile strength over 1 year in vivo[56, 57]. Many in vitro studies have been performed using silk based scaffolds for ACL tissue engineering, evaluating effects of surface treatments, biological factors, and cell types [51, 52, 64, 66, 70-75]. There are also numerous studies that have reported positive results using silk based ACL scaffolds in preclinical animal models[51, 76-78]. A combination of collagen fibers or poly(glycolic acid) with silk scaffolds for ACL reconstruction have been adopted to balance the scaffold behavior of cell ingrowth and tensile strength [79-82]. Safety and efficacy oriented clinical trials of silk based ACL scaffolds in human knees have

also been reported[83]. In short, numerous promising developments have been achieved for silk based ligament scaffold with previous studies, already bringing the concept of a silk-based tissue engineered ACL quite some distance toward clinical application [84, 85].

Open challenges for a tissue engineered ACL

The regeneration of the ligament itself using a silk-based scaffold has been already achieved with some success. Still, just as with use of a autografted tendon, it is by now widely recognized that the largest challenge for a tissue engineered ACL is the integration of the construct with the host bone [86], with the long-term performance of a tissue engineered ACL scaffold believed to mainly depend on successful regeneration of a ligament-bone interface [87]. Many approaches have been tried to enhance the integration of the ligament scaffold to bone in order to achieve improved biological attachment. The major concern is to provide appropriate molecular and cellular cues that result in effective healing between graft and bone. To this end, tissue engineering approaches have employed bone marrow derived mesenchymal stem cells (BMSCs) as potential agents to enhance graft to bone healing[88, 89]. Similarly, osteoinductive bioceramics such as Hydroxyapatite (HA), tricalcium phosphate (TCP), brushite calcium phosphate cement (CPC) have also been adopted to augment graft to bone attachment[90-95]. Bioactive factors including bone morphogenetic proteins (BMPs) and other growth factors have further been implemented for augmented establishment of a graft to bone enthesis [96-99].

Despite the wide range of applied approaches, they have generally focused on biological augmentation while neglecting implications of primary mechanical stability. The apparent intention is that cells in the bone tunnel will recognize the graft surface as a potentially osteoconductive matrix, promoting rapid bone ingrowth that quickly providing secondary mechanical stability and improved attachment of graft to bone. However, until this secondary stability is ensured the graft is susceptible to elongation and slippage at the graft/bone interface. It seems that few researchers have focused on how an osteoconductive/inductive construct might be used to achieve superior biological healing and long-term stability while also providing adequate primary mechanical stability through increased contact between the graft and the bone tunnel walls. In most approaches, classical fixation

methods such as interference screws have been employed, despite their inherent limitations to providing osteogenic contact surfaces and failure to achieve robust short-term mechanical stability[94].

Our strategy for ACL reconstruction

We propose a novel solution to ACL reconstruction combining a silk-based artificial ACL with a TCP/PEEK(polyether ether ketone) fixation device. The design is intended to provide adequate primary graft stability and optimal bone-contact between the ligament scaffold and bone. We test the construct for its ability to provide fixation strength (in vitro) as well as its ability to achieve long-term biological attachment (in vitro). The employed silk scaffold features an architecture that yields similar mechanical properties to the human ACL. This graft is enlaced upon an TCP insert that maximizes contact between the silk surfaces and osteoinductive surfaces (TCP or bone tunnel). A PEEK anchor housing is employed to provide mechanical purchase, retaining the relative orientation of the device components, and shielding the TCP insert from damage. We demonstrate that this concept of a silk-based artificial ACL with TCP/PEEK anchor may offer a promising solution for ACL reconstruction in the near future.

1.2 SPECIFIC AIMS

We pursue the design, fabrication, and testing of a novel hybrid implant for ACL reconstruction. The aims of this doctoral study are to develop and fabricate the scaffold, and perform biomechanical and biological tests to evaluate the efficacy of the system. The ultimate goal of this work is to provide a promising alternative choice for ACL reconstruction. There are four concrete aims as follows:

Aim 1: To develop and fabricate a silk-based scaffold for ACL reconstruction, with similar mechanical properties with human ACL.

Aim 2: To develop and fabricate a TCP/PEEK based anchor for fixing silk scaffold into bone tunnel. To develop the combination methods of silk scaffold and TCP/PEEK anchor.

Aim 3: To develop possible surgical procedures and insertion tools, and to optimize the design of the scaffold, based on in vitro biomechanical tests and pilot animal study.

Aim 4: To test this novel ACL scaffold within a range of animal experiments. To make systematic and detailed evaluation of this scaffold. To propose and implement further improvement of the device.

1.3 DISSERTATION OUTLINE

The dissertation is structured into six chapters. Chapter 2, 3, 4 correspond to three finished research papers. Chapter 5 corresponds to a patent submitted to the European patent office. Chapter 6 corresponds to the conclusion and outlook. The general descriptions of each chapter are listed as follows:

Chapter 1 gives a detailed background of ACL reconstruction.

Chapter 2 focuses on Aim 1 to develop and fabricate a silk-based artificial ligament for ACL reconstruction, which has similar mechanical behaviors of human ACL. A silk-based scaffold with wired architectures was found to provide a biomimetic ACL tissue engineering scaffold.

Chapter 3 focuses on Aim 2 and Aim 3 to develop and fabricate a TCP/PEEK anchor for silk scaffold fixation. The architecture of TCP/PEEK anchor has been optimized with in vitro biomechanical tests, and the surgical procedures and insertion tools have be evaluated and verified with in vivo pilot animal study.

Chapter 4 focuses on Aim 4 to make systematic efficacy test of this novel concept of hybrid artificial ACL in a porcine model. Biomechanical and histological characterization of implant performance was made after three and six post-operative months.

Chapter 5 is the general description of the patent for the novel concept of silk based artificial ligament with TCP/PEEK anchor for ACL reconstruction. Detailed design parameters and fabrication techniques of the artificial ACL as well as the developed surgical tools can be found in this chapter.

Chapter 6 concludes this dissertation with conclusions, limitations and further direction of study protocol for preclinical trial of this study.

CHAPTER II

Silk scaffold preparation

Wired silk architectures provide a biomimetic ACL tissue engineering scaffold

Xiang Li[1,2], Jess G Snedeker[1,2,*]

[1] Department of Orthopedics, University of Zurich, Balgrist University Hospital, Zurich, Switzerland
[2] Department Health Sciences and Technology, ETH Zurich, Switzerland

Abstract

Silk has been increasingly investigated as a scaffold for tissue engineered anterior cruciate ligament (ACL) grafts, pimarily due to a uniquely advantageous combination of biocompatibility and robust biomechanical strength in the short and middle terms. While previous studies have explored the biomechanical and biological effects of graft geometry, these studies have largely ignored the effects of repeated loading on long term biomechanical performance – an important consideration considering the relatively slow rate with which the silk scaffold is remodeled. In the present study, we utilized a tensile bioreactor to carry out cyclic loading tests on various silk ACL scaffold designs. Silk scaffolds were fabricated with three different architectures (wired, braided, and straight fibered). These were tested in static loading, low cyclic loading to 250 cycles, and high cyclic loading to 100,000 cycles. Different scaffold conditions including dry, wet, with cells, without seeded cells were tested and compared. The ultimate tensile strength (UTS), linear stiffness and construct elongation rate were used to compare the structural behavior of each graft architecture. Based upon this analysis, silk scaffolds with a wired structure exhibited biomechanical behavior most similar to the native human ACL. We thus conclude that the wired silk scaffold design we present provides a biofidelic mechanical basis for tissue engineering strategies for ACL reconstruction.

Keywords

Silk scaffold, ligament tissue engineering, ACL reconstruction, Cyclic loading

2.1 INTRODUCTION

Ligament injuries, typically occurring during sports and other rigorous physical activities, are among the most common musculoskeletal disorders. Due to its anatomical location, the anterior cruciate ligament (ACL) is subjected to high forces during even normal daily activities, and is predisposed to traumatic injury. Consequently, ACL rupture is among the most frequent and severe ligament injuries [1]. It has been estimated that more than 250,000 patients per year suffer ACL disruption in the United States (equivalent to 1 in 3,000 from the general population), with approximately 50,000 of these cases treated by surgical reconstruction [2, 3, 57, 100]. Although numerous surgical options exist for ACL reconstruction, including autografts, allografts, xenografts, or synthetic grafts, each is associated with inherent drawbacks, including donor site morbidity in the case of autografts [101, 102], disease transmission[39] and immune response in the case of allografts [40, 41], and more universal issues like ligament laxity, mechanical mismatch, and others [52, 103, 104]. Thus despite a wide range of options for graft-based ACL reconstruction, further improvements are required. It is widely viewed that rapid developments in tissue engineering may offer promise in this regard [51, 57, 59, 66, 73, 77, 105].

Particularly in cases for which a graft is immediately challenged by high mechanical demands, a wise choice of scaffold represents a keystone within a tissue engineering based strategy. In addition to mechanical stability, an ACL scaffold should also be biodegradable, biocompatible, and be suitably cell permissive to allow cell ingrowth and eventual graft remodeling [51, 52]. Silkworm silk fibroin, a natural biopolymer derived by removing the hyper-allergenic sericin component of raw silk [63, 64], has been used as clinical suture material for centuries[65]. Silk fibroin provides an excellent combination of strong yet adjustable mechanical properties (failure stresses up to 4.8 GPa), remarkable toughness and elasticity (up to 35% failure strains), and a large degree of biological stability [56, 66, 67]. As a structural template for eventual tissue remodeling silk fibroin has been shown to be similar to collagen in supporting cell attachment, inducing appropriate morphology and cell growth [68, 69], with a relatively slow degradation rate that involves a gradual loss of tensile strength over 1 year in vivo[56, 57]. Thus, due to its established biocompatibility and well-suited biomechanical properties, silk

fibroin has been increasingly investigated as a potential ligament or tendon graft material in the last decade [50, 58-62, 106].

Many in vitro studies have been performed on silk based scaffolds for ligament tissue engineering, evaluating effects of surface treatments, biological factors, and cell types [51, 52, 64, 66, 70-75]. There are also numerous studies that have reported positive results using silk based ligament scaffolds in preclinical animal models [51, 76-78]. Safety and efficacy oriented clinical trials of silk based ACL scaffolds in human knees have also been reported [83]. While the promise of silk based grafts for ACL reconstruction seems clear, there is still substantial room for improvement particularly at the level of meso-scale (equivalent to collagen fiber and fascicle level) graft architecture [4, 107]. More specifically, the manner in which the silk fibroin is structured can largely dominate the biomechanical performance of the graft (and thus downstream, the biological performance as well). The current study thus focuses on optimizing the architecture of a silk ACL graft. Some progress has been made in this regard by other groups, for instance in the development of cabled silk structures for ligament reconstruction[108]. Other studies have investigated the implications of hierarchical organization of silk matrix using 6-cord wire-rope configurations [56, 57, 109].

One major issue with published studies to date is that they generally neglect to account for changes in the mechanical behavior of the graft after repeated cycling, particularly under wet conditions. Over the course of rehabilitation, an ACL graft will undergo many thousands of cycles before it has been robustly incorporated within the bone tunnels, and its midsubstance has been populated by fibroblastic cells. While medium to longer term cyclic mechanical behavior of silk based ligament scaffolds is at least as important as the initial graft properties, only a few studies have focused on this aspect [57, 110]. We are thus lacking a rigorous evaluation of how silk graft architecture affects the evolution of mechanical properties under cyclic loading.

Therefore, the purpose of this study is to design a silk ACL scaffold with biofidelic mechanical properties, as characterized under functionally meaningful test conditions. We tested different architectures under cyclic loading. A specially designed bioreactor for cyclic loading was implemented. The mechanical properties of different silk ACL scaffolds after cyclic loading (up to 100,000 cycles) were

measured. By comparing the response of various graft architectures with the mechanical properties of human ACL, we were able to identify a suitable architecture for the design of silk ACL scaffolds.

2.2 MATERIALS AND METHODS

Preparation of silk ACL scaffolds

Raw silk fibers (*Bombyx mori*) were obtained from a commercial supplier (Grege 20/22, Trudel Limited, Zurich, Switzerland). All scaffolds were produced using a specially designed wiring machine. Three different classes of hierarchical ACL graft architectures were employed - wired, braided and straight fibered [50, 111, 112]. Across all designs, a consistent size (~30 mm) and total number (3456) of fibers (the basic structural unit) was chosen to facilitate comparison with previously reported designs of silk ACL scaffolds [108, 109]. The geometries of the different hierarchical architectures can be described using a labeling convention of A(a)*B(b)*C(c)*D(d), where A, B, C, D represent increasing hierarchical level -fibers(A), bundles(B), yarns(C) and cords(D)), while a, b, c, d is the twisting level corresponding to the length (mm) per turn on each of the hierarchical levels. For example, a wired ACL scaffold architecture defined as 6(0)*2(2)*144(10)*2(12) indicates 6 fibers in 1 bundle without twist (0 means parallel), 2 bundles in 1 yarn with 2 mm per turn, 144 yarns in 1 cord with 10 mm per turn, 2 cords in 1 ACL scaffold with 12 mm per turn.

A number of different geometries for each architecture were screened in pilot studies before finally fixing the geometry of each architecture for further tests. This pre-selection was based on considerations of scaffold size, initial failure force and feasibility of fabrication. Specifically, silk ACL scaffolds were manufactured in the following designs: wired - 6(0)*2(2)*144(10)*2(12), braided - 6(0)*2(2)*96(10)*3(12), and straight - 6(0)*2(2)*288(10)*1(0) (Figure 2.1).

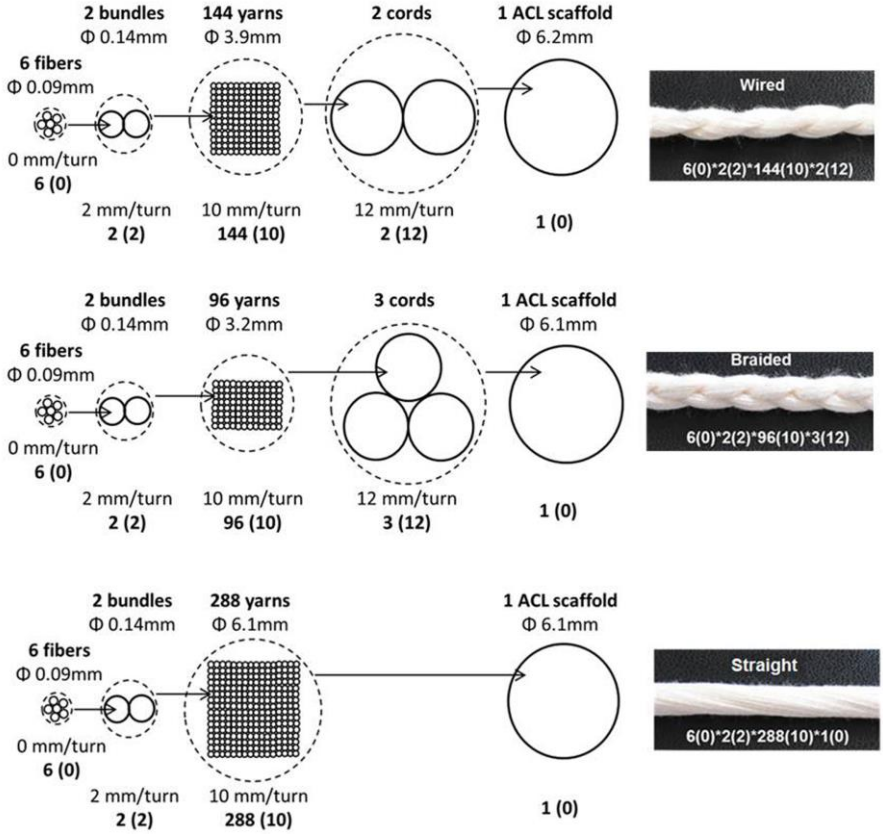

Figure 2.1 Schematic of silk ACL scaffold with three different architectures

Sericin extraction

The silk ACL scaffolds were produced with raw silk yarns. The antigenic protein sericin was removed by immersing the scaffolds into an aqueous solution of 0.5wt% Na_2CO_3 at 90-95 ℃, using a magnetic stirrer (Basic C, IKA-WERKE, Germany) at 300 RPM for 90 minutes, then rinsing with running distilled water for 15 minutes, and air drying at 60 ℃. These procedures were repeated three times. This protocol was based on previous literature [63, 64], but slightly adapted for our study, since the scaffolds we fabricated were tighter and thicker than those reported in the literature[72]. Scanning electron microscopy (FEG-SEM, Zeiss LEO Gemini 1530, Germany) with an in-lens detector was used to view the surface of the silk fiber to

evaluate the efficacy of sericin extraction. Prior to imaging, the scaffolds were coated with platinum to facilitate imaging.

Mechanical test

Tension to failure tests (used for screening various designs), and low-cycle-loading tests were performed on a universal material testing machine (Zwick 1456, Zwick GmbH, Ulm, Germany) with a 20 kN force sensor (Gassmann Theiss, Bickenbach, Germany). Suitable soft tissue fixation clamps were used [113]. The distance between the clamps was 30±1 mm to simulate the normal ACL length[114, 115]. The initial tension to failure tests were applied after a preload of 5 N, and afterwards at a displacement-controlled loading of 0.5 mm/second. For the low-cycle loading tests, after applying a preload of 5 N, 250 cycles from 100 to 250 N, representing the loads of normal walking, were applied using displacement-control and a cycle speed of 0.5 mm/second[116, 117].

To simulate longer term loading of the graft under approximately physiological conditions, a specialized bioreactor was developed, shown in Figure 2.2. A stepper motor (NA23C60, Zaber Technologies Inc, Canada) was used to apply cyclical loads while measuring applied force on a 1 kN load cell (KMM20, Inelta Sensorsystems, Germany). Custom clamps were developed to fix the silk scaffold at an initial length of 28±3mm. A polysulfon (PSU1000, Quadrant AG, Switzerland) environmental chamber was covered with an aluminum foil cap (no contact with the loading piston). The chamber was filled with filled with PBS for the samples without cells and filled with culture media (McCoy's 5A) for the samples with cells. The bioreactors were fixed in an incubator (C150, Binder, Germany) at 37 C, humidity of 100%, 5% CO_2. The bioreactor was controlled using custom software (LabVIEW 9.1) to determine gage length at a preload of 5 N, then apply high-cycle loading using strain control (0-3% strain at 1Hz) for 100,000 cycles. Rest intervals of 30 seconds were applied at increments of 250 cycles, whereupon the gage length was reassessed to account for scaffold creep and/or elongation.

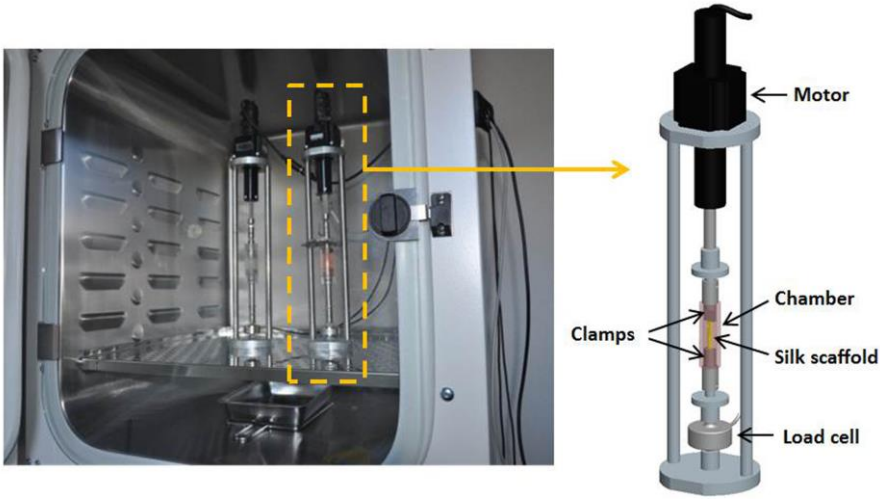

Figure 2.2 Photo of bioreactors fixed in the incubator

Cell seeding

Human foreskin fibroblasts (HFFs) were purchased from American Tissue Culture Collection. Cells were maintained in McCoy's 5A media with 10% fetal calf serum, 1% penicillin/streptomycin, and 1% L-glutamine (all from Invitrogen) with 5% carbon dioxide at 37°C. To assess cell response to various compositions of silk scaffolds, HFFs were prelabeled with Calcein AM (Invitrogen) and seeded on scaffolds for 24 hours. Before seeding, silk scaffolds were first immersed into 75% ethanol solution overnight and then sterilized in an autoclave at 121°C for 20 minutes. The sterile scaffolds were brought into the cell culture hood. Confluent HFF cultures were washed with PBS (Lonza) and overlaid with Calcein AM solution at 5 µM in PBS for 30 minutes at 37°C. Cells were then washed with PBS to remove excess solution. Cells suspensions were created by overlaying trypsin to detach cells, neutralizing with media, and centrifuging cells for 5 minutes at 900 rpm. The supernatant was discarded and the cells were resuspended in complete media. Cell counts were performed, and cells were seeded at 1.36×10^6 cells/cm2. Several samples at both 30 minutes and 24 hours post-seeding, were imaged on an upright Leica microscope with the appropriate excitation and emission filters and a ×20 objective. These samples were then dehydrated in graded ethanol series: 1x10 min. in 25% ethanol, 1x10 min. in 50% ethanol, 1x10 min. in 70% ethanol, 1x10 min. in

85% ethanol, 1x10 min. in 96% ethanol, 3x10 min. in 100% ethanol. After that, specimens were sputter-coated with platinum and imaged by SEM as previously described.

Statistical analysis

Test conditions, groups, and numbers of samples (n) are listed in Table 2.1. All data were expressed as mean ± standard deviation (SD) in quantification. The data were compared with student's t-test, and statistically significant values were defined as $p < 0.05$ (pointed out with asterisk in the chart).

2.3 RESULTS

The ACL graft designs described above were able to be consistently produced in the three architectures (Figure 2.1, above). Scanning electron micrographs indicated that the applied sericin extraction protocol was effective (Figure 2.3). Further, HFF cells were clearly attached to the scaffolds after 30 minutes of seeding and well spread and aligned with the silk fibers after 24 hours (Figure 2.4). Biomechanical analysis of initial properties: The ultimate tensile strength (UTS) of the silk yarns significantly decreased after sericin extraction (Figure 2.5), from 9.4 ± 0.3 N for native silk yarn to 7.3 ± 0.4 N of sericin extracted (dry) and finally to 6.0 ± 0.3 N for sericin extracted silk in wet conditions (PBS), shown in Figure 2.5(A). The stiffness of silk yarns decreased as well after sericin extraction, from 2.0 ± 0.1 N/mm for native silk yarn to 1.4 ± 0.2 N/mm for sericin extracted (dry) to 1.0 ± 0.2 N/mm for sericin extracted in wet conditions, shown in Figure 2.5(B).

The elongation at tensile failure for silk yarns also decreased after sericin extraction, from 9.1 ± 0.3 mm for native silk yarn, to 8.1 ± 0.3 mm for sericin extracted (dry) and finally to 7.0 ± 0.4 mm for sericin extracted yarns in wet conditions, shown in supplementary materials. Tension to failure testing of the assembled silk ACL scaffolds indicated that a straight-fibered architecture had a lower UTS and higher stiffness than the native human ACL [118], whereas the wired and braided architectures were more biofidelic (Figure 2.6).

The UTS of two architectures decreased significantly ($P<0.01$) from 1910 ± 128 N (wired) and 1890 ± 62 N (braided) in dry conditions to 1543 ± 85 N (wired) and 1600 ± 65 N (braided) in wet conditions, with failure values slightly lower than that of

human ACL, shown in Figure 2.6(A). The stiffness of two architectures also decreased significantly ($P<0.01$) from 567 ± 40 N/mm (wired) and 586 ± 41 N/mm (braided) in dry conditions to 289 ± 21 N/mm (wired) and 243 ± 26 N/mm (braided) in wet conditions, falling close to values typical of the human ACL, shown in Figure 2.6(B). Tests on the effects of steam sterilization was also investigated (in wired samples only), but indicated little effect on UTS, linear stiffness, and elongation at failure.

Table 2.1 Overview of test conditions, groups, and numbers of samples

Sample architecture	Sample condition	Test type	Number of samples
Silk yarn	Unextracted, Dry	Tension to failure	10
	Extracted, Dry		
	Extracted, Wet		
Straight	Extracted, Dry	Tension to failure	6
	Extracted, Wet		
Wired	Extracted, Dry	Tension to failure	6
	Extracted, Wet		
	Wet, Sterilized		4
	With cells, 24 hours		3
	With cells, 7 days		
	Extracted, Wet	250 cycles	6
	Extracted, Wet	100,000 cycles	3
	With cells		
Braided	Extracted, Dry	Tension to failure	6
	Extracted, Wet		
	With cells, 24 hours		3
	With cells, 7 days		
	Extracted, Wet	250 cycles	6
	Extracted, Wet	100,000 cycles	3
	With cells		

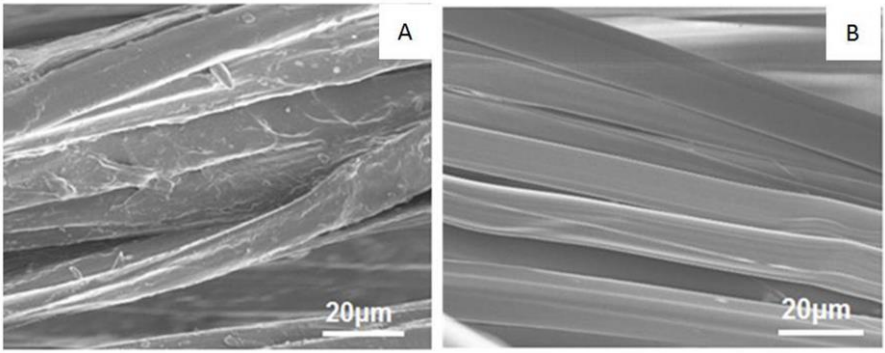

Figure 2.3 The SEM images of the surface of silk fibers.
(A: original raw silk fibers; B: sericin-extracted silk fibers)

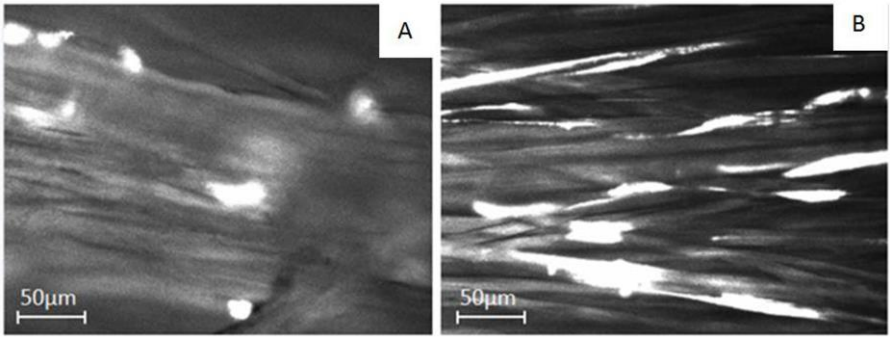

Figure 2.4 Fluorescently labeled HFF cells on silk scaffold.
(A: at 30 minutes; B: at 24 hours)

Biomechanical analysis of properties after cyclic loading: Focusing on the ACL scaffolds yielding the most biofidelic performance (wired and braided architectures), we then tested the evolution of biomechanical properties after repeated cycling to 3% strain at 1Hz (Figure 2.7). Following 250 loading cycles (n=6), UTS in braided and wired samples decreased ~51% and ~41% respectively ($p<0.01$).

Stiffness increased ~114% and ~48% for the braided and wired specimens respectively ($p<0.01$). In more limited testing to 100,000 cycles (n=3), UTS in braided and wired samples decreased ~75% and ~66% respectively ($p<0.01$). Stiffness increased ~128% and ~70% for the braided and wired specimens

respectively ($p<0.01$). There was no significant difference on UTS ($p=0.68$) and stiffness ($p=0.94$) for wired architectures between the silk ACL scaffold with cells and without cells under 100,000 cycles. Although both architectures demonstrated similar functional performance after 100,000 cycles, the wired architecture had generally more stable stiffness and rates of elongation in comparison to the braided construct (Figure 2.8). Analysis of failure mode in the wired architecture revealed differences in failure mode after high cyclic loading, with a more brittle rupture being observed (Figure 2.9).

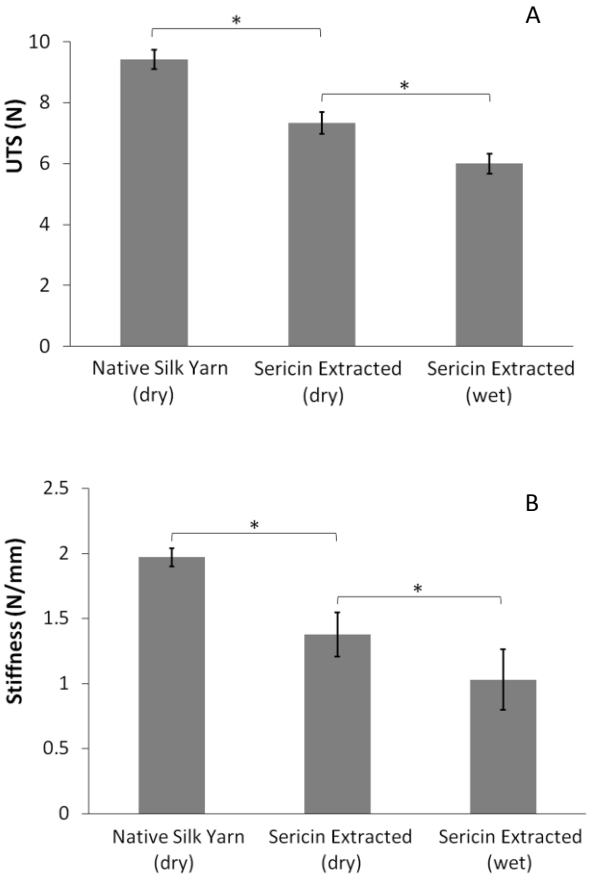

Figure 2.5 UTS and stiffness of silk yarn in different conditions.
(A: UTS; B: Stiffness; $p<0.05$)

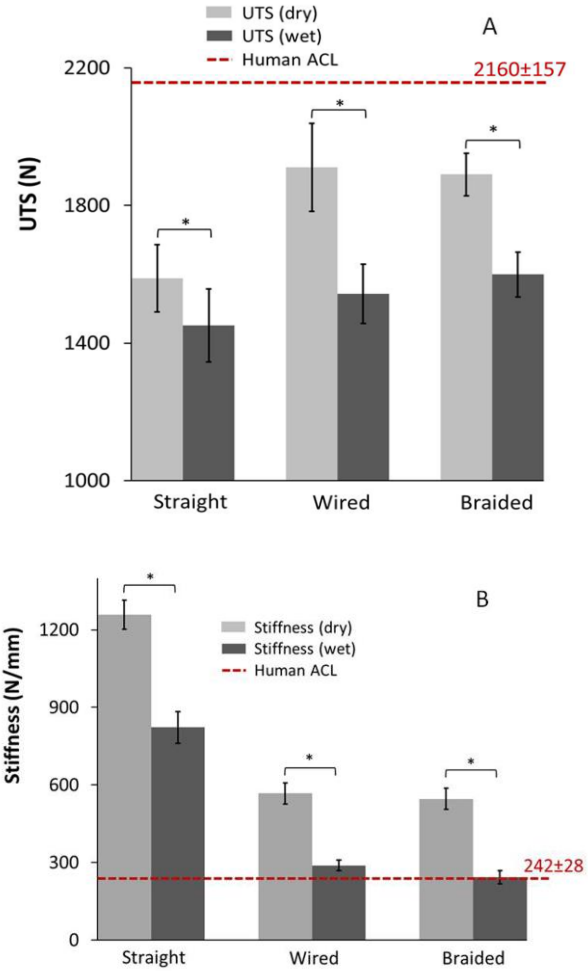

Figure 2.6 UTS and stiffness of silk scaffolds with three architectures. (A: UTS; B: Stiffness; Human ACL value[118]; $p<0.05$)

2.4 DISCUSSIONS

Anterior cruciate ligament reconstruction remains a common, yet often problematic, clinical challenge [119, 120]. In addressing this challenge, silk-based tissue engineering approaches to ACL reconstruction hold substantial promise [77, 121, 122]. De-sericinized silk is highly biocompatible, with a slow rate of

degradation and remarkable mechanical properties. While important progress has been made in advancing the use of this material as an ACL graft, the range of graft architectures that have been explored in the scientific literature is limited to a handful of concepts. Further, the functional characterization of these designs has generally neglected important aspects related to postoperative, *in vivo* performance – specifically moderate and high cycle loading within an aqueous environment.

In the present study, we explored three graft architectures: braided, wired, and straight-fibered. Variants of these architectures have been explored using other synthetic materials [123-125], but to our knowledge they have not been systematically explored using silk constructs to mimic the biomechanical behavior of the human ACL. Of these architectures, the straight-fibered design produced a very strong, but overly stiff graft that we did not further explore in cyclic load testing. The other architectures (wired and braided) were able to approximate the strength and stiffness of the human ACL to varying degrees, yet this depended both upon the graft preparation and the testing conditions in which the functional performance was characterized.

As silk sericin can be a major cause of adverse immune reactions, it is essential to ensure adequate sericin removal before usage. The sericin of the silk ACL scaffolds used in this study was effectively removed using slightly adapted procedures based on the literature. However, the mechanical properties changed remarkably after sericin extraction. For the silk yarns used in all of the ACL architectures investigated in this study, there was a ~22% decrease in UTS (from 9.42 ± 0.33 to 7.34 ± 0.35 N), and a ~30% decrease in linear stiffness (from 1.97 ± 0.07 to 1.37 ± 0.17 N/mm) associated with sericin extraction. These data are similar to reported values for single silk fibers after sericin extraction – 15.2% decrease in UTS, and 28.3% decrease in linear stiffness [109]. The diameter of silk yarn also decreased ~29% after sericin extraction. Because of considerable difference in mechanical properties between raw silk and sericin-extracted silk, any biomechanical characterization of a silk scaffold design should be performed using sericin extracted silk.

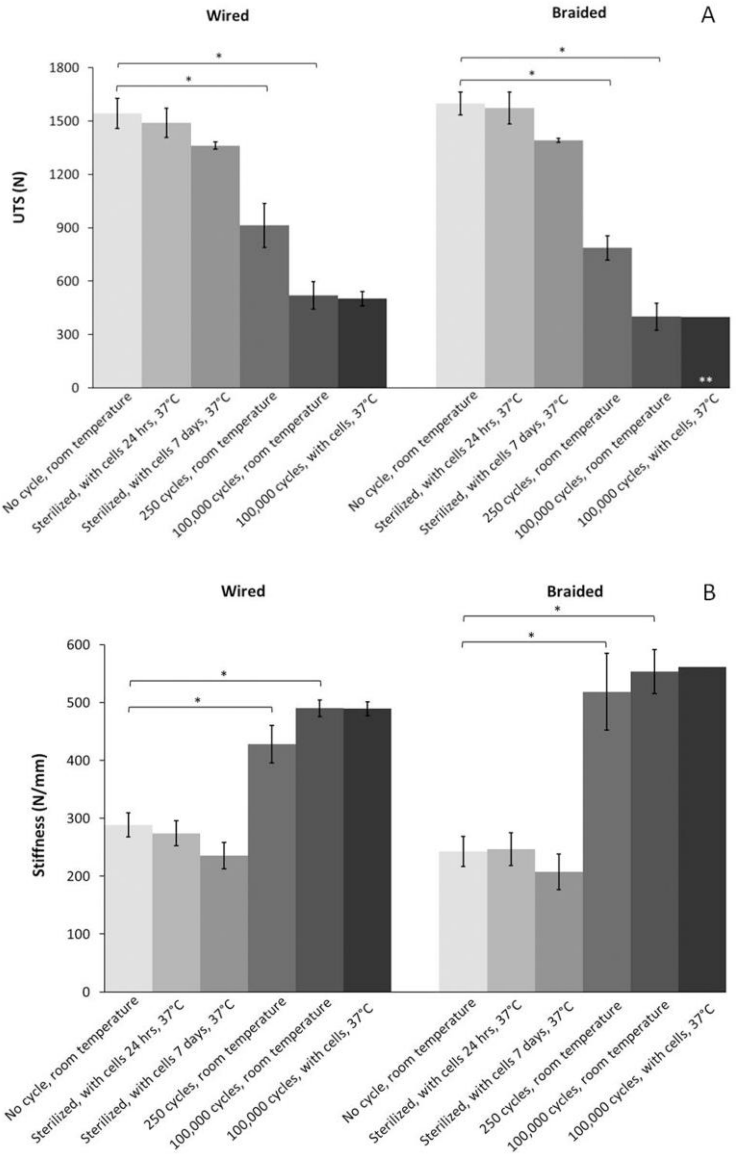

Figure 2.7 UTS and stiffness of wired and braided silk scaffolds under different loading conditions.
(A: UTS; B: Stiffness; $p<0.01$)

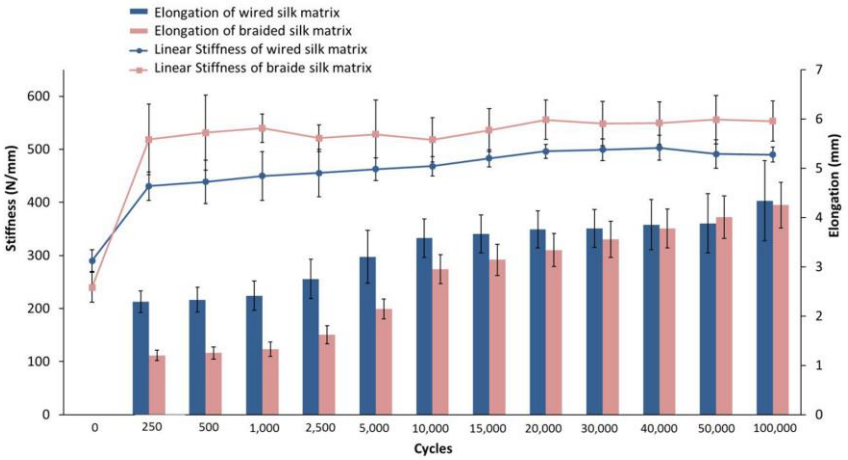

Figure 2.8 The linear stiffness and elongation of wired and braided silk ACL scaffolds under high cyclic loading.

By adopting both dry and wet testing environments, we found that wet testing conditions yielded a large drop in UTS and linear stiffness (~9% decrease in UTS and ~35% decrease in stiffness for straight silk ACL scaffold, while ~20% and ~16% decrease in UTS, ~49% and 56% decrease in stiffness for wired and braided silk ACL scaffolds respectively). It has been suggested that this loss of mechanical strength and stiffness is not due to any chemical destabilization of the structure, but rather that moisture substantially decreases friction between the hydrophobic silk fibers [108]. This likely explains the fact that mechanical properties of the straight-fibered scaffolds were less affected than those of the wired and braided scaffolds, which have considerably more inter-fiber contact and relative movement. Although fluid immersion, progressive loss of hydrophobicity, and an altered state of fiber hydration could explain the slight drop in UTS observed after incubation for 24 hours and 7 days, the exact mechanism behind this drop remains ground for future investigation.

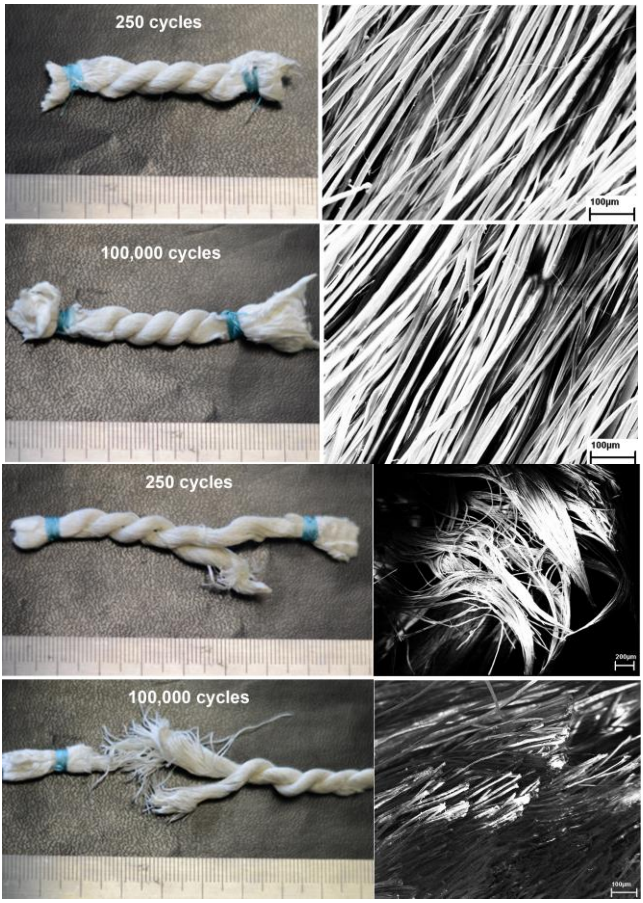

Figure 2.9 The photos and SEM images of the scaffolds after low cyclic loading and high cyclic loading.

While a broad range of sterilization methods could potentially be used for silk ACL scaffolds, we investigated the effects of steam sterilization on the mechanical properties of wired silk scaffolds. Here we found slight, but insignificant differences in UTS ($p=0.19$) and stiffness ($p=0.14$) after sterilization for 20 min at 121 C. Further, as expected, we saw little influence of the sterilization and cell seeding process on the mechanical properties of the wired and braided silk ACL scaffolds. Regarding cell response, we note that this limited set of experiments was performed using HFF cell lines, rather than primary cells that would better reflect clinical reality. The commercially available lines we used were selected for reasons of reproducibility

and standardization, display a uniform phenotype, and can be easily obtained for future study to replicate/build on the results. Further, our previous experience indicates that HFFs are quite representative of primary tendon fibroblast response behavior regarding biocompatibility and early cell attachment, and thus suitable for the focus of this study. Nonetheless, we cannot draw any conclusion regarding cell invasion, proliferation, and eventual construct remodeling, since such experiments should utilize more appropriate cell types at a minimum, and are anyway best studied in vivo.

We note that only one braided sample survived to 100,000 cycles (double asterisk in Figure 2.7) – precluding any statistical analysis. Braided specimen failure was progressive, starting within one cord (each braided sample had three cords). In contrast to the wired specimens, slight differences in the length of the individual cords may have predisposed the shortest cord to higher loading in each cycle. From image analysis of scaffold surfaces after cyclic loading (but before tension to failure), we could not detect differences between low cycle and high cycle sample loading (Figure 2.9). However analysis of internal structures revealed after tension to failure tests did indicate very different failure modes between low and high cycle loading. The failure of scaffold after low cyclic loading was concentrated within a single cord while the high cycle failure was more evenly distributed, indicating more diffuse damage.

In the present study we investigated not only the mechanical properties of a freshly manufactured graft, but also the evolution of those properties during highly repetitive cycling in an aqueous environment. We first assessed biomechanical performance after 250 cycles, a level of loading identified in pilot testing as already sufficient to reveal significant differences in “mechanical preconditioning” that was dependent upon the architectures of the silk scaffold, and logistically possible to achieve before surgical implantation of the graft (to avoid the bulk of post-operative elongation *in vivo*). High cyclic loading to 100,000 cycles at 1Hz with 30 second rest intervals every 250 cycles was also applied, roughly corresponding to one month of typical daily loading of the ACL. With this bout of loading, the UTS of scaffolds substantially decreased, likely due to progressive accumulation of damage within the scaffold. In contrast, the linear stiffness of the scaffolds increased sharply from 0 to 250 cycles (consistent with preconditioning), but then remained relatively steady until testing concluded after 100,000 cycles. We note that the

stiffness of the scaffold mainly depends on the degree of fiber twisting, the primary design variable that can be used to adjust biomechanical behavior of the graft - higher degrees of twist yield lower construct stiffness. Over the course of cyclic stretch, twisting level decreases due to a dynamic creep, corresponding to scaffold elongation and the observed increase in stiffness.

Perhaps the most important outcome of the present study was the identification of ACL scaffold designs (wired and braided) that approximated the biomechanical properties of the human ACL in an aqueous test environment. This stands in contrast to the straight-fibered structure yielding a lower UTS and much higher linear stiffness than the human ACL. Focusing then only on the wired and braided scaffolds as functionally biofidelic designs, we observed that the wired scaffold had relatively higher UTS but a linear stiffness closer to human ACL than the braided structure. Although the elongation of wired scaffold was nearly two-fold higher than the braided scaffold within the first 5,000 cycles, after 5,000 cycles the elongation differences between these structures disappeared. Given its relative simplicity (and corresponding ease of manufacture), we conclude that a wired silk ACL scaffold may represent an ideal choice as a potential ACL scaffold of the three candidate structures, so long as adequate pre-operative graft preconditioning is performed to minimize in vivo elongation.

Admittedly, there are some limitations in this study. Only one specific design for each graft architectural class was thoroughly tested and compared. Thus no detailed insight to the functional effect of the wiring parameters (twisting level, number of fibers per bundle, etc.) could be obtained, a consideration that may be yield room for further optimization. Another ground for future work would be an extensive study characterizing the architecture dependency of seeded cell response under different loading conditions (and biological effects related to local scaffold strain/stress states). The structure will also affect cell ingrowth, and eventual scaffold remodeling – key points that must be eventually considered with in vivo study. Thus, our attempt to identify an ‘optimal’ structure of a silk scaffold for ACL reconstruction was almost exclusively based on the in vitro biomechanical performance of a limited range of candidate architectures. Nonetheless, we believe that this work represents an important step forward in identifying a promising silk ACL scaffold design, and provides a necessary functional baseline for further improvements.

2.5 CONCLUSION

Silk tissue engineering scaffolds for ACL reconstruction with three different structures were compared in this study. These comparisons were based on static and cyclic mechanical tests under different conditions. We found that the tensile strength and stiffness of silk scaffold markedly decreased in wet condition, but was unaffected by steam sterilization or short term cell culture. Cyclic loading decreased the tensile strength of the constructs, with the scaffiolds both elongating and stiffening. Compared to the mechanical properties of the human ACL, a wired structure best approximated the biomechanical behavior of the human ligament. We therefore suggest a wired silk scaffold geometry as a suitable reference for future silk ACL scaffold designs, and will adopted this structure in our own further studies.

Acknowledgement

The authors wish to thank Trudel Limited (Zurich, Switzerland) for providing raw silk for our research. We also thank Mr. Hansruedi Sommer, Dr. Ram Sharma and Ms. Jingyi Rao for their expertise and kind help in the experiments. This study was partly funded by the Chinese Scholarship Council, and the Bonizzi Theler Foundation.

Supplementary Data

Table 2.2 Mechanical properties of silk yarn in three conditions (prior to cyclic loading)

Archi-tecture	Geo-metry	Condition	Length (mm)	Dia. (mm)	Total fibers	UTS (N)	Stiffness (N/mm)	Elongation (mm)	UTS per fiber	Stiffness per fiber
Silk yarn	6(0)*2(2)	Unextracted, Dry	30	0.24	12	9.42 ± 0.33	1.97 ± 0.07	9.08 ± 0.33	0.79	0.16
Silk yarn	6(0)*2(2)	Extracted, Dry	30	0.17	12	7.34 ± 0.35	1.37 ± 0.17	8.14 ± 0.30	0.61	0.11
Silk yarn	6(0)*2(2)	Extracted, Wet	30	0.14	12	6.00 ± 0.33	1.03 ± 0.23	6.94 ± 0.40	0.50	0.09

Table 2.3 Mechanical properties of silk scaffolds with three architectures in dry and wet conditions

Architecture	Geometry	Condition	Lengths (mm)	Diameter (mm)	Cycles	Total fibers	UTS (N)	Stiffness (N/mm)	Elongation (mm)	UTS per fiber	Stiffness per fiber
Straight	6(0)*2(2)*288(10)*1(0)	Extracted, Dry	30 ± 1	~6.7	0	3456	1589 ± 98	1258 ± 57	-	0.46	0.36
Straight	6(0)*2(2)*288(10)*1(0)	Extracted, Wet	30 ± 1	~6.1	0	3456	1452 ± 106	822 ± 60	-	0.42	0.24
Wired	6(0)*2(2)*144(10)*2(12)	Extracted, Dry	30 ± 1	~6.5	0	3456	1910 ± 128	567 ± 40	-	0.55	0.16
Wired	6(0)*2(2)*144(10)*2(12)	Extracted, Wet	30 ± 1	~6.2	0	3456	1543 ± 85	289 ± 21	3.94 ± 0.25	0.45	0.08
Wired	6(0)*2(2)*144(10)*2(12)	Extracted, Wet Sterilized	30 ± 1	~6.2	0	3456	1444 ± 102	251 ± 39	3.93 ± 0.36	0.42	0.07
Braided	6(0)*2(2)*96(10)*3(12)	Extracted, Dry	30 ± 1	~6.6	0	3456	1890 ± 62	546 ± 41	-	0.55	0.16
Braided	6(0)*2(2)*96(10)*3(12)	Extracted, Wet	30 ± 1	~6.1	0	3456	1599 ± 65	242 ± 26	4.75 ± 0.26	0.46	0.07

Table 2.4 Mechanical properties of wired and braided silk scaffolds with three architectures under different conditions

Architecture	Geometry	Condition	Length (mm)	Diameter (mm)	Cycles	Total fibers	UTS (N)	Stiffness (N/mm)	Elongation (mm)	UTS per fiber	Stiffness per fiber
Wired	6(0)*2(2)*144(10)*2(12)	Extracted, Wet	30 ± 1	~6.2	250	3456	913 ± 123	428 ± 32	5.51 ± 0.32	0.26	0.12
Braided	6(0)*2(2)*96(10)*3(12)	Extracted, Wet	30 ± 1	~6.1	250	3456	787 ± 69	518 ± 66	5.56 ± 0.36	0.23	0.15
Wired	6(0)*2(2)*144(10)*2(12)	Extracted, Wet	28 ± 3	~6.2	100,000	3456	520 ± 76	490 ± 14	4.34 ± 0.81	0.15	0.14
Braided	6(0)*2(2)*96(10)*3(12)	Extracted, Wet	28 ± 3	~6.1	100,000	3456	401 ± 76	553 ± 38	4.25 ± 0.46	0.12	0.16
Wired	6(0)*2(2)*144(10)*2(12)	Static cell culture 24 hours	30 ± 1	~6.2	0	3456	1489 ± 82	274 ± 22	-	0.43	0.11
Wired	6(0)*2(2)*144(10)*2(12)	Static cell culture 7 days	30 ± 1	~6.2	0	3456	1362 ± 20	236 ± 23	-	0.39	0.07
Braided	6(0)*2(2)*96(10)*3(12)	Static cell culture 24 hours	30 ± 1	~6.1	0	3456	1572 ± 89	246 ± 28	-	0.45	0.71
Braided	6(0)*2(2)*96(10)*3(12)	Static cell culture 7 days	30 ± 1	~6.1	0	3456	1391 ± 12	207 ± 31	-	0.40	0.06
Wired	6(0)*2(2)*144(10)*2(12)	Dynamic cell culture 48 hours	28 ± 3	~6.2	100,000	3456	502 ± 41	489 ± 12	-	0.15	0.14

CHAPTER III

Hybrid graft designs

A novel silk-TCP-PEEK construct for anterior cruciate ligament reconstruction: An off-the-shelf alternative to a bone-tendon-bone autograft

Xiang Li[1,2], Jiankang He[3], Weiguo Bian[4], Dichen Li[3], Jess G Snedeker[1,2,*]

[1] Department Health Sciences and Technology, ETH Zurich, Switzerland
[2]Department of Orthopaedics, University of Zurich, Switzerland
[3]State Key Lab for Manufacturing System Engineering, Xi'an Jiaotong University, P.R. China
[4]Department of Orthopaedics Surgery, First Hospital of Xi'an Jiaotong University, P.R. China

Abstract

Bone-tendon-bone autograft represents the gold-standard for ACL reconstruction but at the cost of a secondary surgical site that can be accompanied by functional impairment and discomfort. Although numerous in vitro and in vivo studies have investigated tissue engineering alternatives to autografting, the achievement of a functional histological transition between soft and hard tissue remains elusive. To bridge this gap we developed and tested a novel multiphase scaffold of silk, tricalcium phosphate (TCP), and polyether ether ketone (PEEK) for ACL reconstruction. We present in vitro biomechanical tests demonstrating that the construct recapitulates native ACL function under typical physiological loads. A pilot in vivo experiment in pigs with a three-month follow-up showed a robust histological transition between regenerated fibrous tissue and the margins of the bone tunnel, with histological features similar to the native ACL to bone insertion. These histological observations suggest that the construct was stably anchored until TCP incorporation to the host tissues. On the strength of these preliminary results, we conclude that the described approach may offer a promising alternative to autograft for ACL reconstruction. This study thus provides proof for a concept that warrants further development.

Keywords

Silk, TCP, PEEK scaffold, ligament tissue engineering, ACL reconstruction

3.1 INTRODUCTION

Traumatic disruption of the anterior cruciate ligament (ACL) is among the most frequent and severe of ligament injuries[1]. It has been estimated that there are over 250,000 patients per year diagnosed with ACL tear in the United States (roughly 1 in 3,000 of the general population), leading to approximately 75,000 surgical reconstructions performed annually [2-5]. Available surgical grafting options are numerous and varied, with each being accompanied by certain disadvantages. In the case of autograft, donor site morbidity is a primary concern [6, 7], while xenografts present issues related to disease transmission[8] and potential host immune response[9, 10]. All grafting options involve general issues related to ligament laxity and mechanical mismatch [11] among other concerns [12, 13]. Because an improved ACL reconstruction technique is clearly required, scaffold-based tissue engineering strategies have emerged to fill this void [5, 14-20].

Ideally, a scaffold for ACL replacement should be biodegradable and biocompatible, permitting cell ingrowth and tissue remodeling, yet providing joint stability until regenerated tissues can take over this function [12, 14]. Among scaffolding materials for the ligament itself, naturally derived silk fibroin has received increasing attention [18, 21-25]. Removal of the hyper-allergenic sericin component from raw silk [26, 27] results in a biomaterial with outstanding mechanical toughness, failure stresses up to 4.8 GPa, failure strains up to 35%, and excellent environmental stability [15, 28, 29]. As a scaffold for fibrous tissue regeneration, silk fibroin can mimic collagen structures for their ability to support cell attachment, providing an aligned topology that is conducive to ligament-like tissue growth[30, 31]. Silk offers in vivo degradation rates with a gradual loss of tensile strength over 1 year [5, 28]. This characteristic is important for providing immediate support of high mechanical stresses during post-operative rehabilitation, while eventually permitting a progressive transition toward a native tissue.

Studies on the functional implications of silk fiber architectures by our group[32, 33] and others [5, 28, 34, 35] have identified graft designs that can mimic the biomechanical properties of the native ACL. Within the graft itself, in vitro studies have evaluated effects of surface treatment and bioactive factors on cell-material

interactions [12, 14-16, 27, 36-38]. Collectively this work provides a strong foundation of preclinical evidence to guide scaffold development. Silk scaffolds have also been investigated in vivo, including preclinical studies in rabbits, goats and pigs [14, 17, 39, 40], as well as in human clinical trials assessing safety and efficacy for reconstruction of the completely ruptured ACL [41]. Thus much progress has been achieved to bring silk-based ligament scaffolds closer to clinical application [42, 43].

Regardless of the ligament scaffold material, studies on scaffold based ACL reconstruction have largely failed to redress critical shortcomings in the connection of the ligament graft to the bone tunnel. Achieving a rapid and robust interface between the hard and soft tissue remains a highly problematic aspect of post-operative healing, with poor graft incorporation to the bone tunnel widely cited as a major cause of poor clinical outcome[44, 45]. For this reason, the bone-patellar tendon-bone (BPTB) graft has emerged as a gold-standard, exploiting a preexisting histological transition from bone to ligament to rapidly bridge the ligament graft to the bone tunnel [46-48]. Unfortunately BPTB autografting is accompanied by notable donor-site morbidity [20, 49], a factor that often relegates its use to patients seeking a rapid return to high levels of physical activity, but who are willing to risk the post-operative discomfort associated with this graft source. Thus the majority of reconstructions are currently performed using hamstring tendon autograft, despite the slower integration of these grafts to the bone tunnel.

Biomaterial engineers and orthopedic surgeons have done much work attempting to improve functional graft incorporation, with a major thrust of these efforts employing agents within the bone tunnel to elicit more rapid and effective tissue transition from the graft to the host. Bone cements such as calcium phosphate cement (CPC) and tricalcium phosphate (TCP) have been harnessed to augment the peri-graft bone volume and promote bone ingrowth at the healing graft interface, and these have been reported to significantly enhance tendon autograft integration [50, 51]. Cell based approaches have also been employed with reported success [52, 53]. Bioactive factors represent another potentially powerful means of promoting graft to bone healing, with highly osteoinductive properties of bone morphogenetic protein family having been employed to enhance bone ingrowth and accelerate graft to tunnel healing [54, 55].

In these studies and others focusing on biological augmentation of secondary mechanical stability (healing), the critical importance of primary mechanical stability has been largely neglected. Until now, relatively little work has explored on how an osteoconductive/inductive construct might be used to achieve improved healing while also securing adequate primary mechanical stability. Although our group has explored alternative approaches to increase contact pressure between the graft and tunnel to achieve superior primary and secondary stability [56-59], outside of bone-tendon-bone autografting there appears to be no reliable method providing an osteoconductive graft surface within the tunnel while achieving robust primary mechanical stability.

We present a novel approach to ACL reconstruction that is conceptually inspired by the histology of the human bone-tendon-bone autograft, but is extended to incorporate fixation elements that provide primary stability. The implant features a silk fibroin based ligament scaffold enlaced upon a hybrid TCP/PEEK anchor. The silk scaffold is designed to provide mechanical properties similar to the native human ACL. The device features a TCP insert that positions the silk scaffold within the bone tunnel to maximize contact surface area between the silk graft and osteoinductive surfaces within the bone tunnel. To anchor the entire construct while protecting the TCP element from mechanical damage, we employed a PEEK housing that exploits the excellent mechanical properties and biocompatibility of this material. Taken together, the device design was intended to combine a TCP scaffold within a PEEK anchor to provide robust primary mechanical fixation and accelerated graft integration. The following in vitro and in vivo studies were performed to assess whether the device could attain these goals.

3.2 MATERIALS AND METHODS

Silk scaffold design and fabrication

Raw silk fibers (Bombyx mori) were obtained from a commercial supplier (Grege 20/22, Trudel Limited, Zurich, Switzerland). All scaffolds were produced using a specially designed wiring machine. The geometries of the different hierarchical architectures can be described using a labeling convention of A(a)*B(b)*C(c)*D(d), where A, B, C, D represent increasing hierarchical level - fibers(A), bundles(B), yarns(C) and cords(D)), while a, b, c, d represent the twisting level corresponding

to the length (mm) per turn at each of the hierarchical levels. After testing and comparison of different possible structures[126], we selected a wired silk scaffold structure with mechanical properties similar to the native human ACL; this structure was utilized for the present study, with architectural parameters defined as 6(0)*2(2)*144(10)*2(12) meaning 6 fibers in 1 bundle without twist (0 means parallel), 2 bundles in 1 yarn with 2 mm per turn, 144 yarns in 1 cord with 10 mm per turn, 2 cords in 1 ACL scaffold with 12 mm per turn (Figure 3.1).

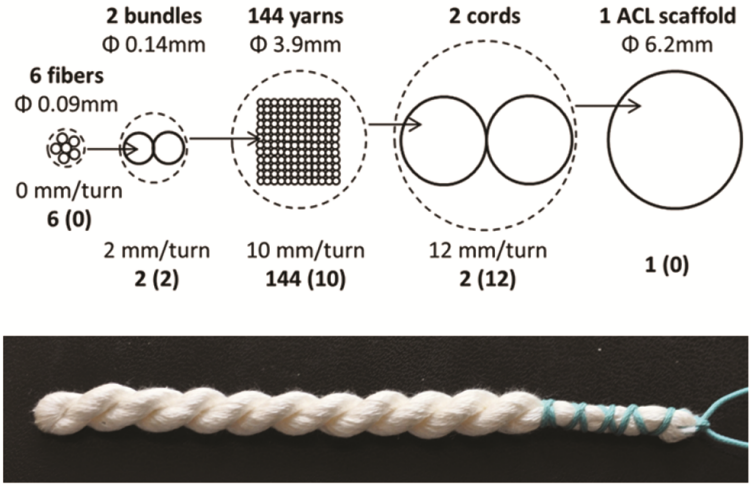

Figure 3.1 Schematic and photo of silk ACL scaffold with wired architecture

The wired silk ACL scaffolds were produced with raw silk yarns. The antigenic protein sericin was then removed by immersing the scaffolds into an aqueous solution of 0.5wt% Na2CO3 at 90-95 ℃, while stirring at 300 RPM using a magnetic stirrer (Basic C, IKA-WERKE, Germany) for 90 minutes. After rinsing with running distilled water for 15 minutes, the grafts were finally air dried at 60 ℃. These procedures were repeated three times per graft.

TCP/PEEK anchor design and fabrication

The anchor design consisted of two parts comprising an osteoconductive insert of porous tricalcium phosphate (TCP) housed within a rigid polymer anchor machined from polyether ether ketone (PEEK). The TCP insert was designed with an 'H'-

shaped form (Figure 3.2A) that accommodated the enlacing silk scaffold around the bridge of the insert that was then press fitted within the external PEEK anchor housing (Figure 3.2B,D,E). A stainless steel insertion tool was developed to secure the PEEK anchor for surgical implantation (Figure 3.2C,F). The outermost perimeter of the TCP insert featured a maximal cross-sectional diameter of 9.0 mm, corresponding to the inner diameter of bone tunnel used in all presented studies. The length of the TCP insert was 11.5 mm. The PEEK anchor featured two arms with anchoring teeth, and a hollow cap with tighter pitched-anchoring teeth. The outside diameter of anchor teeth was 10.4 mm. The diameter of inner circle of the cap and arms was 6.0 mm. The total length of the PEEK anchor was 16.0 mm.

The TCP scaffold was fabricated using techniques combining rapid prototyping and gel-casting methods [127]. Briefly, molds comprising the negative geometry of the TCP insert were designed with a commercial Computer Aided Design (CAD) software (Pro/ENGINEER® Wildfire 5.0). The molds were fabricated on a sterolithography apparatus (SPS 600B) with a commercial epoxy resin (SL14120, Huntsman). The CAD data of the negative pattern (Figure 3.3A) was imported into the prototyping device software, and converted into an appropriate input file for sterolithography. The molds were then fabricated and cleaned with isopropanol alcohol (Figure 3.3B). TCP powder was mixed with monomers (acrylamide, methylenebisacrylamide), and dispersant (sodium polymethacrylate) in de-ionized (DI) water to form a ceramic slurry (Table 3.1).

The prepared slurry was deagglomerated by ultrasound for 5 hours and subsequently degassed under vacuum until absence of released air bubbles was observed. Catalyst (ammonium presulphate) and initiator (N,N,N’N’-tetramethylethylenediamine) were added to the slurry to polymerize the monomers. The amounts of catalyst and initiator were controlled to allow sufficient time to complete the subsequent casting process. Here the TCP slurry was cast into the molds under vacuum to force the TCP powder to migrate into spaces between paraffin spheres of mean diameter 50 μm. The samples were then dried at room temperature for 72 hours. After drying, pyrolysis of the epoxy resin molds and paraffin spheres were conducted in air in an electric furnace with a heating rate of 5℃/h from room temperature to 340℃, holding 5 hours at 340℃ to ensure elimination of most paraffin spheres, and then increasing to 660℃ at a rate of 10℃/h, holding 5 hours at 660℃ to ensure that most epoxy resin was removed.

Afterward the heating rate was increased to 60℃/h to achieve 1200℃, holding 5 hours at 1200℃, and then returning to room temperature over a period of 48 hours. Afterwards, the completed TCP insert was removed from the oven for later use (Figure 3.3C). The PEEK anchor was machined using standard techniques from polyether ether ketone stock material (Ketron PEEK-1000, Angst-Pfister, Switzerland).

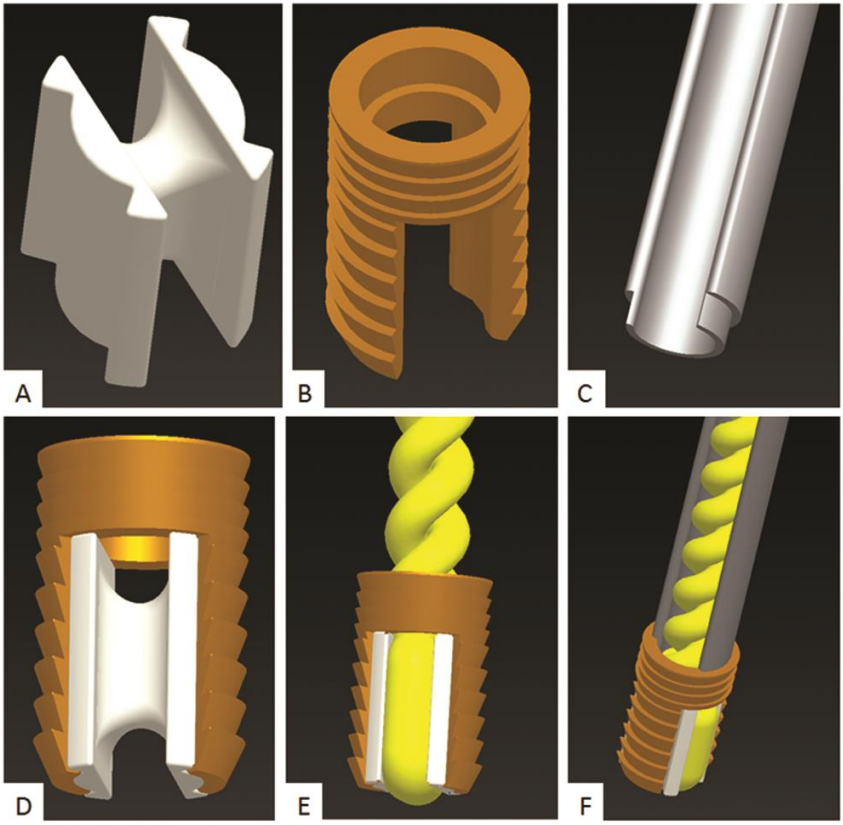

Figure 3.2 CAD images of TCP/PEEK anchor design with and insertion tool. (A) TCP insert; (B) PEEK anchor; (C) Stainless steel insertion tool; (D) Assembled TCP/PEEK anchor; (E) Assembled Silk/TCP/PEEK scaffold; (F) Assembled Silk/TCP/PEEK scaffold mounted for insertion.

Table 3.1 Composition of slurry for scaffold fabrication

	Component	Amount
Solvent:	Deionized water	35g
Ceramic powder:	Beta-tricalcium phosphate	60g
Monomer:	Acrylamide	4g
Cross linker:	Methylenebisacrylamide	0.5g
Dispersant:	Sodium polymethacrylate	0.6g
Initiator:	Ammonium presulphate	0.2g
Catalyst:	N,N,N'N'-tetramethylethylenediamine	0.1g

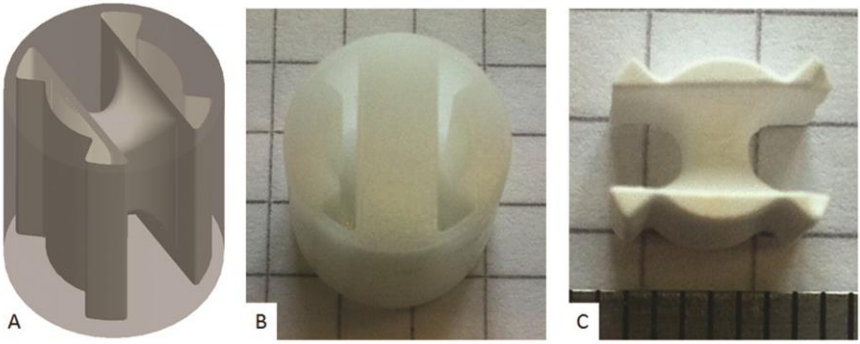

Figure 3.3 The mold for TCP scaffold casting. (A. CAD model; B. Resin mold; C. TCP scaffold fabricated)

In vitro biomechanical test

To assess primary stability of femoral fixation, an in vitro study using porcine knees was performed. Femurs from 3-4 month old pigs were obtained immediately after euthanization at a local abattoir, and then dissected of all soft tissue. Bone tunnels were drilled at the footprint of the native ACL using a 9.0 mm drill (Figure 3.4A). For the left and right femora, the drilling direction was respectively set to 10 or 2 o'clock in the transversal plane, with 45° anterior deviation in the sagittal plane using the femoral axes as a reference. For implant insertion, a specialized anchoring tool secured and aligned the anchor in the desired direction for ready and stable insertion (Figure 3.4B,C). Corresponding control experiments using commercially

available interference screws (Φ8 × 28 mm, Karl Storz Germany) were performed to provide a comparative baseline.

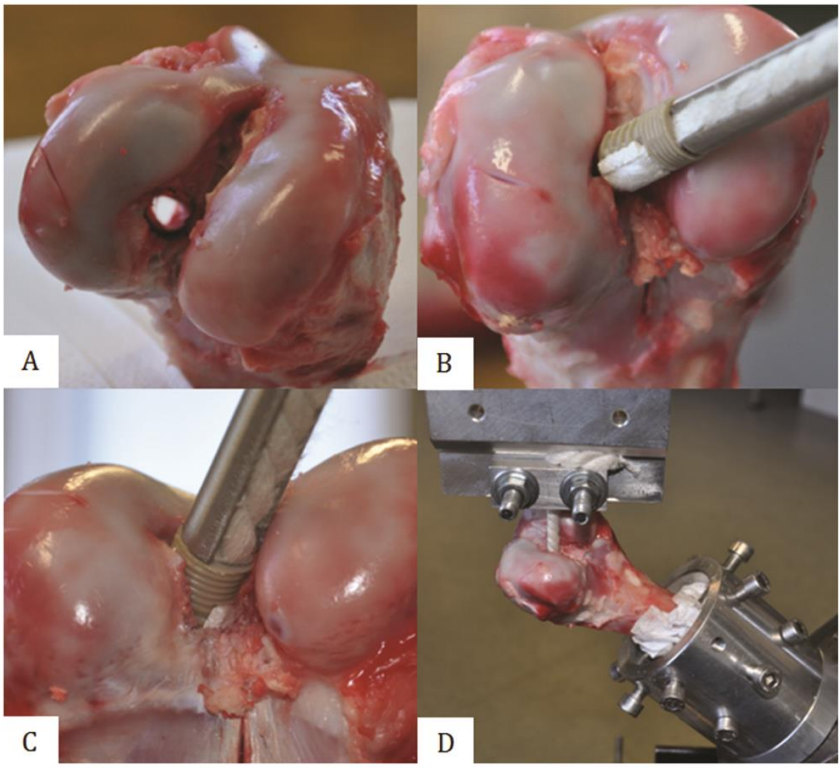

Figure 3.4 In vitro biomechanical testing. (A. drilling of the bone tunnel; B.C implantation; D. Fixation using custom clamps)

Cyclical loading and tension to failure tests were performed with seven samples on a universal material testing machine (Zwick 1456, Zwick GmbH, Ulm, Germany) mounted with a 20 kN force sensor (Gassmann Theiss, Bickenbach, Germany). The femur was secured in an appropriate anatomical position using custom clamps (Figure 3.4D) to provide 30±1 mm of graft length to simulate the normal ACL [114, 115] at a pre-load of 5 N. The samples were then loaded at a rate of 0.5 mm/second from 100 to 250 N over 250 cycles, representing load ranges experienced in normal walking[116], before ramp to failure characterization of ultimate tensile strength.

The force-displacement curve of each test was recorded. Graft elongation/slippage was measured by the difference of displacement between the first cycle and the last cycle to 250N. The ultimate tensile strength was recorded at the first peak in the pull to failure test.

Pilot animal study

All animal experiments were approved and performed according to state and local animal welfare regulations. Two pigs (male, 3 months old, 47kg, 52kg) were used in this pilot animal study. After anaesthetization by pentobarbital, the native ACL of the left knee was removed by blunt dissection at the femoral and tibial surfaces and then immediately reconstructed using the previously described device. Briefly, an open surgical procedure was used. First a longitudinal medial approach skin incision was made 5 cm proximal to the superior margin of the patella to the tibial tubercle. The knee joint was accessed with medial parapatellar capsular approach. Then, the native ACL was carefully cut and removed. A 9.0 mm tunnel was drilled over the footprint of ACL, to 20 mm in depth. To avoid damage to the articular cartilage on the medial condyle, the drilling direction was adjusted to 11 o'clock on the transversal plane, and 45° anterior deviation on the sagittal plane using the femoral axes as a frame of reference. A drilling sleeve was developed to stabilize the drilling instrument, preventing unnecessarily enlarged tunnel apertures and subsequent compromise of implant stability. A corresponding 7.0 mm tunnel was drilled through the tibial ACL footprint using a custom designed synchronizing sleeve. The silk/TCP/PEEK implant was then inserted (press-fit by pushing and tapping with a mallet) into the femoral tunnel using the insertion tool with a hollow cylindrical cross section to accommodate the silk scaffold during insertion. After anchoring of the TCP/PEEK end of the construct within the femur tunnel, the free end of the silk graft was pulled through the tibial tunnel. The knee joint was then flexed at 30°, the silk graft was pulled until tight, and then fixed in place with an interference screw (Φ6 × 19 mm, Anklin AG, Switzerland). A postoperative clinical X-ray and clinical CT were taken to verify that implant position was correct. After recovery from anesthesia, the animals were allowed to move freely without immobilization. Both animals were sacrificed three months later. The regenerated ligament and the insertion to the bone were fixed in 10% formalin. After the specimens were decalcified, they were embedding in paraffin blocks. Sections of

5µm were cut and stained with hematoxylin and eosin (H.E.) for histological observation.

3.3 RESULTS

The silk scaffolds were able to be successfully fabricated, with two cords exhibiting smooth surfaces that were consistent with complete removal of sericin. The ultimate tensile strength and linear stiffness of the silk ligament scaffold was around 1500 N, and 280 N/mm respectively, close to values typical of the native human ACL. The TCP inserts were generated with a porosity of approximately 40% and corresponding compressive strength of approximately 15 MPa [127], with the inserts thus capable of withstanding tensile loads from the silk scaffold of up to 500 N.

In vitro tension to failure tests (n=7) with the assembled silk/TCP/PEEK devices (Figure 3.5) showed that the anchoring system yielded statistically equivalent slippage and graft elongation compared to interference screw fixation (1.65 ± 0.35 mm vs. 1.87 ± 0.67, p=0.49). The pullout strength of the TCP/PEEK anchor developed in this study was 544 ± 98 N, or approximately 170 N lower than pull-out strength of the interference screw (p=0.07).

The surgical procedure was successfully executed on both animals (Figure 3.6). No infections were found after surgery. Both animals recovered well, and could walk on four legs with only a slight degree of observable postoperative lameness after one week. Radiographic imaging of the postoperative reconstruction did indicate that in one animal the TCP insert underwent minor damage upon insertion (Figure 3.7).

The animals were sacrificed three months after the ligament reconstruction surgery. The knee joint was carefully opened and the joint was dissected to leave only the bones and regenerated ligament intact. The silk fibers could still be identified by eye, heavily intermixed with adhered fibrous connective tissue (Figure 3.8). Histological analysis of the ligament scaffold (Figure 3.9A,B) verified that silk fibers were still present at three months, and that these were surrounded by regenerated ligamentous tissues with collagen fibers well-aligned to the silk structures.

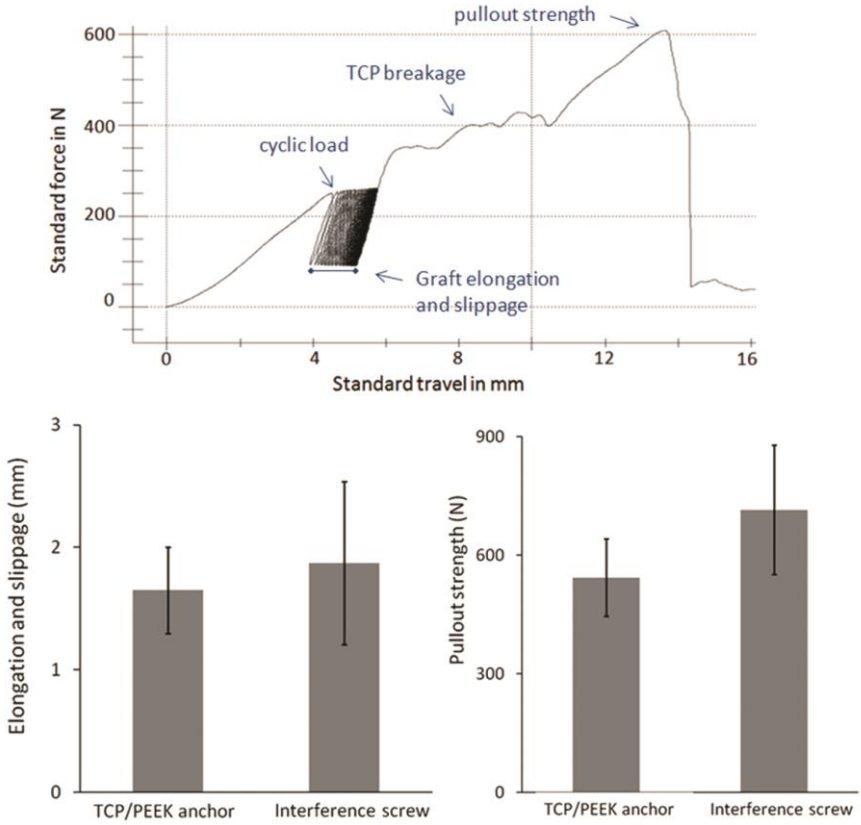

Figure 3.5 The comparison of mechanical behavior between scaffold and interference screw

Analysis of the histological transition zones within the tunnel (Figure 3.9C,D) indicated that the bone tunnel had healed to encapsulate regenerated mineralized and non-mineralized connective tissues among the silk fibers, TCP, and PEEK of the original implant. Regenerated tissues included fibrous tissue and fibrocartilage, as well as clearly demarcated transitional tissue zones resembling “Sharpey’s fibers” that characterize the native histological transition from ligament to bone.

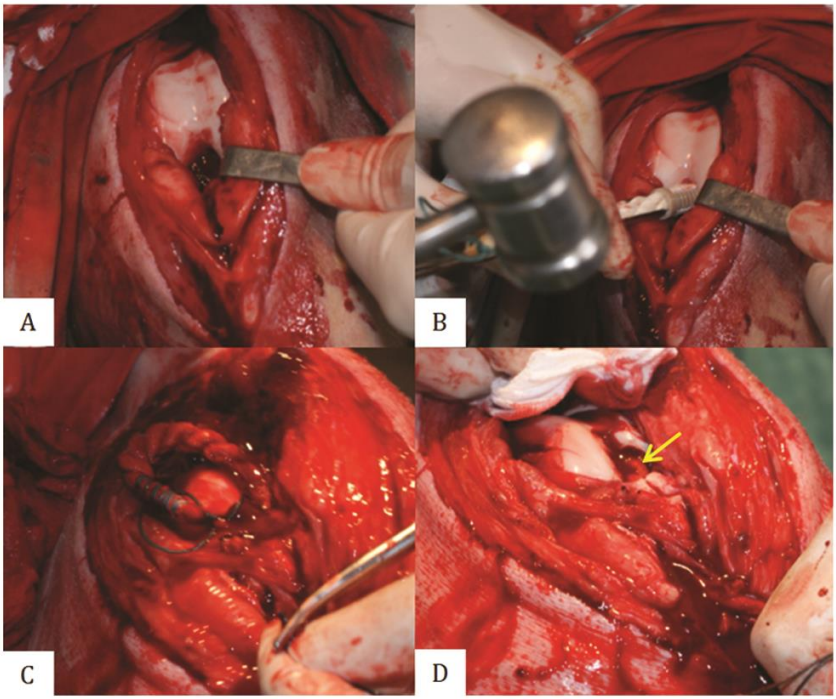

Figure 3.6 The surgery process of scaffold implantation.

3.4 DISCUSSIONS

There are a number of graft choices available to the orthopaedic surgeon for ACL reconstruction. Among these choices, the patellar tendon bone-tendon-bone (BTB) graft has been the "gold standard" graft choice for ACL reconstruction because, aside from an occasionally high degree donor site morbidity, it consistently yields improved clinical outcome in terms of return to pre-injury levels of activity [81].

The idea of this study was to develop and test an alternative grafting solution for ACL regeneration, seeking to mimic certain characteristics of a patellar BTB graft, but using a novel combination of biomaterials to avoid donor site morbidity. We describe a composite scaffold for ACL reconstruction toward achieving this goal.

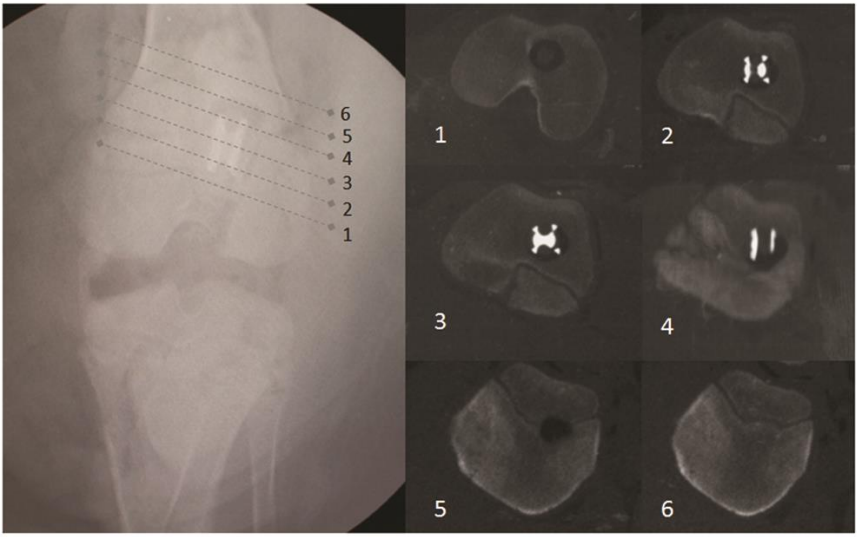

Figure 3.7 Postoperative x-ray (left) and CT images (right) of the operated porcine knee.
(The black ring in (1) is the hollow cap of the PEEK anchor. The middle grey circle is the silk graft. The white parts in (2-4) are the TCP scaffold from top to bottom.)

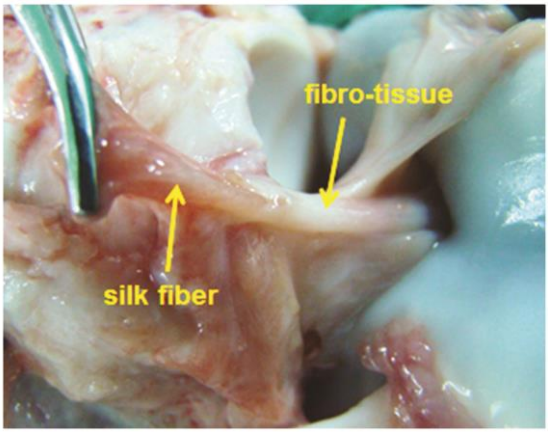

Figure 3.8 Picture of regenerated fibro-tissue euthanasia at three months

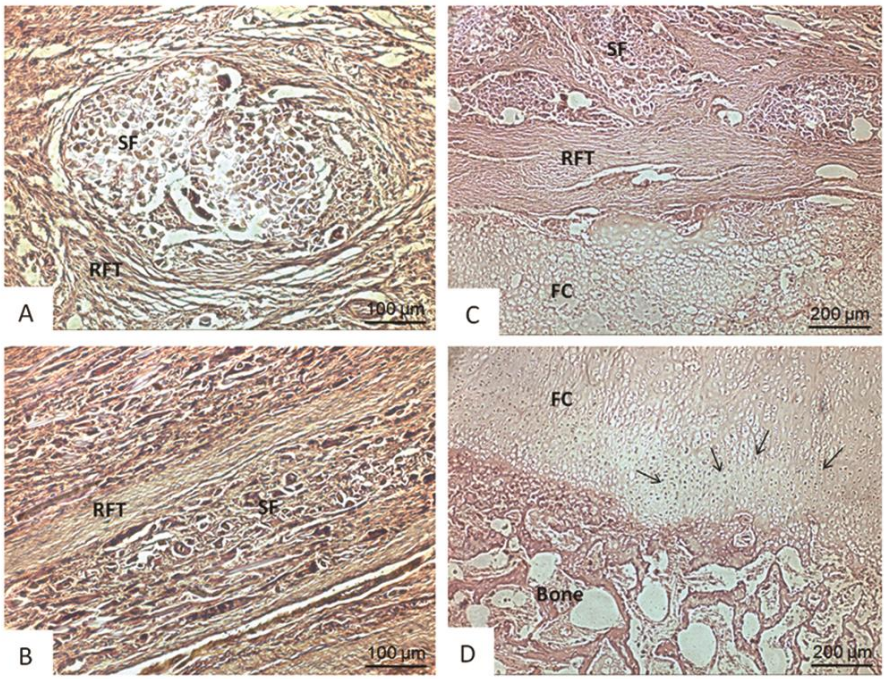

Figure 3.9 Histological observation of regenerated ligament tissues and their transition to the bone tunnel. (SF: silk fiber; RFT: regenerated fibro-tissue; FC: fibrocartilage). (A) Transverse section view of silk fiber with regenerated fibro-tissue. (B) Longitudinal section view of silk fiber with regenerated fibro-tissue. (C) Transitional zone of silk fiber to fibrocartilage. (D) Transitional zone of fibrocartilage.

The ligament graft itself represents a major design concern for which silk has been increasingly employed. Silk offers advantageous biological properties as well as robust biomechanical strength in the short and middle terms [128]. Based on our previous work, we selected a silk scaffold architecture that provides mechanical properties mimicking the native human ACL [128]. After three months of postoperative healing in vivo, the silk scaffolds remained largely intact but were intermixed with regenerated fibrous tissue, the cells of which were well aligned with and often attached to the silk fibers (Figure 9A,B). These observations reflect the characteristically slow degradation of silk, which enables the biomaterial

scaffold to support the functional demands of ligament until the host tissues eventually overtake these loads. These findings are consistent with extensive studies by others using silk grafts for ACL reconstruction[56, 57, 108, 109, 129, 130].

The novel and perhaps most important aspect of the present study concerns conceptual testing of a “hybrid anchor design” featuring a tricalcium phosphate (TCP) insert within a polyether ether ketone housing. While any rigid implant material could in principle be utilized for the anchor housing, we selected PEEK for its biomechanical and biological properties and for the possibility of easy removal in event of complication - factors behind its increasing clinical use. In vitro testing of the hybrid anchor indicated that the system is capable of providing robust mechanical fixation and initial stability, while generally shielding the TCP insert from catastrophic damage. The observed fracture of one TCP insert in the in vivo study reflects the challenge of achieving adequate TCP strength while maintaining high porosity levels that are conducive for cell ingrowth. Still, our more comprehensive in vitro testing results suggest that even in its current form the hybrid anchor can be consistently inserted without damage, suggesting that the surgical technique rather than the implant, requires refinement.

In comparison to silk graft fixation with a standard interference screw, the TCP/PEEK anchor developed for this study had relatively lower pullout strength (~24%) but yielded less slippage (~12%). Still the observed failure forces are more than four-fold higher than ACL forces expected during post-operative recovery and rehabilitation stage [93] and we conclude on this basis that post-operative mechanical loading during gait can be safely supported. Nonetheless, larger scale animal studies are required to verify whether the implant fixation is consistent and sufficiently stable to allow reliable healing and resulting secondary stability.

We view the implant integration and related tissue formation in the bone tunnel to be among the most interesting results of the present study. The native insertion of the ACL to bone contains four histologic transitional zones of ligament, un-mineralized fibrocartilage, mineralized fibrocartilage, and bone that is highly specialized to receive stresses from the attached soft tissues [131]. Recapitulating this tissue transition represents a major research thrust in current orthopedic tissue engineering. In the present study, transitional zones from fibrous tissue to bone were clearly observable after three months (Figure 9C,D). The transitional zones

contained silk fibers, regenerated fibrous tissue, fibrocartilage, intact TCP and regenerated bone. The regenerated soft-to-hard tissue junction appeared morphologically similar to the native ligament to bone insertion, with regions of Sharpey's-like fibers projecting from regenerated fibrous tissue into bone tissue, apparently through regenerated fibrocartilage. Thus the histological assessment of the novel device tested in this study indicated promise for biomimetic ACL regeneration.

The studies performed in this work were designed to provide proof of principle and to test safety and efficacy in a limited population of large animals. While these goals were mostly achieved, certain issues were identified that will require additional research and development to more conclusively assess the potential of this novel strategy for ACL regeneration. For instance, the silk scaffold within the tibial tunnel was fixed using a standard interference screw that yielded comparatively poor graft incorporation to the tibial bone tunnel. How the poor fixation at the tibial tunnel may have impacted implant integration at the femoral tunnel remains to be clarified. This aspect of the device depends heavily on the accompanying surgical technique, and whether the hybrid anchoring concept can be extended to a twin-ended approach. Also to be addressed is the relative fragility of the TCP scaffold used in this study, which was observed to crack upon insertion in one of the two in vivo trials (although not catastrophically, and did not crack during in vitro experiments). Additional investigations utilizing stronger TCP inserts are planned, as well as into the biological implications of the associated reduction in TCP porosity. Finally, longer-term assessment of ligament regeneration and functional (biomechanical) recovery is necessary, and this study must include sufficient statistical power to draw more definite conclusions regarding the clinical promise of the proposed concept. A systematic evaluation of the hybrid ACL scaffold within a larger scale animal experiment is thus required, for which the current study provides a necessary foundation.

3.5 CONCLUSION

A novel silk/TCP/PEEK scaffold for ACL reconstruction was developed in this study. The silk ACL scaffold, with mechanical behavior similar to the human ACL, was enlaced onto the TCP scaffold, and fixed with a PEEK anchor. The proposed concept mimics the human patellar bone-tendon-bone autograft to provide an

osteoinductive element within the bone tunnel. In vitro biomechanical testing verified that the construct provided adequate primary stability. A pilot large animal experiment indicated that after three months the scaffold had been partly remodeled by the host tissues, with histological subregions characteristic of the native ACL and its insertion to bone. We conclude that the hybrid scaffold developed and tested in this study may hold promise as a multi-phase, scaffold-based approach to ACL regeneration.

Acknowledgement

The authors wish to thank Trudel Limited (Zurich, Switzerland) for providing raw silk for our research. We also thank Mr. Hansruedi Sommer, Dr. med. Weijie Zhang, Dr. med. Arnd Viehöfer, Prof. Dr. Marc Bohner, Mr. Zheng Li for their expertise and kind help in various aspects of device prototype fabrication and testing. This study was partly funded by the National Natural Science Foundation of China (No.51105298), Program of Leading Talent in Changshu of China, and the Bonizzi Theler Foundation.

CHAPTER IV

Animal experiments

A novel silk-based artificial ligament and TCP/PEEK anchor for ACL reconstruction – safety and efficacy in porcine model

Xiang Li[1,2], Jiankang He[3], Weiguo Bian[4], Zheng Li[4], Dichen Li[3], Jess G Snedeker[1,2,*]

[1] Department Health Sciences and Technology, ETH Zurich, Switzerland
[2]Department of Orthopaedics, University of Zurich, Switzerland
[3]State Key Lab for Manufacturing System Engineering, Xi'an Jiaotong University, P.R. China
[4]Department of Orthopaedics Surgery, First Hospital of Xi'an Jiaotong University, P.R. China

Abstract

Loss of ligament graft tension in early postoperative stages following ACL reconstruction can come from a variety of factors, with slow graft integration to bone being widely viewed as a chief culprit. Toward an off-the-shelf ACL graft that can rapidly integrate to host tissue, we have developed a silk-based ACL graft combined with a TCP/PEEK anchor. In the present study we tested safety and efficacy of this concept in a porcine model, with postoperative assessments at three months (n=10) and six months (n=4). Biomechanical tests were performed after euthanization, with ultimate tensile strengths at three months of ~370 N and ~566 N at six months - comparable with autograft and allograft performance in this animal model. Comprehensive histological observations revealed that TCP substantially enhanced silk graft to bone attachment. Interdigitation of soft and hard tissues was observed, with regenerated fibrocartilage characterizing a transitional zone from silk graft to bone that was similar to native ligament bone attachments. We conclude that both initial stability and robust long-term biological attachment were consistently achieved using the tested construct, supporting a large potential for silk-TCP combinations in the repair of the torn ACL.

Keywords

Silk, TCP, PEEK, anchor, artificial ACL, ligament tissue engineering, ACL reconstruction

4.1 INTRODUCTION

Anterior cruciate ligament (ACL) ruptures are among the most frequent and severe ligament injuries [1], with between 250,000 to 400,000 diagnosed ACL disruptions in the United States each year [2-4]. ACL reconstruction surgery is increasingly common as well, with more than half of diagnosed complete ACL tears being surgically reconstructed [5, 6]. While ACL reconstruction is generally viewed as a low-risk procedure that provides substantial short- and medium-term patient benefit [6-8], long-term benefit of the procedure is often debated [9-11]. In additional to marginal long-term benefit over conservative treatment, various aspects of the procedure itself, such as donor-site morbidity related to the use of a ligament autograft, leave substantial room for improvement [12-14].

Regarding functional outcome, the major issue of inadequate knee stability most likely relates to loss of graft tension in early postoperative stages[15, 16]. This loss of tension in the replacement ligament can come from a variety of factors, but poor/slow graft integration to the patient's bone is widely considered to be the primary cause. To accelerate bone integration and promote ligament tension, surgeons often employ a bone-tendon-bone (BTB) autograft that is typically extracted from the patient's patellar tendon. Although the transplanted bone blocks at the end of the graft incorporate at the grafting site, the graft extraction itself can be very painful and is a major cause of patient dissatisfaction [17, 18]. For non-professional athletes, doctors thus often employ a hamstring autograft as a less painful alternative source of tissue. While donor site morbidity accompanying a hamstring autograft procedure is generally less than that for a BTB autograft, hamstring grafts are often considered to provide inferior mechanical stability. This inferior stability can be attributed to slow integration of hamstring tendon within the bone tunnel, and associated graft elongation and loosening [19]. By the time the healing phase is complete, a ligament reconstruction using hamstring autograft can often be too slack to ensure normal joint stability.

In general, all currently available choices for ligament grafting material have drawbacks. These include donor site morbidity for autografts [20, 21], disease transmission for allografts [22], and adverse immune response for allografts, xenografts, and synthetic biomaterials [23, 24]. These aspects can compound challenges associated with ligament laxity [25] and mechanical mismatch [26, 27],

and overcoming these challenges has emerged as a major research objective, motivating both biomaterial and tissue engineering approaches to the problem [28-34].

Among these approaches, silk based ACL grafts have been increasingly investigated [28, 32, 35-45], going as far as safety and efficacy oriented clinical trials in humans [46]. Across these many studies, the regeneration of the ligament itself using silk scaffolds has emerged as a viable alternative to autografted tendon. Still, these efforts have not addressed the larger challenge - namely the integration of the ligament graft to the host bone [47, 48]. Many strategies to enhance graft to bone healing have been pursued, including the use of bone marrow derived mesenchymal stem cells [49, 50], bioactive factors like bone morphogenetic proteins [51-54], and/or the incorporation of osteoinductive bioceramics such as hydroxyapatite, tricalcium phosphate (TCP), or brushite calcium phosphate cement [55-60]. However, nearly all of the above studies attempting to enhance graft to bone integration focused primarily on stimulating a biological response, while neglecting the critical considerations of primary mechanical stability (immediate post-operative 'pull-out strength') and confinement of bioactive compounds to the bone tunnel (restriction of such agents from the joint space).

The present study sought to test whether a novel device for ACL reconstruction could achieve these three objectives: robust primary strength, rapid intregration, and restriction of osteoinductive material from the joint space. Toward this goal we combined a TCP/PEEK(polyether ether ketone) anchor with a silk based ACL scaffold [61]. We then evaluated the short- and mid-term safety and efficacy of this system using a porcine model. The results indicate that a combination of TCP and PEEK for ACL graft fixation is not only feasible, but also effective.

4.2 MATERIALS AND METHODS

Silk graft with TCP/PEEK anchor preparation

The general concept of the silk-based ACL graft with TCP/PEEK anchor (Figure 4.1) and detailed design parameters and fabrication techniques are described previously. Briefly, a silk based artificial ACL graft was prepared with an architecture of 6(0)*2(2)*144(10)*2(12), also as previously described[128]. A TCP component with a diameter of 9.0 mm, length of 11.5 mm, and porosity of 45%, was fabricated

using techniques combining rapid prototyping and gel-casting methods[127]. The PEEK anchor with a hollow cap was machined to press-fit with the TCP insert, having an outside diameter of 10.4 mm, inner diameter of 6.0 mm, and featuring two arms with anchoring teeth. All implants were sterilized as follows: After fabrication each component was immersed in 75% ethanol for 24 hours; the TCP components were further treated by Ultraviolet germicidal irradiation at a dose of 100 mJ/cm^2. Afterwards, all parts were assembled in a sterile hood. Finally, the assembled graft was packaged and autoclaved at 121°C for 30 minutes.

Study design

Animal experiments were carried out under the Rules and Regulations of the Animal Care and Use Committee, First Hospital of Xi'an Jiaotong University, P.R. China. The present study was performed with 14 healthy adult male pigs (Chinese tri-hybrid pig: Xianyang breed) aged around four months and weighing 55.2±3.7 kg (mean ± SD) at time of surgery. ACL reconstructions were performed on the left knee. The animals were divided into two study groups with 10 animals planned for sacrifice at a three-month time point, and 4 animals at a six-month time point. Within the three-month group, 7 of 10 animals were used for biomechanical tests, the remaining 3, plus 1 from the biomechanical test samples, (4 animals) were used for histological observation. From the six month group, 3 of 4 animals were used for biomechanical tests, with the remaining specimen combined with one specimen from the 3 biomechanical test samples (i.e. 2 animals) allocated for histological analysis.

Preoperative treatment

The pigs were thoroughly disinfected by spraying with 0.25% didecyl dimethyl ammonium bromide solution two days before surgery. Antibiotics (Penicillin of 800'000 U) were given to each pig by intramuscular injection twice the day before the operation. A sodium pentobarbital solution of 3.5% concentration was used as anesthetic. Each animal was given 0.5ml/kg by abdominal injection, and followed 5 minutes later with additional 0.2ml/kg dose by venous injection. The animal was then positioned supine on the operating table in a specially designed constraint. The left hindleg was shaved, and thoroughly washed with povidone-iodine solution.

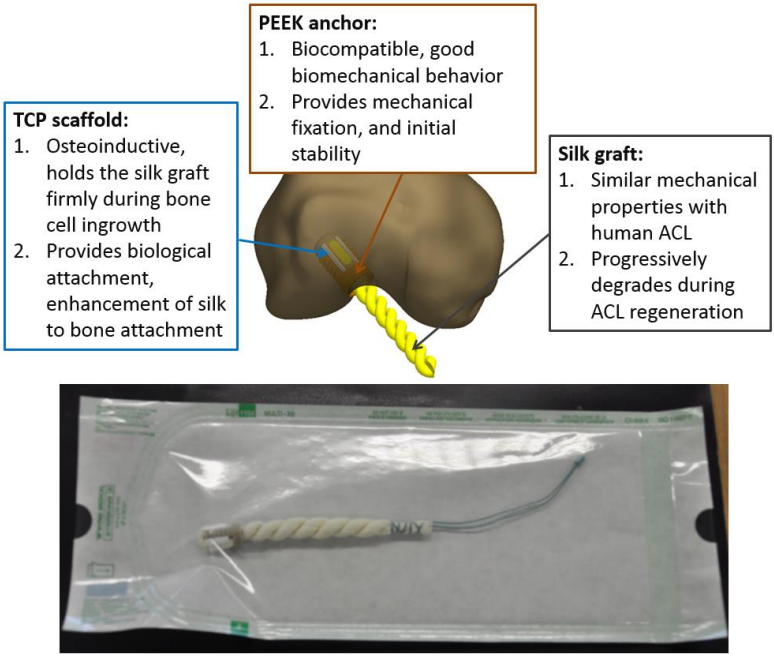

Figure 4.1 The general concept of the silk graft with TCP/PEEK anchor, and the photo of packaged sample ready for animal implantation

Surgical Procedure

An open surgical procedure was used. First a longitudinal, median skin incision was made 5 cm proximal to the superior margin of the patella to the tibia tubercle. The knee joint was accessed with medial parapatellar capsular approach. Then, the joint was positioned to 90° in flexion, and the native ACL was carefully removed at the bone surfaces. A 9.0 mm tunnel was drilled over the footprint of the native ACL, creating a tunnel of 20 mm depth (Figure 4.2A). To avoid damage to the articular cartilage on the medial condyle, the drilling axis was set as 11 o'clock in the transversal plane, and 45° anterior deviation in the sagittal plane using the femoral axes as frame of the reference. A drilling sleeve was developed to prevent slippage and drill wobble, avoiding enlarged tunnel entry and compromised primary stability of the implant. A 7.0 mm tunnel along the same axis was drilled through the tibia with a specially designed synchronizing sleeve (Figure 4.2B). The implant was tapped into the tunnel using a custom insertion tool with a hollow cylindrical cross

section to accommodate the silk graft and secure the PEEK anchor housing. After push-in insertion of the TCP/PEEK scaffold into the femur tunnel, the free distal end of the silk scaffold was drawn through the tibia tunnel with a specially designed retractor (Figure 4.2C). The knee joint was then flexed to 30° before pulling the silk graft tight and fixing with an interference screw (Φ6 × 19 mm, Anklin AG, Switzerland; Figure 4.2D). Upon completion of the graft fixation, the length and cross sectional area of the silk graft was measured and recorded.

Postoperative Treatment

Analgesics (100mg pethidine) were given to each animal twice a day for three days following the surgery. In order to prevent infection, antibiotics (Penicillin of 800'000 U) were given to each animal twice a day until five days after operation. Disinfection solution (0.25% didecyl dimethyl ammonium bromide) was sprayed on the animals and bedding biweekly until the end of the experiment. All pigs were randomly assigned housing in one of three pens (5 × 8 m), and allowed unrestricted daily activity in their pen. Activity level and degree of lameness were monitored.

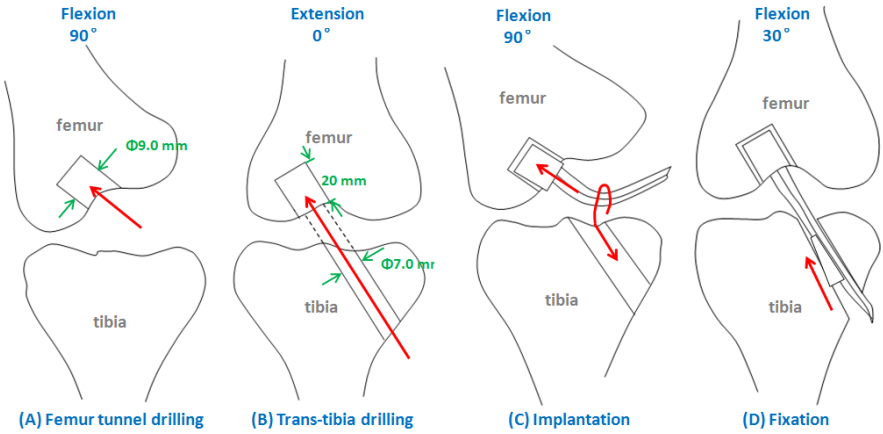

Figure 4.2 Open surgical procedure

As planned, ten pigs were euthanized by lethal injection of thiamylal sodium at a postoperative time point of three months. The remaining four pigs were euthanized at six months. After euthanization both knees were dissected. The samples used for biomechanical test (7 of 10 at three months, 3 of 4 at six months)

were immediately stored at -20 ℃. The remaining samples used for histological observation were cut into small specimens and immediately fixed in a 10% buffered formalin solution. Radiological observation using standard c-arm device was performed on three pigs on the first postoperative day. At each euthanization time point, three additional knees were imaged for qualitative evaluation of TCP degradation and a rough characterization of new bone formation in the femur tunnel.

The lengths and cross sectional areas of the regenerated ACL (left knee) and native ACL (right knee) were measured after removal of surrounding soft tissues. The length was measured three times for each sample using calipers, with the mean value used for statistical analysis. The cross sectional area of the native ACL was calculated as width multiplied by thickness, and the cross sectional area of regenerated ACL was calculated using the diameter. Three different measuring points were chosen, since the cross section was not uniform, and the mean value was adopted for statistical analysis

Biomechanical testing

Samples used for biomechanical testing were thawed overnight at 4 ℃ prior to testing. All surrounding soft tissues on both knees were removed, leaving only the ACL graft (or native ACL in control knees) connecting the tibia and femur (Figure 3). Cross sectional area and length were measured as described above, and recorded. Cyclic loading and tension to failure testing was performed on a universal material testing machine mounted with a 5kN load cell (Sans s-503, MTS Corporation., Minnesota, US). A specially designed clamp was used to fix the femur and tibia, to ensure that the ACL graft was fully aligned with the machine test axis. The tests were applied a pre-conditioned loading of 5 N, and afterwards applied a force-controlled cyclic loading of 0.5 mm/second from 100 to 250 N over 250 cycles, representing the loads of normal walking [116]. Finally, tension to failure was applied to determine the ultimate tensile strength. The force-displacement curves of each cycle were recorded. Dynamic creep of the construct was analysed by calculating the difference in machine displacement after the first cycle and the final cycle. The ultimate tensile strength was determined as the first peak (a more than 50% drop in attained force) in the force displacement curve.

Histological Observation

The samples used for histological observation were fixed in buffered formalin solution for two months. A first group was embedded in resin and specimens were sectioned parallel to the longitudinal axis of the bone tunnel. The section slides were stained with Goldner's trichrome for general assessment of bone, PEEK, newbone, TCP, cartilage, silk graft, and transitional zone. A second group of specimens were decalcified and embedded in paraffin after removal of the PEEK or interference screw, since these materials cannot be sectioned with paraffin embedding. The paraffin embedded sections were stained with Hematoxylin and Eosin, Gomori, and Masson for evaluating the bone, cartilage, graft, transitional zone as well as Sharpey's fibers.

Statistical Analysis

All data were expressed as mean ± standard deviation. Data were compared with a two-tailed student's t-test, and statistically significant values were defined as $p < 0.05$ (significance indicated in all figures using asterisk).

4.3 RESULTS

General observations

After ligament reconstruction all animals were standing upon three legs by the third postoperative day. All animals were walking on four legs with a detectable degree of lameness within 5 to 7 days postoperatively. Activity levels increased gradually after one week, until resumption of normal activity and no discernable lameness by the second postoperative week. At time of euthanization no animal exhibited graft failure or apparent degenerative changes in surrounding tissues of the knee (articular cartilage, menisci, other ligaments). Analysis of blood chemistry indicated no systemic markers of inflammation.

Lateral X-Ray images of the knee joint at three time points indicated progressive resorption of TCP (Figure 4.3). The edge of the bone tunnel was clearly visible in the postoperative X-ray images, as was the TCP within the tunnel. At three months, an observable zone with a gradient of grey scales from TCP to the bone tunnel was present, demarcating regions of new bone formation. At six months, observable

TCP regions were much smaller, but still present. The grey scale intensity of the bone tunnel was higher at six months compared to that at three months, qualitatively indicating increased presence of new bone and increased bone volume.

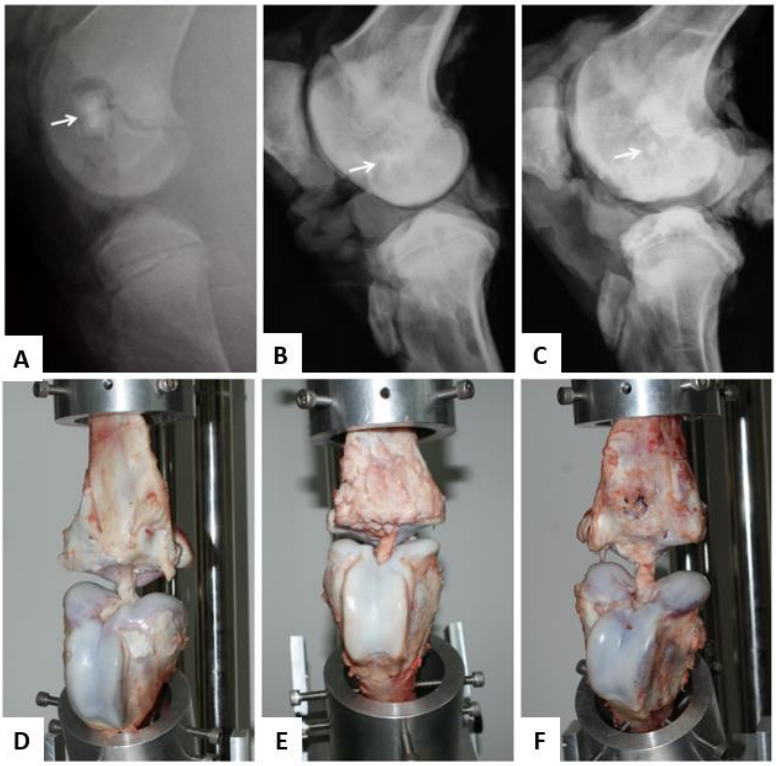

Figure 4.3 X-ray images of the knee with reconstructed ACL, at different postoperative time points.
(A: Day one; B: Three months; C: Six months; D: Native ACL; E: Regenerated ACL at three months; F: Regenerated ACL at six months)

Biomechanical evaluations

The length of silk graft at implantation was 33.6 ± 4.2 mm (n=14). The length of the regenerated ACL was 42.2 ± 3.4 mm at three months (n=7), and 43.3 ± 2.9 mm at six months (n=3). The length of the native ACL was 37.4 ± 3.2 mm at three months

(n=7), and 37.3 ± 2.1 mm at six months (n=3). Comparison of graft length to the contralateral (native) ligament revealed these differences to be non-significant (Figure 4.4A). The cross section area of silk graft at implantation was 30.2 ± 2.3 mm^2 (n=14). The cross section area of the regenerated ACL was 57.5± 8.1 mm^2 at three months (n=7), and 84.6 ± 11.5 mm^2 at six months (n=3). The cross section area of the native ACL was 23.6 ± 4.8 mm^2 at three months (n=7), and 30.3 ± 4.4 mm^2 at six months (n=3). The comparison of the graft cross section areas indicated significant differences between area at time of implantation and then at three months ($p<0.01$), with a further significant increase between three months and six months ($p=0.016$; Figure 4.4B).

Two regenerated ACL specimens sacrificed at 3 months failed prior to onset of cyclic loading (151 N and 184 N). Although the loading mode of these two failed samples were different with other samples, we also included UTS statistical analysis, but excluded for stiffness analysis. The UTS of native ACL was 1384 ± 181 N at three months (n=7), and increased but not significantly ($p=0.14$) to 1749 ± 284 N at six months (n=3), similar to reports in the literature [9]. The UTS of the regenerated ACL was 311 ± 103 N at three months (n=7), and increased significantly ($p<0.01$) to 566 ± 29 N at six months (n=3) (Figure 4.4C). All failures occurred in the midsubstance of the regenerated ACL - with no pullout failures observed at either the femoral tunnel or tibial tunnel. The stiffness was calculated as the slope of the force-displacement curve between 100 N and 250 N of the 250^{th} cycle. The stiffness of native ACL was 192 ± 22 N/mm at three months (n=5), and increased significantly ($p<0.01$) to 259 ± 15 N/mm at six months (n=3). The stiffness of regenerated ACL was 148 ± 19 N at three months (n=5), and increased significantly ($p=0.035$) to 183 ± 10 N at six months (n=3) (Figure 4.4D).

Compared to the graft length at time of implantation, there was a significant increase ($p=0.04$) in length of the regenerated ACL after three months in vivo – an increase in length that was larger than elongation observed after 100’000 cycles of in vitro testing (Figure 4.5A). This parameter reflects any slippage of the anchor or interference screw, and creep in the graft. The graft length at peak load for the regenerated ACL was 14.6 ± 6.5 mm at three months (n=7), and increased but not significantly ($p=0.27$) to 18.1 ± 3.0 mm at six months (n=3), which was ~10% lower than the value of native ACL (~20mm) (Figure 4.5B).

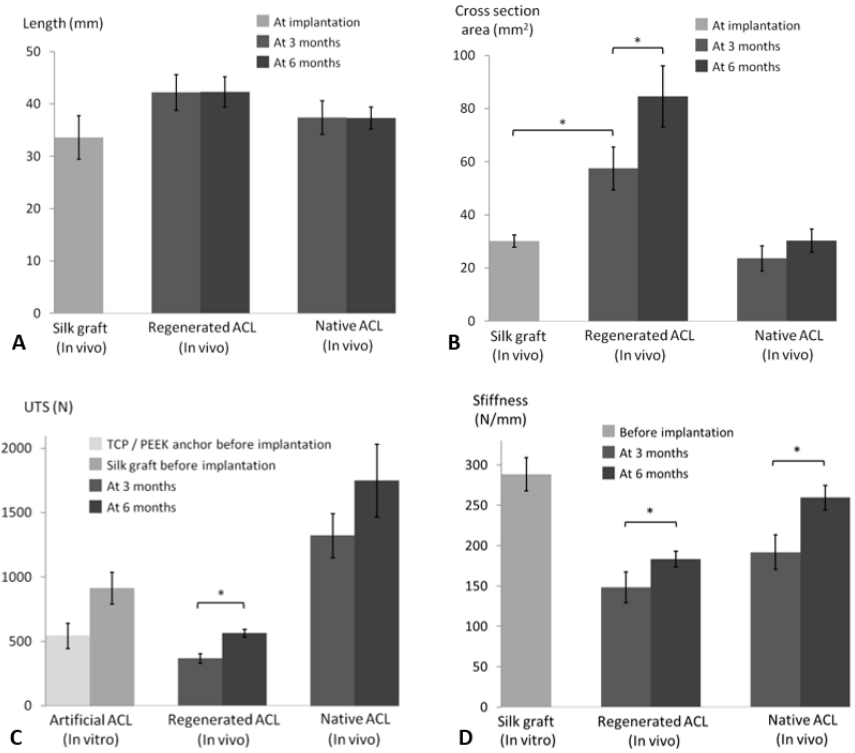

Figure 4.4 Comparison of geometry and mechanical properties of the construct properties at the time of implantation [128], against the regenerated ACL and native ACL at different time points. (* indicates $p<0.05$, Native ACL not used for statistical analysis.); A: Length; B: Cross section area; C: UTS; D: Stiffness

The dynamic creep of native ACL was 0.74 ± 0.21 mm at three months (n=5), and 0.88 ± 0.30 mm at six months (n=3). The dynamic creep of regenerated ACL was 1.48 ± 0.49 mm at three months (n=5), and decreased but not significantly (p=0.145) to 1.07 ± 0.25 mm at six months (n=3). There was a significant decrease (p=0.046) in dynamic creep comparing the TCP/PEEK anchor and the regenerated ACL at 6 months against in vitro data and the regenerated ACL at three months (Figure 4.5C).

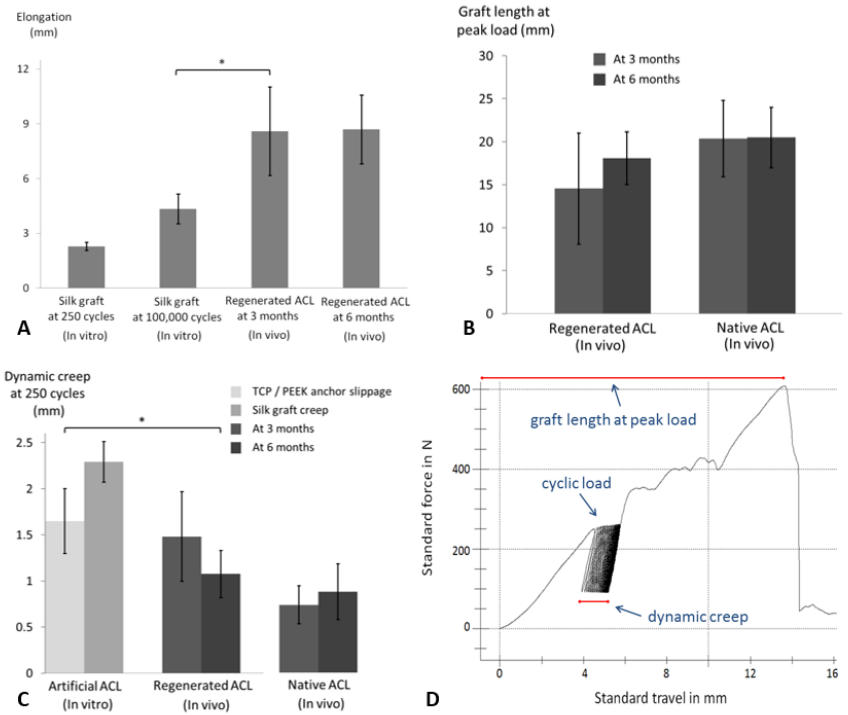

Figure 4.5 Comparison of mechanical properties of silk graft[128], TCP/PEEK anchor, regenerated ACL, native ACL at different time point. ($p<0.05$)
A: Elongation (calculated as the final graft/ligament length minus the length of the silk graft at implantation)
B: Graft length at peak load (calculated with the distance from preload of 5 N to failure point)
C: Dynamic creep (calculated as the shift distance between the first cycle and 250th cycle)
D: Force displacement loading curve (Load to failure distance and dynamic creep indicated in red lines)

Histological observations

Hematoxylin and eosin staining of longitudinal sections (along the axis of the tunnel) and transverse sections (perpendicular to the tunnel) indicated substantial

fibrous tissue formation surrounding the silk fibers, with slightly increased presence at six months (Figure 4.6).

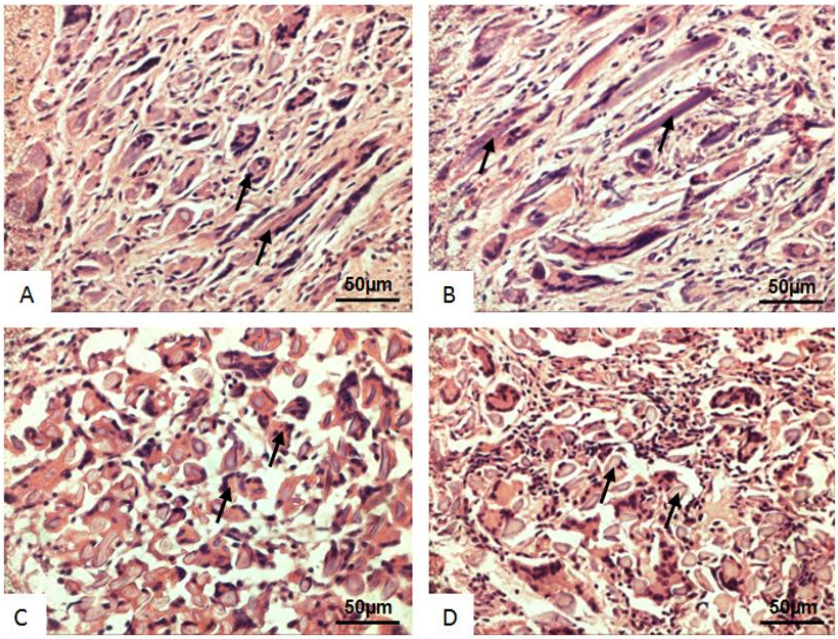

Figure 4.6 Hematoxylin and eosin stain of the silk graft with the regenerated fibro tissues at three months (A,C)and six months(B,D) time point (Black arrows point the silk fiber).
A,B: Longitudinal section; C,D: Transverse section

Goldner's trichrome stain was adopted to observe the regenerated tissue in the bone tunnel[132]. The TCP could still be located at three months, with regenerated new bone tissue observed to surround the TCP (Figure 4.7A). New bone tissue was increasingly present at six months, with fibrocartilage observed to lie between silk fibers and the new bone tissue (Figure 4.7G). The silk to bone transitional area was characterized with Hematoxylin and Eosin stain in terms of silk, fibrous tissue, fibrocartilage, and bone (Figures 4.7C at three months and Figure 4.7I at six months). The regenerated fibrous tissue layer characterized using Masson stain at six months (Figure 4.7K) was nearly twice as thick as that at three months (Figure 4.7F), reflecting the regeneration of fibrous tissue surrounding the silk graft. The

connection of fibrous tissue to bone through a fibrocartilage zone, and Gomori staining revealed interdigitated (Sharpey's) fibers in fibrocartilage zones. Numerous such fibers could be seen both at three months (Figure 4.7E) and six months (Figure 4.7J).

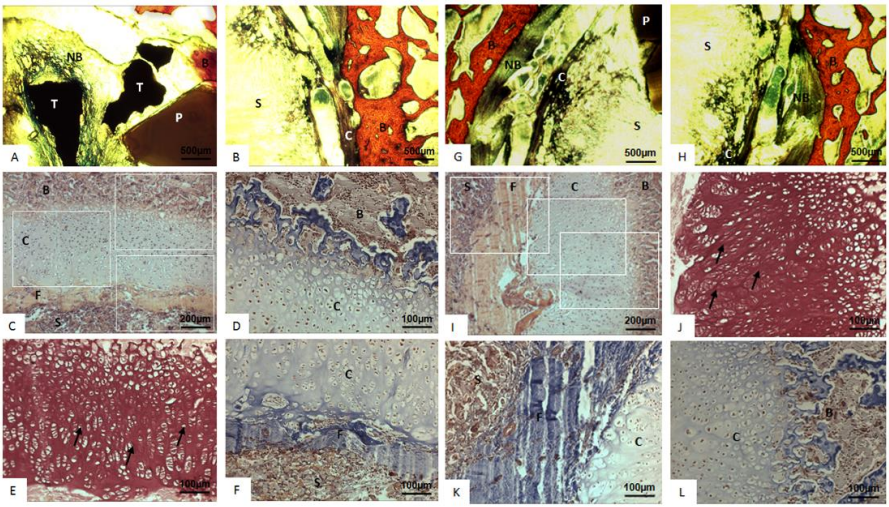

Figure 4.7 Histological images of silk graft to bone transitional zone in the femur tunnel.
(A to F: at three months; G to L: at six months)
(T: TCP ; P: PEEK; B: bone; NB: newbone; C: fibrocartilage; F: fibrous tissue; S: silk)
A,B,G,H: Goldner's trichrome stain (TCP - black; PEEK - brown; bone - red; newbone - green; cartilage - purple; silk - yellow)
C,I: Hematoxylin and Eosin stain (white rectangles are shown in Figure D,E,F,J,K,L)
D,F,K,L: Masson stain
E,J: Gomori stain (Sharpey's fiber pointed with black arrows)

At regions of contact between the silk, interference screw (IS), and bone in the tibial tunnel, cartilaginous tissue was observed at the silk-IS-bone interface at three months (Figure 4.8A). This cartilagenous layer at the silk-IS-bone corner was even more pronounced at six months (Figure 4.8B). However, at the interface of silk to bone the transition was characterized by the presence of silk, fibrous tissue, and

bone tissue only, with no cartilaginous layer observable at three months (Figure 4.8C) or six months (Figure 4.8D,E). There were only a few cases showing a thin, non-continuous layer of fibrocartilage at six months (Figure 4.8F). Comparison between the tibial and femoral tunnels revealed a relative absence of new bone formation in the tibial tunnel, with a corresponding lack of a cartilagenous silk to bone transition in the tibia tunnel.

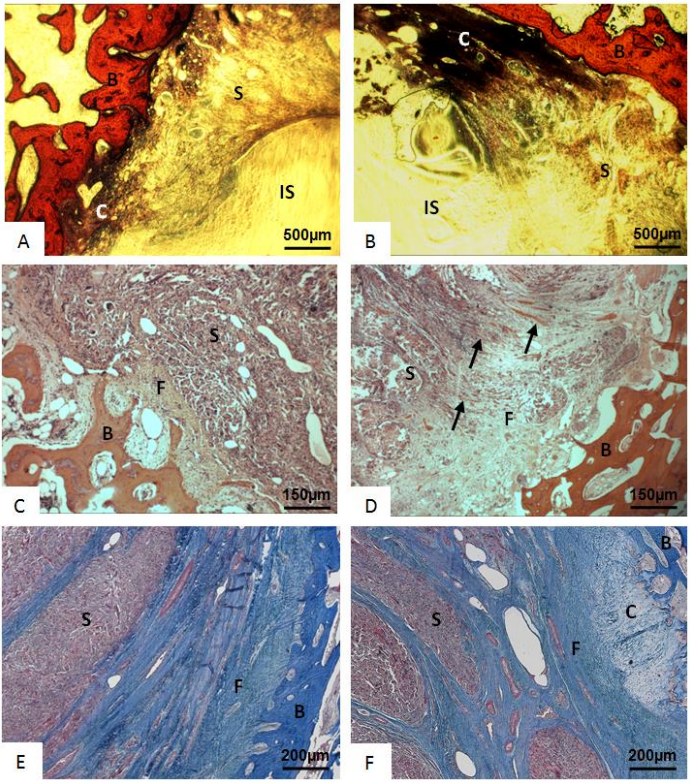

Figure 4.8 Histological images of silk graft to bone transitional zone in the tibia tunnel.

(A,C: three months; B,D,E,F: six months)

(IS: interference screw; B: bone; C: fibrocartilage; F: fibrous tissue; S: silk)

A,B: Goldner's trichrome stain

C,D: Hematoxylin and Eosin stain

E,F: Masson stain

4.4 DISCUSSIONS

The so-called 'Gold Standard' graft choice for torn ACL reconstruction is a bone-patellar tendon-bone autograft (BPTB). Except for donor site morbidity, BPTB reconstructions have consistently yielded favorable clinical outcomes with a 90-95% success rate in terms of a return to pre-injury activity level [81]. We have designed and developed a synthetic alternative to a BPTB autograft with analogous structural, biological, and mechanical properties. The present study tested the efficacy of this concept in a large animal model.

Because of a uniquely advantageous combination of biocompatibility and robust biomechanical strength in the short- and middle-term, sericin extracted silk fibers were adopted as the ligament graft in the device, implemented with a wired architecture that provides mechanical behaviour similar to the the human ACL [128, 133]. To stimulate integration of the silk within the bone tunnel, we employed a porous TCP scaffold – a well characterized and FDA approved osteoinductive biomaterial. To overcome the notorious fragility of porous TCP scaffold we introduced a PEEK anchor housing to provide initial fixation stability. The present study examined both the overall functional (biomechanical) performance of the assembled construct, as well as the host-implant integration at the various biomaterial-tissue interfaces.

Functional Outcome

From a functional standpoint, this efficacy study focused on the mechanical strength and stiffness of the regenerated ACL. The UTS of the regenerated ACL increased by ~82% (Figure 4C) from three months to six months. Although the absolute strength of the graft was still far from that of the native ACL, these values fall safely below typical maximal ACL loads associated with normal daily activity (~250 N; [116]). The UTS values we recorded at 3 months compare favorably with other ACL reconstruction studies using porcine models with sacrifice after three months [134, 135], although UTS values we recorded at 6 months were approximately 40% lower than another study with a similar time course [136]. Also as in previous studies, failures almost nearly occurred in the midsubstance of the reconstructed ACL, with no incidence of tunnel pullout failure. It should be noted that graft elongation at failure typically exceeded 15 mm (Figure 5B), a distance at

which recruitment of other stabilizing structures (muscles, other ligaments) would reasonably be expected to prevent graft failure.

Graft slippage and elongation also play a critical role in functional performance, as these aspects are closely related to loss of graft tension and relative joint laxity. The elongation of the regenerated ACL compared to graft length at implantation was ~8.6 mm for both three months and six months (Figure 5A), although interpreting these values is difficult in view of the fact that the animals were growing over the course of the experiment. More conclusively, elongation of silk graft during cyclic load (dynamic creep) of the regenerated ACL decreased by ~38% from three months to six months, indicating that the graft become less viscoelastic in this timeframe. Still, because any measure of graft elongation includes effects from both the femoral side (silk/TCP/PEEK) and the tibial side (silk-IS), it was not possible to assess the relative contribution of either side to the overall function. Nonetheless when compared to in vitro biomechanical test data, dynamic creep of the regenerated ACL was ~35% lower after 6 months than the original graft (Figure 5C), clearly indicating that the implant became more elastic (less viscoelastic) over the course of healing – and was comparable to the native ACL.

Histological assessment

Silk-based scaffolds have been increasingly investigated as a potential graft material for tendon and ligament regeneration [52, 73, 77, 79, 112, 137, 138]. This owes in part to the advantageous biological properties of silk as well as robust biomechanical strength in the short- and middle-term. After three months of postoperative healing, we observed that the silk scaffolds remained largely intact but were intermixed with regenerated fibrous tissue, the cells of which were well aligned with and often attached to the silk fibers (Figure 6A,C). After six months the regenerated fibrous tissue that was intermixed with silk fibers appeared to be increased, although not substantially (Figure 6B,D). The silk graft remained around 70% intact even at six months, reflecting the characteristically slow degradation of silk, which enables the biomaterial scaffold to continue supporting functional demands of the ligament until the host tissues eventually overtake these loads. These findings are consistent with extensive studies by others using silk grafts for ACL reconstruction [56, 57, 108, 109, 129, 130]. The fibrous tissues covered around the silk graft were disorganized and can be regarded as some kind of scar tissue.

There were plenty of blood vessels in the scar tissue (pink color in Figure 3E, 3F), which made it grown thicker over the regenerating process. The cross sectional area of regenerated ACL at six months was ~47% larger than that at three months (Figure 4B), which was mainly attributed by the growth of scar tissue. This scar tissue blocked the interstitial fluid to go deeper into the silk graft, which is the essential factor for silk degradation process. This is the reason that the degradation speed of silk graft was slower over the regenerating process.

The present study differentiates itself from previous studies, in its use of a porous TCP scaffold (mimicking a bone block) combined with a PEEK anchor. From histological observation, we found that the porous TCP scaffold substantially increased silk graft to bone attachment. There was a clear tendency toward new bone formation in the femur tunnel in contrast to the tibial tunnel which lacked presence of TCP (Figure 7). At three months the TCP scaffold could still be seen clearly, while at six months considerable less TCP material could be identified, comparable to degradation rates reported in the literature[139]. Over the course of TCP remodeling, the enlaced silk graft was apparently incorporated within the tunnel leading to accelerated biological fixation by three months and robust incorporation to the tunnel by six months. In contrast, there was little new bone tissue formation observed in the tibial tunnel, particularly at the margins of the silk graft pressed against one side of the tunnel by the interference screw. Lacking a histological transition from the silk to the host bone, it would appear that silk graft fixation would remain dependent on mechanical purchase of the screw (Figure 8A,B) and could thus remain susceptible to subsequent loosening.

In femur tunnel we conclude that the presence of TCP provoked formation of tissue transitions from silk, into regenerated fibrous tissue, into regenerated fibrocartilage, and eventually into bone (Figure 7C,I). These transitions reflect those present in the attachment of the native ACL to bone - a highly specialized tissue transition that effectively transmits forces from soft to hard tissues. The histological examination of the implanted constructs exhibited such regions already at three months (Figure 7F) and becoming further pronounced at six months (Figure 7K). Interestingly, numerous interdigitated (Sharpey's) fibers were observed to project from regenerated fibrous tissue into newly generated bone tissue through similarly generated fibrocartilage (Figure 7E,J). Thus a relatively biomimetic attachment of the silk graft to the femoral bone tunnel was achieved. In contrast, the tibial tunnel

showed comparatively no fibrocartilage layer at the silk graft to bone interface (Figure 8C,D). While we attribute this to the absence of TCP, other factors could potentially have played a role – for instance the relative mechanical stability of the different anchoring systems applied to each tunnel.

Limitations

The main limitations of the study regard the use of young pigs (similar to a Yorkshire breed) that grew considerably over the course of the study. The surgery was performed at four months of age, corresponding to adolescence. These animals grow approximately 3kg/week until seven months of age and then ~2kg/week until ten months of age. Taking this into consideration, results of the present study should be considered in relative terms, particularly with regard to the substantial regenerating capacity of adolescent mammals compared to adults. Another limitation imposed by the animal model was the inability to perform functional clinical joint tests (such as the drawer test, or Lachman test), which in man represent important criteria for postoperative evaluation of ACL reconstruction. More detailed evaluation in other animal models represents the next step of our research.

4.5 CONCLUSION

A silk.-based artificial ACL graft combined with a TCP/PEEK anchor was tested and evaluated in a porcine model of ACL reconstruction, and evaluated at three and six months. A series of biomechanical tests were performed, and a detailed histological analysis was made. We found that incorporation of the silk graft to bone was markedly enhanced in tunnels augmented with a TCP block enlaced to the end of the silk graft. Histological transitions from the silk graft to bone were similar with features of native ACL to bone attachment. We conclude that the concept of a TCP/PEEK anchored silk graft performs well as a synthetic alternative to autograft. This study provides a basis for eventual safety and efficacy testing in man.

Acknowledgrement

The authors wish to thank Trudel Limited (Zurich, Switzerland) for providing raw silk for our research. We also thank Mr. Hansruedi Sommer, Mr. Wenyou Zhang, Dr. med. Arnd Viehöfer, Prof. Dr. Marc Bohner, and Dr. Xiaojun Wang for their

expertise and kind help in the experiments. This study was partly funded by the National Natural Science Foundation of China (No.51105298), Program of Leading Talent in Changshu of China, and the Bonizzi Theler Foundation.

CHAPTER V

Detailed design parameters

Device for fixation of a flexible element, particularly a natural or synthetical ligament or tendon, to a bone

Applicant: **University of Zurich**

Inventors: **Jess Snedeker[1,2], Xiang Li[1,2], Hansruedi Sommer[2]**

[1]Department Health Sciences and Technology, ETH Zurich, Switzerland
[2]Department of Orthopaedics, University of Zurich, Switzerland

Abstract

The invention relates to a device (1) for fixing a flexible element (10), particularly in the form of an artificial or natural ligament or a tendon, to a bone (20), comprising: an insert (100) being designed to hold said flexible element (10), and an anchor (200), wherein the insert (100) is designed to be inserted into said anchor (200), and wherein the anchor element (200) is designed to be inserted into a bore hole (2) of said bone (20) together with said insert (100) inserted into the anchor (200) to fix the flexible element (10) to the bone (20).

5.1 SPECIFICATION

The invention relates to a device for fixing a flexible element, particularly in the form of an artificial or natural ligament or an artificial or natural tendon, to a bone, preferably to a human bone.

Due to anatomical locations, such flexible elements, like the anterior cruciate ligament (ACL) for instance, are subjected to bear tremendous forces during sports and other daily activities. The ACL rupture is regarded as the most frequent and severe ligament injury[1]. It has been estimated that there are around 250,000 (or 1 in 3,000 in the general population) patients per year diagnosed with ACL disruption in the United States, with approximately 75,000 performed surgical reconstructions annually[2, 3, 57, 100]. In Switzerland, there are around 5,000 ACL reconstructions each year. Although many surgical options for ACL reconstruction, including autografts, allografts, xenografts, or synthetic grafts, have been practiced for the restoration of knee joint stability, several unavoidable drawbacks exist, such as donor site morbidity[101, 102], disease transmission[39], immune response[40, 41], ligament laxity[103], mechanical mismatch, and so on[52, 104]. Therefore, more optimal reconstructive techniques for ACL repair are required and should be developed. The rapid development of tissue engineering technique offers a promising approach of regenerating functional tissues to treat ACL injuries[51, 55, 57, 66, 81, 105, 140].

It is regarded that biomaterial scaffolds are a key factor in tissue engineering. An ideal ACL replacement scaffold should be biodegradable, biocompatible, with suitable porosity for the cell ingrowth, and sufficient mechanical stability[51, 52]. Silkworm silk fibroin, a natural biopolymer usable after removal of the hyper-allergenic sericin component from raw silk[63, 64], has been used as clinical suture material for centuries[65]. Silk fibroin provides an excellent combination of outstanding and customizable mechanical properties (up to 4.8 GPa), remarkable toughness and elasticity (up to 35%), and environmental stability [56, 66, 67]. As a structural template, silk fibroin has been shown to bear equivalence to collagen in supporting cell attachment, inducing appropriate morphology and cell growth[68, 69], with a degradation rate that involves a gradual loss of tensile strength over 1 year in vivo[56, 57]. Thus, because of good biocompatibility, biomechanical properties, and optimal degradation rates for replacement of load bearing tissues,

silk fibroin has been increasingly investigated as a potential ligament or tendon graft in recent decades[50, 55, 58, 60-62]. A number of researchers have been working on silk based ACL scaffold. Horan and Altman et al. did a study on the architectures of silk matrix and determined the cabled structure would be optimal for ligament reconstruction[108]. A series of additional studies have been performed on hierarchical organization of silk matrix, and a 6-cord wire-rope silk fiber matrix is suggested for ligament regeneration[56, 57, 109]. Many in vitro studies have been performed on silk based scaffold for ligament tissue engineering, to evaluate the effect of surface treatment, biological factors, or cell types on the biological and mechanical behavior for tendon or ligament scaffold[51, 52, 64, 66, 70-73]. There are also quite a few studies that have tested the silk based ligament scaffold in the animals. Rabbits, goats and pigs are frequently used animal models for evaluation of in vivo response of silk based ligament scaffolds[51, 77, 130, 141]. For a silk based ACL scaffold named SeriACL a human clinical trial has been conducted in Europe to assess the safety and efficiency for a completely ruptured ACL reconstruction[83]. Thus many promising developments have been achieved for silk based ligament scaffold in previous studies, bringing silk based tissue engineered ACL much closer to widespread clinical application[84, 85].

However, most of the previous studies on ACL scaffolds have only focused on the scaffold itself, largely ignoring he critical the connection site of the ACL scaffold to the bone tunnel, which is very important for successful ACL repair. Since it is similar to hamstring autograft reconstruction, the scaffold to bone integration is almost always poor. Bone tunnel expansion can occur, predisposing the scaffold to pullout. To avoid bone tunnel expansion and achieve effective attachment of ACL scaffold into the bone tunnel, sufficient surface contact between scaffold and bone, and suitable biomechanical stimulation are essential for scaffold to bone attachment. Although some fixation methods, such as interference screws, can be adopted to anchor the ACL scaffold into bone tunnel, these methods impose a decidedly non-physiological barrier to healing.

Many approaches have been tried by biomaterial engineers and orthopaedic surgeons to achieve a better biological attachment. The major concern is to provide appropriate cellular cues that result in an effective healing response between e.g. tendon and bone. Due to good properties regarding osteoconductivity and bioresorption, bone cements, such as brushite calcium phosphate cement (CPC)

and injectable tricalcium phosphate (TCP), can augment the peri-tendon bone volume and promote bone ingrowth into the healing interface and significantly enhance the tendon-bone integration after tendon or ligament reconstruction[90, 91]. Cell based therapies have also been employed. Since a sufficient amount of stem cells is probably necessary for optimal tissue regeneration, mesenchymal stem cells (MSCs) have been applied as potential agents to enhance tendon healing into the bone tunnel. MSCs coated scaffolds have been reported to develop an interpositional zone of fibrocartilage between tendon and bone during tendon reconstruction, had high quality of osteointegration and perform significantly well on biomechanical testing[88, 89]. Bioactive factors represent another potentially powerful means of promoting tendon to bone healing. The highly osteoinductive properties of bone morphogenetic proteins (BMPs) are now widely recognized, and implemented within daily clinical practice. Endogenous BMP-2 and BMP-7 participate in tendon to bone healing and their functions involve downstream signal transduction mediators. The BMP-2 can enhance bone ingrowth and accelerate the healing process when a tendon scaffold is transplanted into a bone tunnel[96, 142].

But nearly all pre-clinical studies listed above have focused primarily on cell biology aspects (cell sources or osteoinductive/conductive agents) that can applied at the tendon/scaffold to bone interface, and neglect implications of primary mechanical stability. They hope that cells in the bone tunnel might recognize the tendon/scaffold surface as a potentially osteoconductive matrix, promoting rapid bone ingrowth that quickly provides secondary mechanical stability through an improved attachment of tendon to bone.

Few researchers have focused on how an osteoconductive/inductive construct might be used to achieve superior biological healing and secondary stability while also providing adequate primary mechanical stability.

Therefore, the problem motivating the present invention is to provide for a device for fixing a flexible element such as a synthetic or natural ligament or tendon to a bone that is improved concerning mechanical stability and particularly allows for an efficient biological healing at the same time.

This problem is solved by a device having the features of claim 1.

According thereto, the device for fixing a flexible element, particularly in the form of an artificial or natural ligament or a tendon, to a bone, comprises: an insert being designed to hold said flexible element, wherein particularly the flexible element contacts the insert, and an anchor, wherein the insert is designed to be inserted into said anchor, and wherein the anchor is designed to be inserted into a bore hole of said bone together with said insert inserted into the anchor, in order to fix the flexible element to the bone.

Preferably, the insert is formed out of an osteoconductive and/or osteoinductive material or comprises an osteoconductive and/or osteoinductive material.

In this regard, an osteoconductive material is material that is designed to serve as a scaffold or guide for the reparative growth of bone tissue. Osteoblasts from the margin of the bone bore hole utilize such a material as a framework upon which to appropriately spread, migrate, proliferate, and ultimately generate new bone. In this sense an osteoconductive material may be regarded as a “bone compatible” material.Further, an osteoinductive material is a material that is designed to stimulate osteoprogenitor cells to preferentially differentiate into osteoblasts that then begin new bone formation. An example for such osteoinductive cell mediators are bone morphogenetic proteins (BMPs), and tri-calcium phosphate bearing biomaterials. Thus, an insert that is osteoconductive and osteoinductive will not only serve as a scaffold for currently existing osteoblasts but will also trigger the formation of new osteoblasts, and thus allows for faster integration of the insert into the bone.

The described invention allows one to adequately provide for robust initial mechanical stability due to the anchor, while at the same time promoting contact between the insert/flexible element and the walls of the bore hole or bone tunnel can be established that promotes the afore-mentioned biological healing, e.g. ingrowth of the bone into the insert.

According to an embodiment of the invention, the anchor is designed to be inserted into said bore hole (also denoted as bone tunnel) of the bone along an insertion direction together with said insert inserted into the anchor, wherein the insert is preferably designed to be inserted into the anchor counter to said insertion direction.

According to an embodiment of the invention, the anchor comprises a head part and a first and a second leg facing each other, wherein said legs preferably protrude from said head part along the insertion direction. Particularly, the legs are integrally formed with the head part. Further, the anchor is designed to be inserted into the bore hole of the bone with the legs ahead so that the head part is particularly flush with the surface region of the bone around the bore hole.

In an embodiment of the invention, particularly for the use with synthetical flexible elements (e.g. ligaments or tendons, particularly ACL scaffolds), the head part comprises an annular shape, wherein particularly the head part comprises a central opening designed for passing through said flexible element.

In an alternative embodiment, particularly for the use with natural flexible elements (e.g. ligaments or tendons, particularly autografts), the head part comprises two opposing cut-outs designed for receiving/bypassing the flexible element, wherein each cut-out is formed in a boundary region of the head part extending from one leg to the other.

According to a further aspect of the invention, the insert is preferably arranged between the legs of the anchor when the insert is inserted into the anchor as intended.

For proper insertion of the insert into the anchor, the insert preferably comprises a first and a second guiding recess according to a further embodiment of the invention, wherein these recesses are preferably designed to receive the legs of the anchor in a form fitting manner when the insert is inserted into the anchor.

Preferably, each guiding recess is delimited by a surface of the insert forming the bottom of the respective guiding recess, wherein the two surfaces face away from each other, and two opposing boundary regions protruding from the respective surface and extending along the insertion direction forming the side walls of the respective guiding recess. In a variant of the invention, the two surfaces are convex, i.e. bulged towards the respective leg that slides along the surface of the associated guiding recess upon insertion of the insert into the anchor.

Further, each of said boundary regions preferably comprises a contact surface being designed to contact the bone when the anchor is inserted into the bore hole

of the bone together with the insert as intended, which contact surface extends along the respective guiding recess. In this way, bone cell ingrowth into the insert around which the flexible element is laid is achieved that finally results in a bone firmly holding the flexible element. Further, also the anchor comprises an outside for contacting the bone, wherein preferably said outside comprises a toothed surface in order to increase friction between the outside of the anchor and the walls of the bore hole. Particularly, the contact surfaces of the boundary regions of the insert are essentially flush with said outside of the anchor when the insert is inserted into the anchor as intended. Hence, while the outside of the anchor serves for mechanical stability right from the start, the contact surfaces of the insert are designed to promote biological healing and thus provide additional stability in the long term.

To further increase mechanical stability, the insert is at least in sections tapered in a variant of the invention, so that upon inserting the insert into the anchor, said surfaces of the insert press the legs away from each other, wherein particularly the anchor is designed to be inserted into the borehole in the insertion direction with the insert being inserted into the anchor in a first position, in which the insert is not fully inserted into the anchor, wherein the insert is designed to be pulled into a second position counter to the insertion direction when the anchor is inserted into the bore hole of the bone as intended, in which second position the insert is fully inserted into the anchor and thus presses the legs against the wall of the bore hole.

According to a further aspect of the invention, the legs preferably comprise an inner surface, wherein the two inner surfaces face each other, and wherein particularly said inner surfaces are concave so as to match with the surface of the respective guiding recess, i.e., each inner surface is preferably designed to slide along the surface of the respective guiding recess when inserting the insert into the anchor, and to rest on the associated surface of the insert thereafter. Further, each leg preferably comprises two lateral surfaces coming off the respective inner surface, wherein particularly the lateral surfaces of a leg face away from each other, and wherein particularly each lateral surface rests on an associated boundary region, when the insert is inserted into the anchor as intended. Further, each lateral surface preferably encloses an angle of particularly 45° with an extension plane along which the respective leg extends.

Particularly, according to a further aspect of the invention, the insert comprises a first wall region and a second wall region, wherein particularly the first guiding recess is formed in the first wall region, and wherein particularly the second guiding recess is formed in the second wall region. Preferably, the two wall regions are integrally connected by a connecting region of the insert, which connecting region preferably comprises a concave surface.

Further, for receiving the flexible element, the insert preferably comprises a groove or an open channel, wherein particularly said groove is formed by the two wall parts and the connecting region. The groove is preferably formed such that the flexible element can be laid around the connecting region and is then arranged at least in sections in said groove tightly contacting the insert.

In case the head part of the anchor comprises an annular shape with a central opening, the flexible element passes through the opening of the head when the insert is inserted into the anchor as intended and when the flexible element is arranged with respect to anchor and insert as intended.

Alternatively, in case the head comprises said two opposing cut-outs, the flexible element preferably extends through the cut-outs of the head when the insert is inserted into the anchor as intended and the flexible element is arranged with respect to anchor and insert as intended.

As mentioned before, the flexible element may be a natural ligament or a natural tendon.

Particularly, the flexible element is a synthetic ligament or tendon, particularly an anterior cruciate ligament (ACL) scaffold.

According to a further embodiment of the present invention, such a flexible element comprises two twisted cords, wherein particularly the cords have a turn every 12mm. Further each cord comprises 144 twisted yarns, wherein particularly the yarns have a turn every 10mm. Each yarn comprises two twisted bundles, wherein particularly each bundle has a turn every 2mm. Finally, each bundle comprises 6 fibres, which fibres preferably comprise fibroin, e.g. silk.

According to a further alternative embodiment of the present invention, the flexible element comprises three braided cords, wherein particularly the cords have a turn every 12mm. Further, each cord comprises 96 twisted yarns, wherein particularly the yarns have a turn every 10mm. Each yarn comprises two twisted bundles, wherein particularly each bundle has a turn every 2mm. Finally, each bundle comprises again 6 fibres, which fibres preferably comprise fibroin, e.g. silk.

According to a further embodiment of the present invention, the insert comprises one of the following substances: tricalcium phosphate, hydroxylapatite, calcium phosphate, particularly as a component of a of bone cement, calcium silicate, particularly as a component of a bone cement, or silicate-substituted calcium phosphate or other osteoinductive/osteoconductive bioceramics/bioglasses.

Further, according to yet another embodiment of the present invention, the anchor comprises one of the following substances: polyether ether ketone, poly lactic acid, poly lactic-co-glycolic acid, poly-ε-caprolactone, titanium-based alloy, or magnesium-based alloy. The anchor may also comprise or may be formed out of another biopolymer or implantable metal.

According to another aspect of the present invention, a tool set is provided for inserting a device according to the invention into a bore hole or bone tunnel.

According to claim 28 such a tool set comprises at least a first tool for pressing the device into said bore hole, wherein said first tool comprises an elongated shaft having a free end that is designed to engage with the anchor, particularly with the head part of the anchor, for pressing the device into said bore hole or bone tunnel, wherein said elongated shaft further comprises a groove for receiving the flexible element extending from the anchor/insert upon insertion of the device into the bore hole of the bone.

In a variant of the invention, the first tool comprises at its first end a plurality of protrusions (particularly three protrusions) that are designed to engage with corresponding recesses formed in the head part of the anchor, particularly in a periphery of the opening of the annular head part.

In a further variant of the first tool the free end is shaped hollow cylindrical and comprises a discontinuation extending along the longitudinal axis of the shaft

corresponding to said groove of the shaft. Wherein the shaft preferably comprises a step at the free end such that the free end has a reduced outer diameter compared to the remaining shaft, wherein the cylindrical free end is designed to engage in a form fitting manner with said opening of the annular head part of the anchor for pressing the anchor into the bore hole of the bone.

Further, the tool set may comprise a second tool comprising a handle and a drill sleeve protruding from a free end of the handle for guiding a drill for drilling said bore hole into the bone, wherein a free end of the drill sleeve may be tapered or sharpened for assuring a good grip on the bone while pressing the free end of the drill sleeve against the bone.

Further, the tool set may comprise a third tool for positioning the second tool, wherein the third tool comprises a first leg extending along an extension direction, as well as a second and a third leg extending from opposite ends of the first leg so that particularly a u-shaped or arc-shaped body of the third tool is formed, wherein a plug protrudes from a free end of the second leg along the extension direction for insertion into the bore hole of the bone (e.g. into the distal femur in case the flexible element replaces the anterior cruciate ligament, for instance). Further, the third leg opposing the second leg preferably comprises a through-opening aligned with said plug, so that when the plug is inserted into the bore hole of the bone (e.g. distal femur), the second tool can be inserted with its drill sleeve into the through-opening of the third leg, so that a bore hole (e.g. tunnel) can be drilled into another bone (e.g. the tibia in case the flexible element replaces the anterior cruciate ligament for instance) in axial alignment with the bore hole of said bone (e.g. distal femur). Then, the free end of the flexible element distal to the anchor/insert can be passed through said bore hole or tunnel of the further bone (e.g. tibia) and fixed to said further bone, for instance by means of an interference screw.

Finally, another aspect of the present invention is to provide for a method for inserting a device according to the invention into a bore hole of a bone, particularly using said tool set, wherein the method comprises the steps of drilling a bore hole into a bone, particularly into the distal femur, and pressing the anchor with inserted insert with the legs of the anchor ahead into said bore hole in an insertion direction, wherein particularly the insert is fully inserted into the anchor upon inserting the anchor into the bore hole or wherein particularly the insert is inserted into the

anchor in a first position, in which the insert is not fully inserted into the anchor, wherein, when the anchor is inserted into the bore hole of the bone as intended, the insert is pulled into a second position counter to the insertion direction by means of the flexible element, in which second position the insert is more or fully inserted into the anchor and the legs of the anchor are pressed against a wall of the bore hole of the bone by means of the insert.

According to a further aspect of this method, before drilling said bore hole, a small lateral incision is made to put an endoscope into the knee joint.

According to a further aspect of the method, a trans-tibial bone tunnel is then drilled, as well as said bore hole in the distal femur, wherein particularly said bone tunnel and said bore hole have a diameter of 4 to 8 mm, and wherein particularly said bore hole has a depth of 15 to 30 mm (typically 7mm), wherein said bone tunnel and said bore hole are particularly drilled such that said bone tunnel is aligned with said bore hole.

According to a further aspect of the method, the knee is then bent, and a medial incision is made.

According to a further aspect of the method, said bore hole is then enlarged to 7 to 12 mm (typically 9mm) diameter, particularly through said medial incision.

According to a further aspect of the method, the insert is then inserted (e.g. as described above) into said bore hole, particularly by means of the first tool, through the medial incision.

According to a further aspect of the method, a free end of the flexible element is then pulled through the trans-tibial bone tunnel.

According to a yet further aspect of the method, the flexible element is then pulled tight, wherein the tension is particularly adjusted by the surgeon, and fixed with a fixing element, particularly with an interference screw (Φ6 × 19 mm), to the tibia, wherein said fixing element is particularly screwed into the trans-tibial bone tunnel.In the following, an alternative variant of the method is described.

According to an aspect of this alternative method, a longitudinal medial skin incision is made, particularly 5 cm proximal to the superior margin of the patella to the tibial tubercle.

According to a further aspect of the alternative method, the knee joint is then accessed with a medial parapatellar capsular approach.

According to a further aspect of the alternative method, the native ACL is cut and removed.

According to a further aspect of the alternative method, said bore hole, particularly of diameter 9 mm, is then drilled over the footprint of ACL in the femur, particularly 20 mm in depth.

According to a further aspect of the alternative method, particularly to avoid damage to the articular cartilage on the medial condyle, the drilling direction is adjusted to 11 o'clock on the transversal plane, and 45° anterior deviation on the sagittal plane using the femoral axes as frame of reference.

According to a further aspect of the alternative method, the second tool is used to guide the drill used for drilling said bore hole, particularly so as prevent slipping and/or wobbling of said drill.

According to a further aspect of the alternative method, a trans-tibial bone tunnel, particularly 7.0 mm in diameter, is then drilled along the axis of said bore hole in the distal femur, wherein particularly the third tool is used to guide the drill used for drilling said further tunnel into the tibia.

According to a further aspect of the alternative method, the insert is inserted (e.g. as described above) into said bore hole, particularly by means of the first tool.

According to a further aspect of the alternative method, a free end of the flexible element is then pulled through the trans-tibial bone tunnel.

According to a further aspect of the alternative method, the knee joint is then flexed to 150°.

According to a yet further aspect of the alternative method, the flexible element is then pulled tight, wherein the tension is particularly adjusted by the surgeon, and fixed with a fixing element, particularly with an interference screw (Φ6 × 19 mm), to the tibia, wherein said fixing element is particularly screwed into the trans-tibial bone tunnel.

5.2 DESCRIPTION

Further features and advantages of the invention shall be described by means of detailed descriptions of embodiments with reference to the Figures.

Figure 5.1 shows a device 1 according to the invention for fixation of a flexible element 10 to a particularly human bone 20, e.g. distal femur in case the flexible element 10 is used for ACL reconstruction. The device 1 according to the invention comprises an insert 100 for holding the flexible element 10, which is particularly looped around the insert 100 as well as an anchor 200 into which said insert 100 is inserted. When inserted into a bore hole 2 of said bone 20, the anchor 200 contacts the walls of the bore hole 2 with its toothed outside 200a. At the same time the insert 100 is inserted such into the anchor 200 that also contact surfaces 112a, 113a, 122a, 123a of the insert 100 (cf. also Figure 5.6 and 5.7) contact the walls of the bore hole 2.

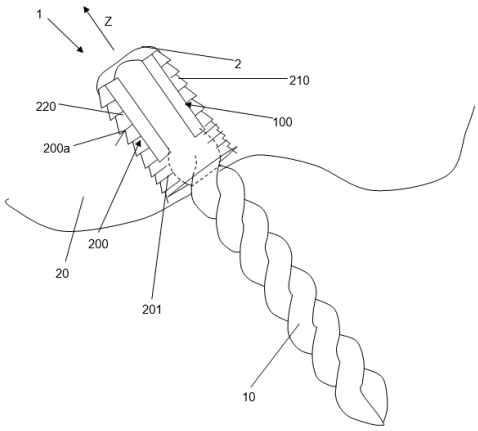

Figure 5.1 a schematical, partly cross sectional view of a device according to the invention inserted into a bore hole in a bone.

Preferably, the anchor 200 is made out of or comprises polyether ether ketone (PEEK) whereas the insert 100 preferably contains tricalcium phosphate (TCP). While the anchor 200 serves to provide adequate mechanical fixation the beginning and thus good initial stability, the TCP insert 100 that holds the flexible element 10 is designed to promote bone cell ingrowth into the porous TCP scaffold, so that the flexible element, which may be a silk ACL scaffold or tendon autograft, see below, will be hold by the TCP/bone interface within the bore hole 2 of the bone 20. In the long-term, the TCP scaffold provided by insert 100 will be fully regenerated with the new born bone, and the flexible element 10 (e.g. silk ACL scaffold or tendon autograft) will be attached onto the native bone tissue firmly. The biological fixation will be finally achieved.

Figure 5.2 to 5.7 show the components of a device according to the invention that is preferably used for a fixation of a synthetical flexible element 10 such as an ACL scaffold shown in Figure 5.12 and 5.13. As shown in Figure 5.2 to 5.5, the anchor 200 of the device 1 comprises a head part 201 having an annular shape and delimiting an opening for passing through the flexible element 10 as shown in Figure 5.1.

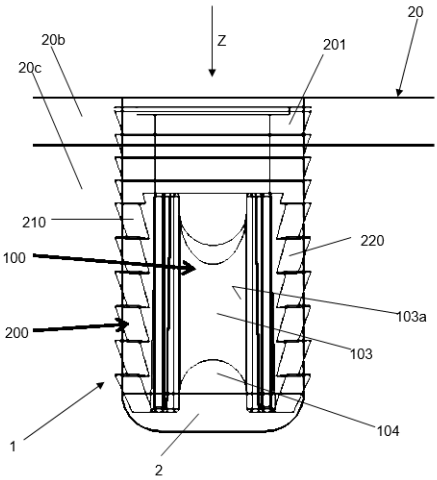

Figure 5.2 a lateral view of an anchor and an insert of the device according to the invention inserted into a bore hole of a bone for use with a synthetical flexible element (for instance ACL scaffold)

The anchor 200 further comprises two legs 210, 220 protruding from the head part 201 along an insertion direction Z along which the anchor 200 and inserted insert 100 is inserted into the bore hole 2 with the legs 210, 200 of the anchor 200 ahead. The legs 210, 220 each comprise a concave inner surface 210a, 220a, which concave inner surfaces 210a, 220a face each other. Further, each leg 210, 220 comprises two lateral surfaces 210b, 220b, as indicated in Figure 5.4 and 5.5, coming off opposing edges 210c, 220c of the respective inner surface 210a, 220a. The lateral surfaces 210b, 220b are tilted by an angle W' of 45° with respect to an extension plane spanned by said edges 210c of the respective leg 210, 220 (cf. Figure 5.4).

According to Figure 5.6 and 5.7, the insert 100 comprises a first and a second wall region 101, 102 integrally connected by a connecting region 103, which comprises a concave surface 103a. The two wall regions 101, 102 and the connecting region 103 form a groove or open channel circulating around the connecting region 103 for receiving the flexible element 10, when the latter is laid around the connecting region 103 contacting the concave surface 103a of the connecting region 103 and the adjacent surfaces of the two opposing wall regions 101, 102.

The two wall regions 101, 102 each comprise a guiding recess 110, 120 extending along the insertion direction Z or longitudinal axis L of the insert 100 for guiding the insert 100 with respect to the anchor 200 upon insertion of the insert 100 into the anchor 200 counter to the later insertion direction Z. Each guiding recess 110, 120 is delimited by a convex surface 110a, 120a of the respective wall region 101, 102, wherein the surfaces face away from each other, and wherein each surface 110a, 120a is a section of a surface area of a cone, so that the surfaces 110a, 120a comprise a central radius R that decreases along the longitudinal axis L of the insert. This means that the insert 100 is correspondingly tapered in the region of the surfaces 110a, 120a. Further, each guiding recess 110, 120 is delimited by two opposing boundary regions 112, 113, 122, 123 extending along the longitudinal axis L of the insert 100. Each boundary region may comprise a wedge-like shape having an angle of W=45° particularly, as shown in Figure 5.6.

Each boundary region 111, 112, 122, 123 of the insert further comprises a contact surface 111a, 112a, 122a, 123a which is essentially flush with the outside 200a of the anchor 200 when the insert 100 is inserted into the anchor 200. These contact surfaces 111a, 112a, 122a, 123a serve for forming an interface between the TCP

insert 100 and the walls of the bore hole 2, thus promoting bone cell ingrowth into the insert 100.

When inserting the insert 100 into the anchor 200 as shown in Figure 5.3 the concave inner surfaces 210a, 220a of the legs 210, 220 of the anchor 200 slide on the convex surfaces 110a, 120a of the respective guiding recess 110, 120 of the insert 100 and press the legs 210, 220 away from each other, which allows for anchoring the anchor 200 in the bore hole 2. For this the anchor 200 is inserted into the bore hole 2 when the insert 100 is not fully inserted into the anchor 200. Once the anchor 200 is in place, the insert 100 is pulled via the flexible element 10 attached to the insert 100 into its final position thereby pressing said legs 210, 220 away from each other so that the legs 210, 220 are pressed against the walls of the bore hole 2.

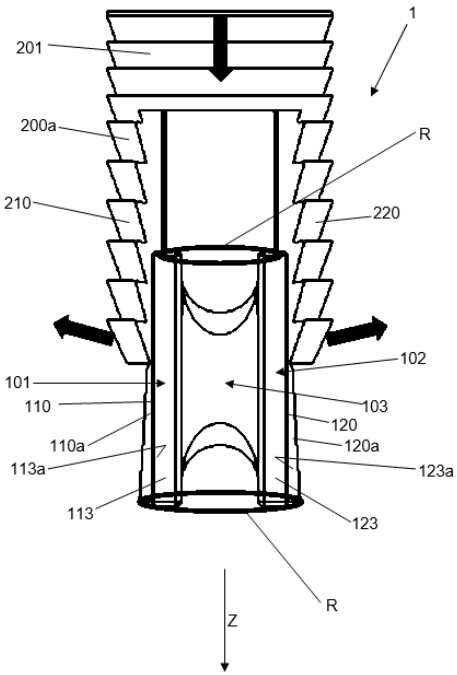

Figure 5.3 a lateral view of the insert and the anchor of the device according to the invention upon insertion of the insert into the anchor.

Further, when inserting the insert 100 into the anchor 200, the four lateral surfaces 210b, 220b of the legs 210, 220 slide along the boundary regions 111, 112, 113, 123 of the insert 100, thus prohibiting turning of the insert 100 with respect to the anchor 200. In this way the legs 210, 220 of the anchor 200 are guided in a form-fitting manner in the guiding recesses 110, 120 of the insert 100 upon insertion of the insert 100 into the anchor 200.

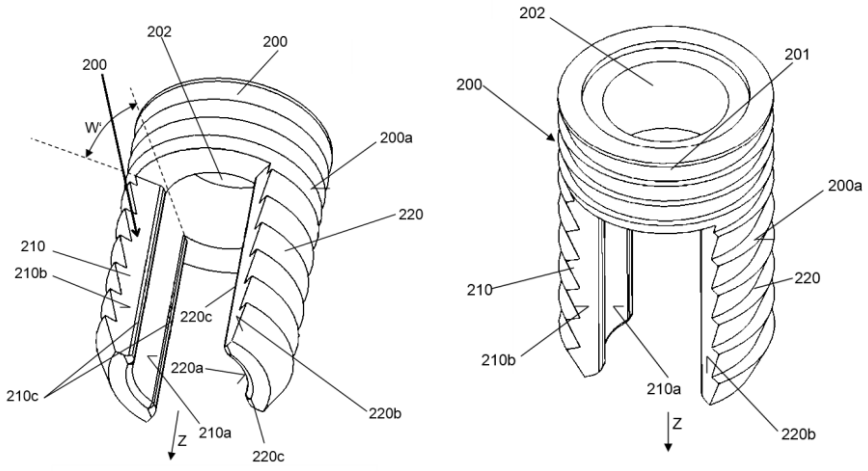

Figure 5.4(left) **5.5**(right) perspective views of the anchor shown in Figure 5.1 to 5.3

In other words, by means of the central Radius R (besides its spreading function) a primary guiding system is established which is supported by a secondary guiding system provided by the tilted (angle W') lateral surfaces 210b, 220b, which avoids turning of the insert 100 while implanting the device 1. As a second function, the secondary guidance system provides a contact zone (via contact surfaces 111a, 112a, 122a, 123a) between the TCP insert 100 and the bone 20, which is crucial for the osteoinduction.

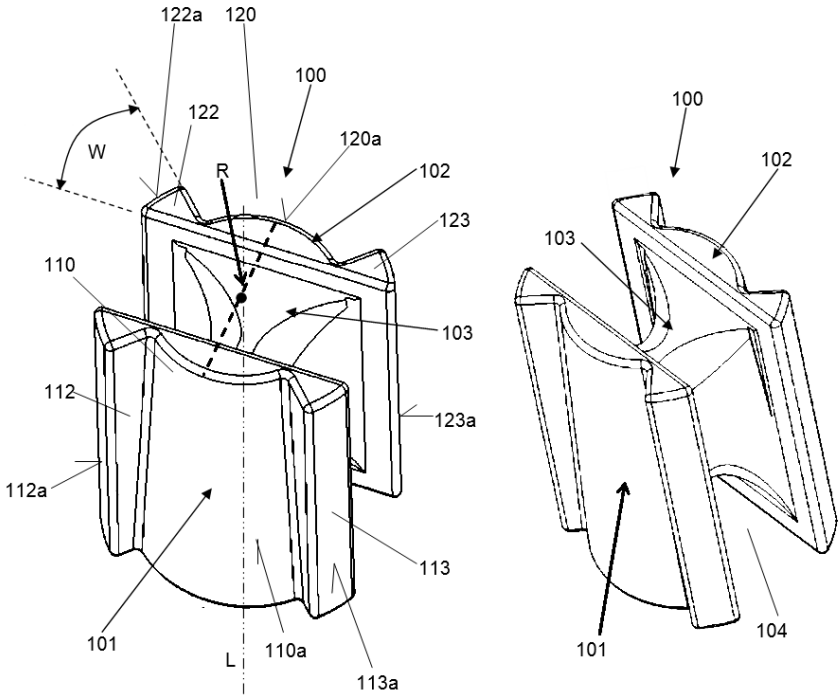

Figure 5.6(left) **5.7**(right) perspective views of the insert shown in Figure 5.1 to 5.3

Further, Figure 5.8 to 5.11 show a further embodiment of a device 1 for fixation of a flexible element to a bone 20, which is preferably used for natural flexible elements 10 such as ligament or tendon autografts. The device 1 has the same features as described above, but in contrast to the device 1 shown in Figure 5.2 to 5.7, the insert 100 has no tapered surfaces 110a, 120a. Further, the legs 210, 220 are relatively thinner, and the head part 201 does not comprise an annular shape, but two opposing cut-outs 203, 204 as shown in Figure 5.8 and 5.9, which receive the flexible element 10, so that the latter can be passed by the head part 201.

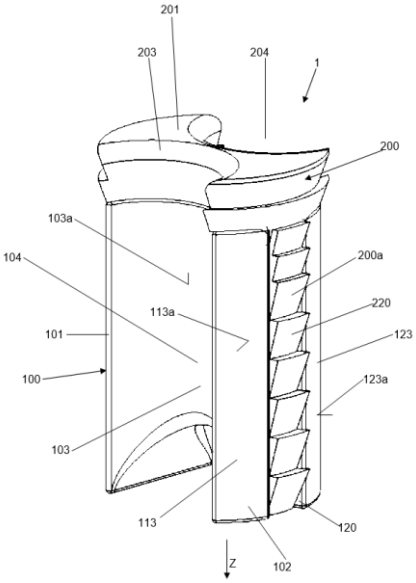

Figure 5.8 a perspective view of an alternative embodiment of the device according to the invention for fixation of a natural flexible element (e.g. autograft) to a bone

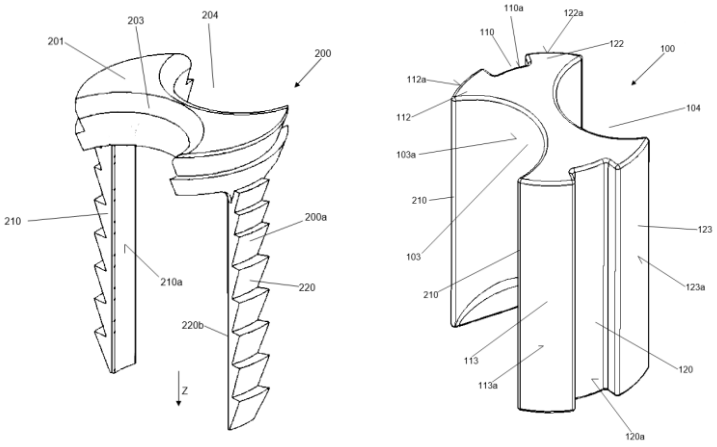

Figure 5.9(left) **5.10**(right) a perspective view of an anchor and insert of the device shown in Figure 5.8

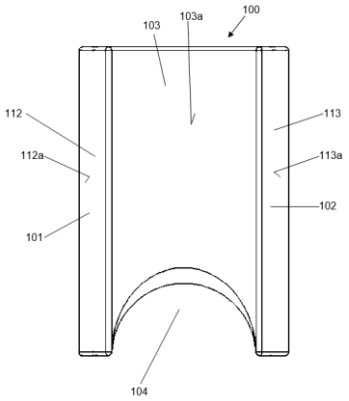

Figure 5.11 a lateral view of the insert of the device shown in Figure 5.8

In case the insert 100 comprises no tapered regions (see above), the anchor 200 is pressed into the bore hole 2 with the insert 100 being fully inserted into the anchor 200.

Preferably, the afore-described anchors 200 are formed out of PEEK. PEEK anchors 200 can be fabricated with traditional machine tools. However, for the TCP insert 100, the geometry is quite complicated, which is not easy to produce by traditional machine tools. So we used an advanced manufacturing technique of combining rapid prototyping and gel-casting methods. The negative pattern of the TCP insert 100 was designed with a commercial Computer Aided Design (CAD) software (Pro-engineer). The molds were fabricated on a stereolithography apparatus (SPS 600B, xi'an jiaotong university, Xi'an, China) with a commercial epoxy resin (SL14120, Huntsman). The CAD data of the negative pattern was converted into STL data by Pro-engineer, imported into Rpdata software, and converted into an input file for stereolithography. The molds fabricated were then cleaned with isopropanol alcohol. TCP powders along with monomers (acrylamide, methylenebisacrylamide), and dispersant (sodium polymethacrylate) was mixed with deonized (DI) water to form a ceramic slurry.

The slurry prepared was deagglomerated by ultrasonic for 5 hours and subsequently deaired under vacuum until no further release of air bubbles from the sample. Catalyst (ammonium presulphate) and initiator (N,N,N'N'-

tetramethylethylenediamine) were added to the slurry to polymerize the monomers. The amount of which were controlled to allow a sufficient time for casting process. The TCP slurry was cast into the molds under vacuum to force the TCP powders to migrate into the interspaces of the paraffin spheres. The samples were dried at room temperature for 72 hours. After the drying, pyrolysis of the epoxy resin molds and paraffin spheres were conducted in air in an electric furnace with a heating rate of 5°C/h from room temperature to 340°C, holding 5 hours at 340°C to ensure most paraffin spheres were burn out, and then sintered to 660°C at a rate of 10°C/h, holding 5 hours at 660°C to ensure most epoxy resin was burn out. After that the heating rate went up to 60°C/h till 1200°C, holding 5 hours at 1200°C, and then decreased to room temperature in 48 hours.

The mechanical property of porous TCP inserts or scaffold 100 varies with different porosities. The TCP inserts with different porosities have different elastic modules, and different failure stresses. To choose the proper porosity of porous TCP insert 100, a finite element analysis (FEA) was used to find out the stress and strain distribution on a TCP insert 100 while anchoring and pulling. Three different porosities, namely 40%, 60%, and 80%, were used in this study. It was found, that the maximum stress point is on the lower middle of the connecting region 103 of the TCP insert 100. For 60% porosity, under 1,000 N pullout force, the maximum stress on the TCP insert 100 is ~1 GPa.

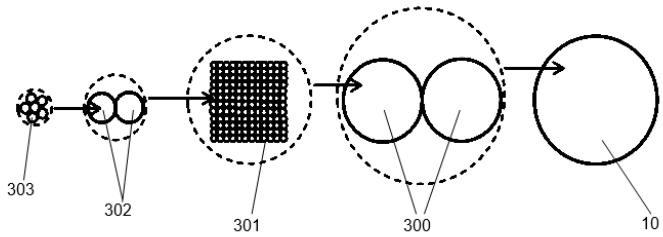

Figure 5.12 a schematical illustration of the structure of an embodiment of a synthetical flexible element (e.g. ACL scaffold)

According to a preferred embodiment of the invention ACL scaffolds based on silk as shown in Figure 5.12 and 5.13 are used as flexible elements 10.

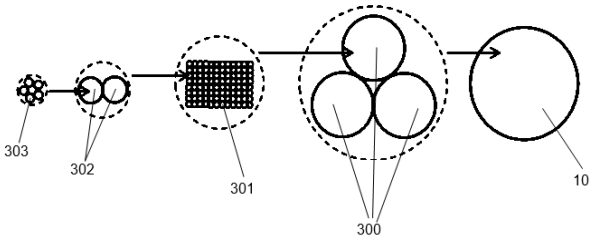

Figure 5.13 a schematical illustration of the structure of an alternative embodiment of a synthetical flexible element (e.g. ACL scaffold)

For producing such flexible elements 10 raw silk fibers (Bombyx mori) were obtained from Trudel Limited (Zurich, Switzerland). A special designed wiring machine was used to fabricate silk ACL scaffolds. For description purposes, the geometries of different hierarchical architectures were labeled as A(a)*B(b)*C(c)*D(d), where A, B, C, D represent the structural levels, which means number of fibers(A), bundles(B), yarns(C) and cords(D) in the final structure, while a, b, c, d is the twisting level, which means the lengths (mm) per turn on each of the hierarchical levels. After comparison and test with different structures, a wired silk scaffold structure was found to have the similar mechanical properties with human ACL. The structure parameter is defined as 6(0)*2(2)*144(10)*2(12), which means 6 fibers 303 in 1 bundle without 302 twist (0 means parallel), 2 bundles 302 in 1 yarn 301 with 2 mm per turn, 144 yarns 301 in 1 cord 300 with 10 mm per turn, 2 cords 300 in 1 ACL scaffold 10 with 12 mm per turn.

Figure 5.13 shows an alternative embodiment of a flexible element 10 in the form of a braided ACL scaffold. Here, the structure parameter is defined as 6(0)*2(2)*96(10)*3(12), which means 6 fibers 303 in 1 bundle 302 without twist (0 means parallel), 2 bundles 302 in 1 yarn 301 with 2 mm per turn, 96 yarns 301 in 1 cord 300 with 10 mm per turn, 3 braided cords 300 in 1 ACL scaffold 10 with 12 mm per turn.

The flexible elements in the form of silk ACL scaffolds 10 depicted in Figure 5.12 and 5.13 were produced with raw silk yarns. The hyper-antigenic protein sericin was removed by immersing the scaffolds 10 into an aqueous solution of 0.5wt% Na_2CO_3 at 90°C -95°C, 300 RPM in a magnetic stirrer (Basic C, IKA-WERKE, Germany) for 90 minutes, then rinsing with running distilled water for 15 minutes, and air

dried at 60°C. These procedures were repeated three times, then the sericin was thoroughly extracted.

For biomechanical testing of the silk-based flexible elements 10 in vitro pull to failure tests and low-cycle-loading tests were performed on a universal material testing machine (Zwick 1456, Zwick GmbH, Ulm, Germany), wherein a 20 kN force sensor (Gassmann Theiss, Bickenbach, Germany) was used. A special fixation clamp was developed. The distance between the clamps was 30±1 mm to simulate the normal ACL length[114, 115]. For the initial pull to failure tests a pre-conditioned loading of 5 N was applied to the scaffold 10, and afterwards a displacement-controlled loading of 0.5 mm/second was applied to the scaffold 10. For the low-cycle loading test, after applying a pre-conditional loading of 5 N to the scaffold 10, a force controlled cyclic loading from 100 N to 250 N over 250 cycles, representing the loads of normal walking[118], were applied with a loading speed of 0.5 mm/second.

To simulate long term loading of flexible elements (e.g. ACL scaffolds) 10, a specialized bioreactor 400 shown in Figure 5.14 was employed. A stepper motor 401 (e.g. NA23C60, Zaber Technologies Inc, Canada) was used to apply cyclic load, and a 1 kN load cell (e.g. KMM20, Inelta Sensorsystems, Germany) 404 was used to acquire the force. For holding the flexible element to be tested, said bioreactor 400 comprises two clamps 402 and a chamber 403, particularly in the form of a tube made of Polysulfon (PSU1000, Quadrant AG, Switzerland) surrounding the scaffold 10 to be tested as well as the clamps 402. The bioreactors 400 were fixed in an incubator (C150, Binder, Germany), and controlled by a special developed program with LabVIEW (9.x).

The length of the tested silk scaffolds 10 between the clamps was 28±3mm. The chamber 403 was filled with PBS and covered with an aluminum foil cap. The temperature in the incubator was 37°C. The humidity was 100%, and the CO2 concentration was 5%. After applying a pre-conditional loading of 5 N, the high-cycle loading was applied with a strain control at 1Hz frequency of 3% strain over 100,000 cycles with an interval rest of 30 seconds between every 250 cycles.

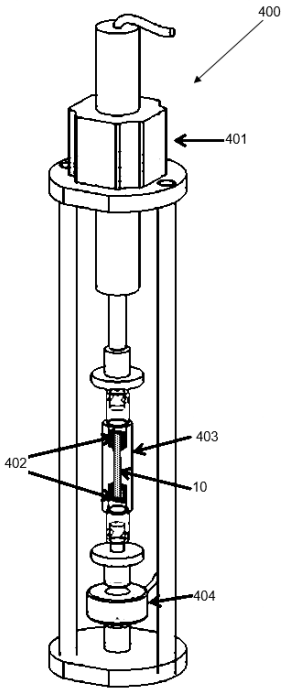

Figure 5.14 a perspective view of a bioreactor for simulating long term loading of a flexible element (e.g. ligament)

Mechanical properties of silk yarns with different conditions had been tested. The lengths of each sample is 30mm, and the diameter is 0.24 mm of native silk yarn, 0.17 mm of sericin extracted (dry), and 0.14 mm of sericin extracted (wet). The UTS of silk yarns decreased quite remarkably after sericin extraction, from 9.42 ± 0.33 N of native silk yarn to 7.34 ± 0.35 N of sericin extracted (dry) and 6.00 ± 0.33 N of sericin extracted (wet), respectively. The stiffness of silk yarns decreased as well after sericin extraction, from 1.97 ± 0.07 N/mm of native silk yarn to 1.37 ± 0.17 N/mm of sericin extracted (dry) and 1.03 ± 0.23 N/mm of sericin extracted (wet), respectively. The stiffness of silk yarns reduced significantly ($p<0.01$) in wet condition. The failure elongation of silk yarns also decreased after sericin extraction, from 9.8 ± 0.33 mm of native silk yarn, to 8.14 ± 0.30 mm of sericin extracted(dry) and 6.94 ± 0.40 mm of sericin extracted (wet) respectively.

Pull to failure tests had been performed on silk ACL scaffold 10 with different architectures. All the samples were sericin-extracted, tested in dry and wet conditions respectively. The architectures of silk ACL scaffolds are: parallel 6(0)*2(2)*288(10)*1(0), wired 6(0)*2(2)*144(10)*2(12), and braided 6(0)*2(2)*96(10)*3(12), as described previously. The results shows that the silk ACL scaffold 10 with parallel architecture has a lower UTS and higher stiffness, which is much farther from the value of human ACL taken from Woo et al[118]. The UTS of wired and braided architectures decreased significantly ($P<0.01$) from around 1900 N in dry condition to around 1500 N in wet condition. Although the value is lower than that of human ACL, it is still acceptable in ACL tissue engineering, since the earlier report shows that the UTS of human ACL varies according to the ages, up to 1730 N in people aged 16-26 years, but much less in people aged 48-86 years, with a mean average for approximately 734 N[143]. The stiffness of wired and braided architectures also decreased significantly ($P<0.01$) from around 550 N/mm in dry condition to around 250 N/mm in wet condition, which is quite close to the value of human ACL. To find out the effect of sterilization procedures on mechanical properties of silk ACL scaffolds 10, three samples of wired silk ACL scaffolds after sterilization had been tested. The UTS, linear stiffness, and failure elongation were 1444 ± 102 N, 251 ± 39 N/mm, and 3.93 ± 0.36 mm respectively.

Cyclic load tests had been performed on silk ACL scaffolds 10 with wired and braided architectures (cf. also Figure 5.12 and 5.13). The UTS and linear stiffness of scaffolds were compared under the following loading conditions: without loading, low cycle loading and high cycle loading. Cells were seeded on the scaffolds 10 to find out the effect of cell on the mechanical behavior of silk ACL scaffold 10 under different loading conditions. For the samples without cyclic loading, the UTS decreased slightly after immersed into the PBS solution for 7 days, from 1543 ± 85 N to 1362 ± 20 N for wired architecture, and from 1599 ± 65 N to 1391 ± 12 N for braided architecture. After cyclic loading, the UTS reduced significantly, to ~900 N (wired) and ~800 N (braided) after 250 cycles, to ~500 N (wired) and ~400 N (braided) after 100,000 cycles. The linear stiffness of samples without cyclic loading also decreased slightly after immersed into PBS solution for 7 days, from 289 ± 21 N/mm to 236 ± 23 N/mm for wired architecture, and from 242 ± 26 N/mm to 207 ± 31 N/mm for braided architecture. After cyclic loading, the linear stiffness increased significantly, to 428 ± 32 N/mm (wired) and 518 ± 66 N/mm (braided) after 250 cycles, to 490 ± 14 N/mm (wired) and 553 ± 38 N/mm (braided) after

100,000 cycles. There is no significant difference on mechanical properties (P>0.05) for wired architectures between the silk ACL scaffold 10 with cells and without cells under high cyclic loading.

The linear stiffness and elongation of silk ACL scaffold 10 under high cyclic loading were recorded. The linear stiffness of silk ACL scaffold 10 increased sharply from 289 ± 21 N/mm (wired) and 242 ± 26 N/mm (braided) at 0 cycle, to 428 ± 32 N/mm (wired) and 518 ± 66 N/mm (braided) at 250 cycles, then increased slightly to 496 ± 13 N/mm (wired) and 556 ± 37 N/mm (braided) at 20,000 cycles, and remain stable at ~500 N/mm (wired) and 550 N/mm (braided) until 100,000 cycles. The elongation of silk ACL scaffold 10 increased sharply from 0 at the beginning to 2.3 ± 0.2 mm (wired) and 1.2 ± 0.1 mm (braided) at 250 cycles, and increased gradually to 3.6 ± 0.4 mm (wired) and 3.0 ± 0.3 N/mm (braided) at 10,000 cycles, then increased slightly to 4.3 ± 0.8 mm (wired) and 4.3 ± 0.5 mm (braided) at 100,000 cycles.

The PEEK anchors 200 were tested on a universal material testing machine (Zwick 1456, Zwick GmbH, Ulm, Germany), the testing protocol was the same as previously described. The distance between the clamps was 30±1 mm to simulate the normal ACL length[114, 115]. For the tests a pre-conditioned loading of 5 N was applied to the anchor 200, and afterwards a displacement-controlled loading of 0.5 mm/second from 100 to 250 N over 250 cycles was applied to the anchors 200, representing the loads of normal walking[116], and then a pullout to get the ultimate tensile strength. Three types of anchors, V0, V1, and V2, were tested. V0 denotes an insert having parallel wall regions 101, 102 (i.e. non-tapered insert 100), which have no spreading effect on the anchor 200. The V1 and the V2 system have a small wedge and a bigger wedge respectively (cf. Figure 5.3). We found out from the results that the anchors 200 with spreading effect as shown in Figure 5.3 have a better survival rate.

Regarding the slippage in pig bone, the results of the V1/V2-system are quite good. The mean values of these two systems are around 0.7 mm, which is an improvement of around 56% compared with the V0-system. As it was intended to keep the slippage below a value of 1.5 mm, the system can in this sense be regarded as successful. The untimate tensile strengths (UTS) are shown in Figure 5.22. As can be seen from Figure 5.22, the V2-System is comparable to an 8/28 Interference

screw (IS). In mean, the IS is slightly higher than the V2 (715N to 684N). However, the median of the V2 is slightly higher than the median of the IS (698N to 694N). A T-Test comparing the V2 with the IS-Groups shows no significant difference of the mean values (P = 0.695) between these groups. In this sense, the V2 can be regarded as an equivalent system to the IS regarding the ultimate tensile strength.

The surgical processes can be inferred from Figure 5.15. A first approach is minimally invasive, similar to ACL repair surgery currently used in clinics. First, make a small lateral incision to put endoscope into the knee joint. Then, a trans-tibial bone tunnel 2d of 7 mm diameter is drilled, as well as a bore hole 2 of 20 mm length in the femoral distal. Then, bend the knee, and make a medial incision. Enlarge the bore hole 2 to 9 mm diameter through the medial incision. Afterwards, the insert 1 is inserted and anchored using the first tool 40, through the medial incision. Then, the free end of the flexible eleement (e.g. ACL scaffold) 10 is pulled through the tibia tunnel 2d. The silk scaffold 10 is pulled tight, tension is adjusted by the surgeon, and fixed with a standard interference screw (Φ6 × 19 mm).

For the animal studies an open surgical procedure (second approach) was favored to an arthroscopic approach because of a better overview and the lack of sophisticated tools for an arthroscopic anchor fixation. Because of the orientation of the femoral bone tunnel, the medial approach of accessing to the knee joint, where the patella is flipped laterally out of the way of drilling instruments, is adopted in this study. First a longitudinal median skin incision is made 5cm proximal to the superior margin of the patella to the tibial tubercle. Then a medial parapatellar capsular approach gives the surgeon access to the knee joint. The quadriceps and patellar tendon are disconnected from the joint calpsule and the vastus medialis is liberated from its insertion to the patella. Special attention should be given not to injure the patellar tendon and the medial collateral ligament. Keeping the cutting line close to the patella when liberating it from the joint capsule ensures that no damage occurs to the medial collateral ligament. Once the extensor apparatus is free, the patella can be flipped to the lateral side and the knee joint bent carefully to hold the luxated patella in its position.

For insertion of the anchor 200 / insert 100 into the bore hole 2, a first tool (also denoted as insertion tool) 40 with a hollow cylindrical cross section and three protrusions (also denoted as pods) 44 was used (cf. Figure 5.17). Due to the hollow

cylindrical cross section, the shaft 41 of the insertion tool 40 comprises a groove 43 for receiving the flexible element 10 upon insertion of the anchor 200 / insert 100 into the respective bore hole 2.

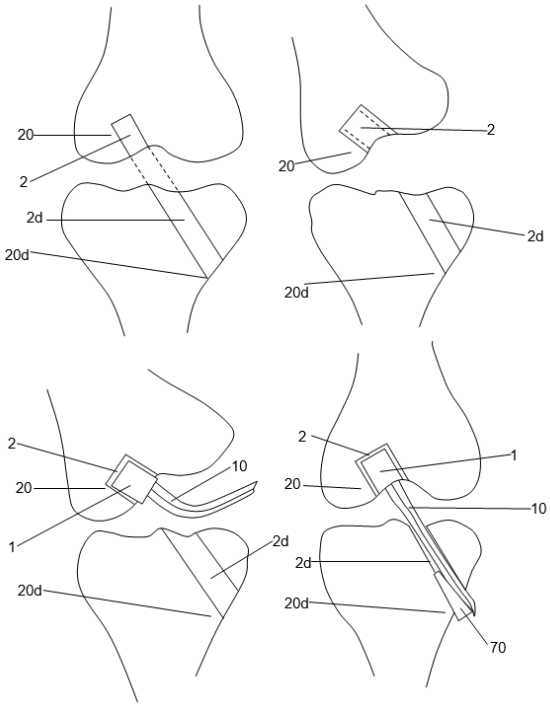

Figure 5.15 a method for inserting a device according to the invention into the femur, particularly for ACL reconstruction

Some anchors 200 tilted in the bone tunnel 2 and once contact was lost between the instrument 40 and the anchor 200, a reinsertion of the pods 44 into corresponding recesses 202b of the head part 201 of the anchor 200 as shown in Figure 5.16 was very difficult. Hence a new insertion tool 40 with a reduced wall thickness (external radius reduced by 0.5 mm) of the distal 5 mm was developed as shown in Figure 5.19. Correspondingly, the PEEK anchor 200 used with this insertion tool 40 (cf. Figure 5.18) has a central opening 202 adapted to the free end 42 of the first tool 40 shown in Figure 5.19.

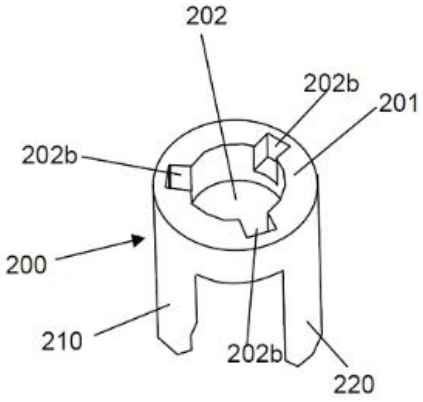

Figure 5.16 a perspective view of a head part of an anchor of a device according to the invention

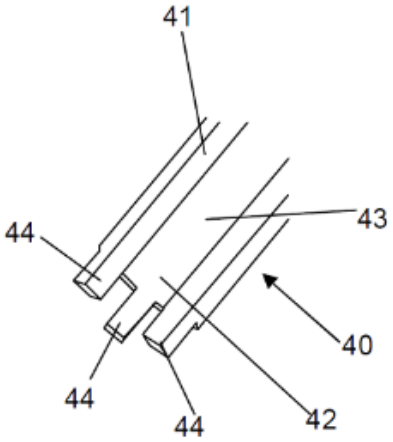

Figure 5.17 a portion of a first tool for engaging with the head part shown in Figure 5.16 for pressing the device according to the invention into a bore hole of a bone

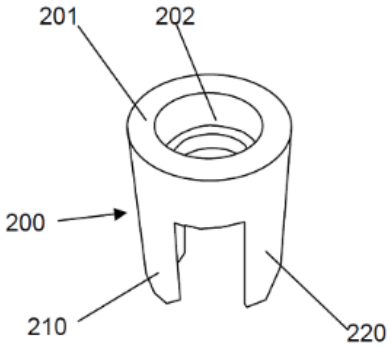

Figure 5.18 a perspective view of an alternative head part of an anchor of a device according to the invention

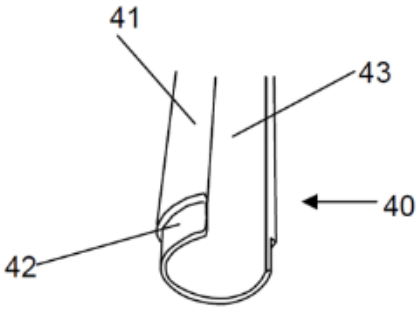

Figure 5.19 a portion of an alternative first tool for engaging with the head part shown in Figure 5.18 for pressing the device according to the invention into a bore hole of a bone

To prevent slipping and wobbling of the drilling instrument used to drill the bore hole 2 for anchoring the device 1, which can cause an enlarged tunnel entry and a subsequent loss of fixation stability of the implant 1, a second tool 50 as shown in Figure 5.20 is provided. The second tool 50 comprises a handle 51 having a free end 52, from which a cylindrical drill sleeve 53 surrounding a channel 55 for receiving a

drill protrudes, wherein the drill sleeve 53 comprises a sharpened free end 54 that ensures a firm grip in the femoral notch and the handle 51 allows accurate positioning of the drilling instrument. To ensure a reproducible angulation of the femoral bone tunnel 2 the following procedures are proposed: A level rod is pressed against the anterior side of the thigh aligned with respect to the longitudinal axis of the femur; the second tool 50 (also denoted as holding instrument) is positioned at 45° angulation in the sagittal plane and 30° deviation to the lateral side. In order to ensure axial alignment of the tibia 2d and femoral bone 2 tunnels (cf. Figure 5.15), a third tool 60 (for instance out of aluminum) as shown in Figure 5.21 may be used. The third tool comprises a first leg extending along an extension direction and a second and a third leg connected to the free ends of the first leg so that an arch is formed. A 9mm plug protrudes from a free end of the second leg along said extension direction, wherein the third leg comprises a trough-opening aligned with said plug in which the drill sleeve 53 of the second tool can be inserted and fixed in different positions along the extension direction by a fixation means 66 such as a screw, to ensure that the instrument 60 can be adapted to different knee sizes.

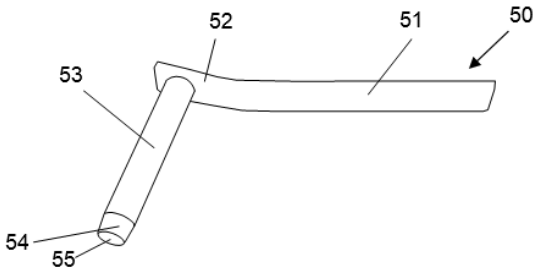

Figure 5.20 a perspective view of a second tool providing a drill sleeve for guiding a drill being used for drilling a bore hole for insertion of the device according to the invention

After the femoral bore hole 2 is drilled (cf. Figure 5.15), the plug of the third tool 60 is inserted into the femoral bore hole 2, then the knee joint is extended until the drill sleeve 53 extending trough trough-opening 65 of the third tool 60 can be adjusted to the tibia edge 20d. The tibia tunnel 2d is now drilled in axial alignment with the femoral bore hole 2, shown in Figure 5.15. The anchor 200 with insert 100

and silk ACL scaffold 10 is then inserted into the bore hole 2, leaving particularly the PCL just behind the ACL intact.

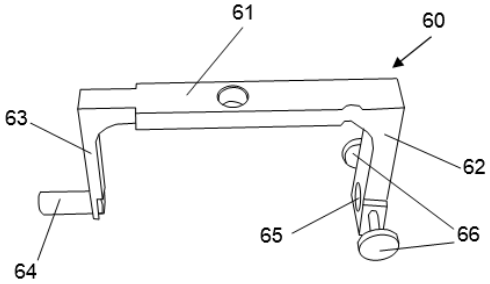

Figure 5.21 a perspective view of a third tool by means of which the second tool can be positioned in order to drill a further bore hole / tunnel into a further bone so that the further bore hole/tunnel is in axial alignment with the bore hole for the device according to the invention

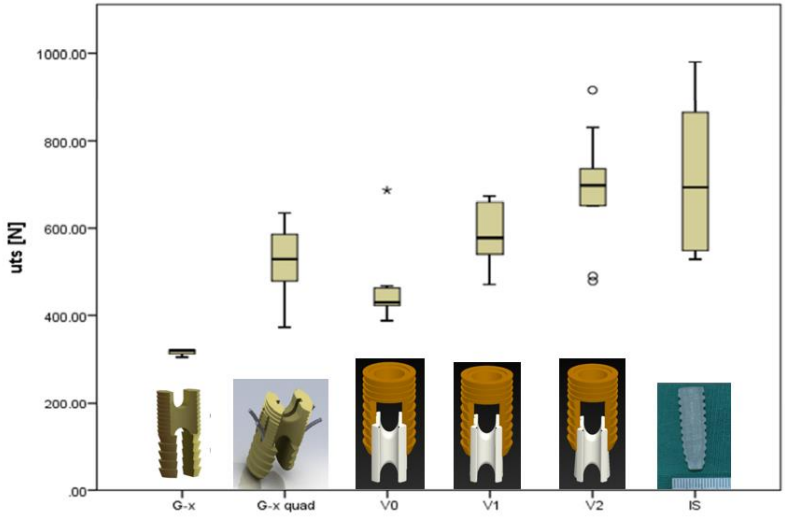

Figure 5.22 The UTS of the device according to the invention in pig bone for different insert/anchor configurations V0, V1 and V2 of the device according to the invention

5.3 CLAIMS

1. Device for fixing a flexible element (10), particularly in the form of a natural or synthetical ligament or tendon, to a bone (20), comprising: an insert (100) being designed to hold said flexible element (10), an anchor (200), wherein the insert (100) is designed to be inserted into said anchor (200), and wherein the anchor element (200) is designed to be inserted into a bore hole (2) of said bone (20) together with said insert (100) inserted into the anchor (200) to fix the flexible element (10) to the bone (20).
2. Device as claimed in claim 1, **characterized in that** the insert (100) is formed out of an osteoinductive or osteoconductive material or comprises an osteoinductive or osteoconductive material.
3. Device as claimed in one of the preceding claims, **characterized in that** the anchor (200) is designed to be inserted into said bore hole (2) along an insertion direction (Z) together with said insert (100) inserted into the anchor (200).
4. Device as claimed in one of the preceding claims, **characterized in that** the anchor (200) comprises a head part (201) and a first and a second leg (210, 220) protruding from said head part (201), wherein particularly the legs (210, 220) are integrally formed with the head part (201) and wherein particularly the legs (210, 220) protrude from the head part (201) in the insertion direction (Z).
5. Device as claimed in claim 4, **characterized in that** the head part (201) comprises an annular shape, wherein particularly the head part (201) comprises an opening (202) for passing through said flexible element (10).
6. Device as claimed in claim 4, **characterized in that** the head part (201) comprises two opposing cut-outs (203, 204) for bypassing the flexible element (10), wherein each cut-out (203, 204) is formed in a boundary region of the head part (201).
7. Device as claimed in one of the claims 4 to 6, **characterized in that** the insert (100) is arranged between the legs (210, 220) of the anchor (200) when the insert (100) is inserted into the anchor (200).
8. Device as claimed in claim one of the claims 4 to 7, **characterized in that** the insert (100) comprises a first and a second guiding recess (110, 120)

being designed to receive the legs (210, 220) in a form fitting manner when the insert (100) is inserted into the anchor (200).

9. Device as claimed in claim 8, **characterized in that** each guiding recess (110, 120) is delimited by a surface (110a, 120a) of the insert (100), wherein the two surfaces (110a, 120a) face away from each other, and two opposing boundary regions (112, 113, 122, 123) protruding from the respective surface (110a, 120a), wherein particularly the two surfaces (110a, 120a) are convex.
10. Device as claimed in claim 9, **characterized in that** each boundary region (112, 113, 122, 123) comprises a contact surface (112a, 113a, 122a, 123a) being designed to contact the bone (20) when the anchor (200) is inserted into the bore hole (2) of the bone (20) together with the insert (100) as intended, which contact surface (112a, 113a, 122a, 123a) extends along the respective guiding recess (110, 120).
11. Device as claimed in one of the preceding claims, **characterized in that** the anchor (200) comprises an outside (200a) for contacting the bone (20), wherein particularly said outside (200a) comprises a toothed surface, and wherein particularly the respective contact surface (112a, 113a, 122a, 123a) is flush with said outside (200a) of the anchor (200).
12. Device as claimed in claim 4 or one of the claims 5 to 11 when referred back to claim 4, **characterized in that** a region (110a, 120a) of the insert (100) is tapered so that upon inserting the insert (100) into the anchor (200), the insert (100), particularly by means of the surfaces (110a, 120a) of the insert (100), presses the legs (210, 220) away from each other, wherein particularly the anchor (200) is designed to be inserted into the bore hole (2) in the insertion direction (Z) with the insert (100) being inserted into the anchor (200) in a first position, in which the insert (100) is not fully inserted into the anchor (200), wherein particularly the insert (100) is designed to be pulled into a second position counter to the insertion direction (Z) when the anchor (200) is inserted into the bore hole (2) of the bone (20) as intended, in which second position the insert (100) is fully inserted into the anchor (200) and thus presses the legs (210, 220) against the bone (20).
13. Device as claimed in claim 4 or one of the claims 5 to 12 when referred back to claim 4, **characterized in that** each of the legs (210, 220) comprises

an inner surface (210a, 220a), wherein the two inner surfaces (210a, 220a) face each other, and wherein particularly said inner surfaces (210a, 220a) are concave.

14. Device as claimed in claims 9 and 13, **characterized in that** each inner surface (210a, 220a) is designed to rest on an associated surface (110a, 120a) of a guiding recess (110, 120).
15. Device as claimed in one of the preceding claims, **characterized in that** the insert (100) comprises a first wall region (101) and a second wall region (102), wherein particularly the first guiding recess (110) is formed in the first wall region (101), and wherein particularly the second guiding recess (120) is formed in the second wall region (102).
16. Device as claimed in claim 15, **characterized in that** the two wall regions (101, 102) are integrally connected by a connecting region (103), wherein particularly the connecting region (103) comprises a surface (103a) for contacting the flexible element (10), wherein particularly said surface (103a) is concave.
17. Device as claimed in one of the preceding claims, **characterized in that** the insert (100) comprises a groove (104) for receiving the flexible element (10), wherein particularly said groove (104) is delimited by the two wall regions (101, 102) and the connecting region (103).
18. Device as claimed in one of the preceding claims, **characterized in that** the device (1) comprises said flexible element (10),
19. Device as claimed in claim 18, **characterized in that** the flexible element (10) is laid around the insert (100), particularly around the connecting region (103), particularly such that it contacts the insert (100), wherein particularly said flexible element (10) is arranged in said groove (104).
20. Device as claimed in claim 5 and in claim 18 or 19, **characterized in that** the flexible element (10) passes through the opening (202) of the head part (201).
21. Device as claimed in claim 6 and in claim 18 or 19, **characterized in that** the flexible element (10) passes by the cut-outs (203, 204) of the head part (201).
22. Device as claimed in one of the claims 18 to 21, **characterized in that** the flexible element (10) is a natural ligament or tendon.

23. Device as claimed in one of the claims 18 to 21, **characterized in that** the flexible element (10) is a synthetic ligament or tendon, particularly an ACL scaffold.
24. Device as claimed in claim 23 or one of the clams 18 to 21, **characterized in that** the flexible element (10) comprises two twisted cords (300), each cord (300) comprising 144 twisted yarns (301), each yarn (301) comprising two twisted bundles (302), each bundle comprising 6 fibres (303), which fibres particularly comprise fibroin.
25. Device as claimed in claim 23 or one of the claims 18 to 21, **characterized in that** the flexible element (10) comprises three braided cords (300), each cord (300) comprising 96 twisted yarns (301), each yarn (301) comprising two twisted bundles (302), each bundle (302) comprising 6 fibres (303), which fibres particularly comprise fibroin.
26. Device as claimed in one of the preceding claims, **characterized in that** said insert (100) comprises one of the following substances: tricalcium phosphate, hydroxylapatite, calcium phosphate, calcium silicate, or silicate-substituted calcium phosphate.
27. Device as claimed in one of the preceding claims, **characterized in that** the anchor (200) comprises one of the following substances: polyether ether ketone, poly lactic acid, poly lactic-co-glycolic acid, poly-ε-caprolactone, a titanium-based alloy, or a magnesium-based alloy.
28. Tool set for inserting a device (1) according to one of the preceding claims into a bore hole (2) in a bone (20), comprising at least a first tool (40) for pressing the device (1) into said bore hole (2), wherein said first tool (40) comprises an elongated shaft (41) having a free end (42) that is designed to engage with the anchor (200), particularly with the head part (201) of the anchor (200), for pressing the device (1) into said bore hole (2), wherein said elongated shaft (41) comprises a groove (43) for receiving the flexible element (10) upon insertion of the device (1) into the bore hole (2) of the bone (20).

CHAPTER VI

Synthesis

6.1 CONCLUSIONS

Injuries of the ACL are increasingly common, and the demand for ACL reconstruction is increasing year by year. There are many options available to the orthopaedic surgeons with regard to the method of repair. Among the most critical of these is the choice of graft used in the reconstructive surgery. Each choice has both advantages and drawbacks. Of clinically available graft options, a bone-patellar tendon-bone (BPTB) autograft reconstruction is commonly employed for patients seeking the most rapid return to pre-injury activity levels, and for which rapid graft-host integration is essential. This graft features two bony ends and a very strong bone-tendon interface, with the bone blocks at being fixed into the bone tunnel. As bone to bone healing is significantly faster and more robust than tendon to bone healing, BPTB autografts have been regarded as the gold standard for ACL reconstructions for decades. However, the functional efficacy of this approach comes at the cost of potentially substantial donor site morbidity. Therefore, numerous alternative approaches have pursued novel solutions with efficacy similar to the BTB autograft. Of these, tissue engineering approaches to ACL repair have emerged as a promising direction.

Tissue engineering approaches to ACL repair represent a huge topic, encompassing a variety of complex aspects such as cell source, cell signaling, bio factors, biomaterials, scaffold design, and so on. Concerning our research backgrounds and expertise, we focused only on the scaffold aspect in this study. Particularly in cases for which a scaffold is immediately challenged by high mechanical demands, a wise choice of scaffold represents a keystone within a tissue engineering based strategy. While many biomaterials have been investigated for fabrication as a tissue engineering scaffold for ACL reconstruction, silk has been increasingly investigated as a scaffold for tissue engineered ACL grafts, primarily due to a uniquely advantageous combination of biocompatibility and robust biomechanical strength in the short and middle terms. There are numerous studies that have reported positive results using silk based ligament scaffolds in preclinical animal models, and safety and efficacy oriented clinical trials of silk based ACL scaffolds in human knees have also been reported. In these latter studies, it appears that silk based scaffolds for ACL regeneration have achieved promising success to some extent. However, silks have still not been translated into a clinically available graft material for ACL reconsitruction. Beyond the ligament graft itself, it is by now widely appreciated

that the biggest challenge to achieving a long-term clinical success is attaining rapid integration of the graft within the host bone tunnels. Accordingly, many approaches have been attempted to enhance graft to bone integration. Generally, these have applied bioactive agents, cells, or osteoinductive biomaterials that seek to provoke tissue integration at the interface between the scaffold and bone. However, primary mechanical stability and adequate contact surface between scaffold and bone have been largely neglected in published studies. Although conventional fixation methods like interference screws attempt to achieve this goal, there still remains no method that seems able to attain adequate contact surface to achieve consistently robust mechanical stability. The current body of work has focused on developing a novel approach to overcome this long-standing challenge of tissue engineered ACL scaffold to bone healing.

To this end we proposed a novel concept of a silk-based artificial ACL with bone-like ends (TCP/PEEK anchor), designed to be roughly biomimetic of a BPTB autograft. We have shown that this concept can provide not only adequate contact force and area between graft to bone for long-term biological integration, but is also capable of fixation strength adequate to provide initial stability. The concept has been tested and evaluated step by step in this work. First, the design and preparation of silk-based artificial ligament was presented in Chapter 2. Here, scaffolds with different candidate architectures were tested using a specially designed bioreactor under various loading conditions including static, low cycle, and high cycle loading. The architecture of silk scaffold with a similar biomechanical behavior to the native human ACL was found, and used as a basis for further investigations. Following the establishment of the silk ligament construct, a hybrid TCP/PEEK anchor is developed. In vitro biomechanical tests were performed on different anchor designs, and an optimized design was selected for combination with the silk-based artificial ligament. This hybrid graft was first tested in vivo with the small-scale pilot animal study discussed in Chapter 3. On this basis, larger scale evaluate of efficacy was performed as discussed in Chapter 4. Biomechanical tests and histological observations were used at two time points: three months and six months to evaluation the regeneration properties. Indicating what may be remarkable promise, numerous Sharpey's fibers could be clearly observed at the transitional zone between silk graft to bone, implying a biological integration of the silk graft to bone that appeared similar to the native ACL to bone insertion. Recognizing these large-animal results as clinically promising, we filed a preliminary

patent on these concepts with the European Patent Office. The claims of this patent including detailed design parameters and fabrication techniques of the hybrid graft, as well as the developed surgical tools are described in Chapter 5.

6.2 OUTLOOK

Admittedly, there are many limitations in this study. We focus on the architecture design of scaffold, but the architecture we presented as 'optimized' in this study, is merely the best design one among all the candidate ones. The architecture of this hybrid silk graft with TCP/PEEK anchor can still be improved. Before implantation, we didn't do any pretreatment or preincubation with some potential agents such as biofactors or specific cells on the graft. The results could be possibly better if we conduct such procedures. Only one side (femur) of silk scaffold was fixed with TCP/PEEK anchor, while the other side (tibia) of silk scaffold was fixed with interference screw, which increases the risk that the scaffold pullout from tibia tunnel due to tibia tunnel widening in long term. A better design with both bony ends should be considered. The porcine model is adopted to evaluate the efficacy of the hybrid graft. But the functional tests such as drawer test or Lachman test cannot be performed with porcine, since the fat and muscles of porcine is too thick to accurately measure the joint mobility. Other animal models should be adopted in further study.

The next step of our study is to do the translation work of this concept into clinical application. To make this step easier, we separated the hybrid graft into two parts - the silk based artificial ACL and the TCP/PEEK anchor. We chose the TCP/PEEK anchor part for the first step of translation since we believe it is closer to a clinical application. Animal experiment for preclinical trial of device safety and efficacy in a canine model has been started already, detailed study protocol is listed in the following paragraph.

Study protocol of preclinical trial (next step)

Hybrid TCP insert / PEEK anchor housing

The device contains TCP insert and PEEK anchor housing, shown in Figure 6.1. The TCP insert was fabricated with an indirect 3D printing (combination of gel-casting

and rapid prototyping). The TCP insert has an outside diameter of 5 mm, and length of 10 mm, with a microporosity of approximately 45%, pore size of approximately 5 μm on average. The PEEK anchor housing was fabricated with a traditional machine tool. The PEEK anchor housing has an outside diameter of 5.5 mm, and length of 13 mm (arm: 10 mm, cap: 3 mm). The sterilization processes were firstly conducted on each part separately. Each part after fabrication was put into 75% ethanol solution for 24 hours. And the TCP part was secondly treated by gamma radiation in a dose of 30kGy. Afterwards, two parts were assembled in a clean hood. Then, the assembled TCP/PEEK anchor was packaged and autoclaved at 121℃ for 30 minutes. The photos of each separated part, assembled part, and packaged sterile part ready for animal implantation are shown in Figure 6.2.

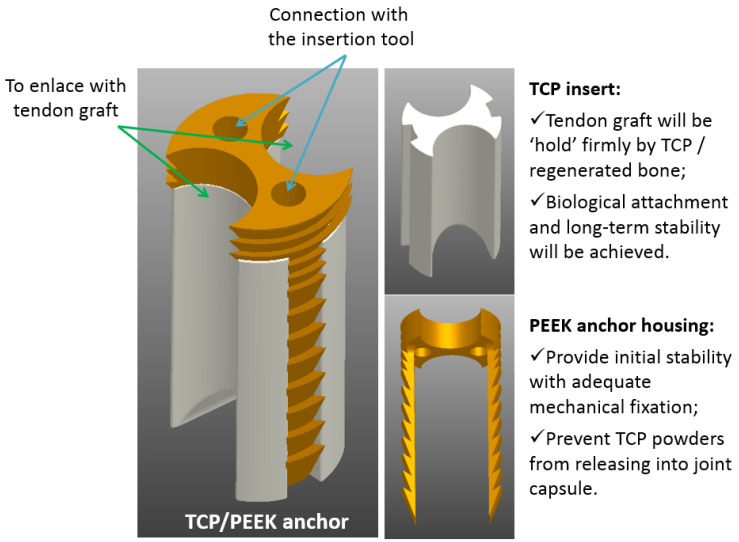

Figure 6.1 The design of hybrid anchor with TCP insert and PEEK anchor housing.

Study design

The present study was performed with 24 healthy adult male beagles aging around one and half years old, weighing 12.0 ± 1.1 kg (mean ± SD). Animal experimentation was carried out under the Rules and Regulations of the Animal Care and Use Committee, First Hospital of Xi'an Jiaotong University, P.R. China. The ulnar carpal flexor in left forelimb was used as tendon autograft. The CCL reconstructions were

performed on the right knee. The canines were divided into three study groups for three months, six months, and twelve months with 8 canines at each time point. For each time point, 6 animals were used for mechanical tests and morphological observation, the remaining 2, plus 2 from the 6 mechanical test samples, namely 4 animals were used for histological analysis. The drawer test and Lachman test were performed with all samples. The detailed study design is shown in Table 6.1.

Preoperative treatment

The canines were thoroughly disinfected(spray) with 0.25% didecyl dimethyl ammonium bromide solution two days before operation. Antibiotics (Penicillin of 800'000 U) were given to each canine by intramuscular injection twice a day at one day before operation. A sodium pentobarbital solution of 3.5% concentration was used as anesthetic. Each canine was give 0.5ml/kg with abdominal injection, and followed 5 minutes later with additional 0.2ml/kg dose with vein injection. Then, the canine was positioned on its back on the operating table in a specially designed holding tray. The left forelimb and right hindleg were shaved, and washed with povidone-iodine solution thoroughly.

Figure 6.2 The photos of TCP insert, PEEK anchor housing, assembled anchor, and sterilized anchor.

Table 6.1 Overview of animal study for CCL reconstruction in canine model

Time (months)	Clinical X-Ray, CT, Drawer test, Lachman test								
3, 6, and 12	Mechanical test, Morphology		Histology, Micro-CT						
Total Number: 24 n=8 at each time point	Sample (n)	Control	Sample (n)			Control			
	6	Contralateral CCL	4 *			Tibia side			

Processes	Samples (n)	1	2	3	4	5	6	7	8
CCL reconstruction (right knee)	8	•	•	•	•	•	•	•	•
Clinical X-Ray at Day 1 (bilateral knees)	3	•	•	•					
Clinical CT at Day 1 (bilateral knees)	3	•	•	•					
Euthanization at 3, 6, and 12 months	8	•	•	•	•	•	•	•	•
Dissection (keep both knees)	6	•	•	•	•	•	•	•	•
Clinical X-Ray immediately following euthanization (right knee)	8	•	•	•	•	•	•	•	•
Clinical CT immediately following euthanization (right knee)	8	•	•	•	•	•	•	•	•
Drawer test, Lachman test (bilateral knees)	8	•	•	•	•	•	•	•	•
Open the joint, remove unnecessary tissues	6			•	•	•	•	•	•
Morphology evaluation (bilateral knees)	6			•	•	•	•	•	•
Mechanical test (bilateral knees)	6			•	•	•	•	•	•
Dissection and Cut into small blocks for histology (bilateral knees)	4	•	•	•	•				
Micro-CT	4	•	•	•	•				
Paraffin embedded (PEEK removed)	2	•		•					
Resin Embedded (including PEEK)	2		•		•				
Freeze at -20 C for further test	4					•	•	•	•

* Two samples of which are from the samples after mechanical tests.

Surgical Procedure

A tendon stripper was used to access and cut the ulnar carpal flexor from left forelimb. The flexor tendon was trimmed and combined with TCP/PEEK anchor. The tendon ends were sutured with bioresorbable sutures, shown in Figure 6.4(A). An open surgical procedure was used. First a longitudinal median skin incision was made 3 cm proximal to the superior margin of the patella to the tibia tubercle. The knee joint was accessed with medial parapatellar capsular approach. Then, the joint

was bended at 90°, and native CCL was carefully cut and removed. A 5.0 mm tunnel was drilled over the footprint of ACL, with ~15 mm in depth, shown in Figure 6.3(A). To avoid damage the articular cartilage on the medial condyle, the drilling direction was 11 o'clock on the transversal plane, and 45° anterior deviation on the sagittal plane using the femoral axes as frame of the reference. A drilling sleeve was developed to prevent slipping and wobbling of the drilling instrument, which can cause an enlarged tunnel entry and a subsequent loss of fixation stability of the implant. A 5.0 mm tunnel in same axis was drilled through the tibial with a special designed synchronizing sleeve, shown in Figure 6.3(B). An insertion tool for CCL graft implantation was developed, with a hollow cylindrical cross section for tendon graft, and an adapted end for holding PEEK anchor. After anchoring of the TCP/PEEK scaffold into the femur tunnel, the other end of tendon graft was brought through the tibia tunnel with a specially designed retractor, shown in Figure 6.3(C). Then the knee joint was flexed at 30°. The tendon graft was pulled to tight, and fixed with an interference screw (Φ3.7 × 10 mm, Smith & Nephew, UK), shown in Figure 6.3(D).

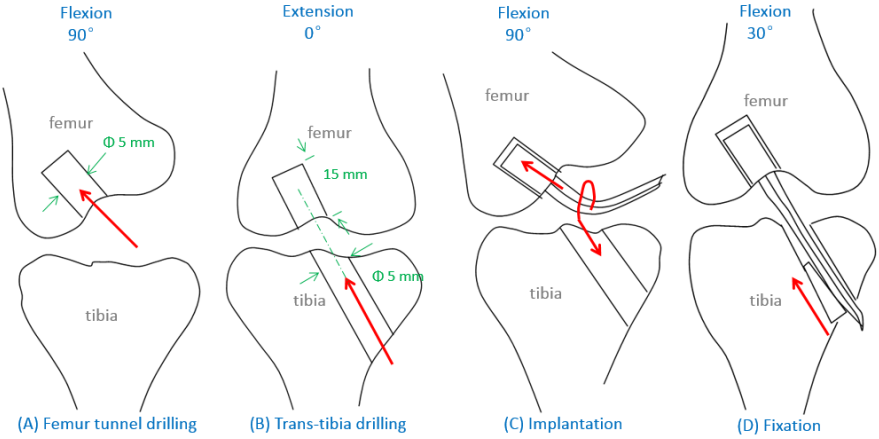

Figure 6.3 Open surgical procedures for canine CCL reconstructions

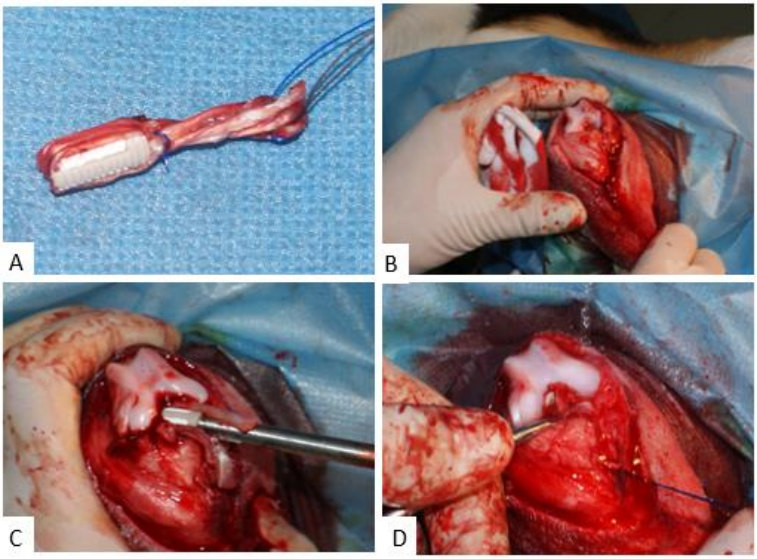

Figure 6.4 Photos during surgical procedures for canine CCL reconstructions.

Postoperative Treatment

If a canine died within one month after operation, another surgery would immediately be performed on a backup canine. If a canine died after one month, we just recorded the results, and excluded it from the 5 samples for mechanical test in 12 months period. Each canine was put into its own cage (120 × 100 × 75 cm), and unrestricted daily activities within cage was allowed. Analgesics (Pethidine of 100mg) were given to each canine twice a day for three days right after operation to release the pain. In order to prevent infection, antibiotics (Penicillin of 800'000 U) were given to each canine twice a day until five days after operation, and spray disinfection with 0.25% didecyl dimethyl ammonium bromide solution were performed on canines as well as cages biweekly until the end of animal experiment. The normal activities and degree of lameness were monitored.

Note: This study is ongoing. The following measurements haven't been done yet. This study is expected to be finished in September 2014. And results will be presented in our further published papers.

Outcome evaluation

Euthanization time points

3 months, 6 months, 12 months.

Euthanize 8 canines at each time point with lethal injection of thiamylal sodium.

Test group

4 canines are used for clinical X-Ray, CT at DAY 1 after operation. All 8 canines are used for clinical X-Ray, CT, Drawer test, and Lachman test, at 3, 6, and 12 months. 6 canines are used for biomechanical tests, and morphology evaluation. 4 canines are used for histology evaluation, Micro-CT image. (2 of which are from samples after mechanical tests)

Functional test

(n=8 at each time point, contralateral knee used as control.)

Cranial drawer test: The knee is flexed at 90 degrees, the tibia is then drawn forward anteriorly. The amount of anterior tibial translation is recorded.

Lachman test: The knee is flexed at 30 degrees, the tibia is then pulled with a motion in comparison to the femur. The amount of motion is recorded.

Endpoints: Clinically relevant function assessment of reconstructed knee(right, device) compared to the control knee (left, sham operated) across different time point.

Radiological evaluation

X-Ray and CT images are taken at DAY 1 after surgical operation(n=4). X-Ray images are taken at 3 months, 6 months, 12 months after reconstruction, immediately following euthanization(n=8). Micro-CT are taken at femur bone tunnel 3 months, 6 months, 12 months after euthanization(n=4).

Endpoints: Tracking of tunnel closure/widening (estimate TCP resorption rate). Micro-CT based analysis of new bone formation volume at various subregions and different time points.

Morphology evaluation

(n=6 at each time point)

Native ACL width and length are measured at operation. Contralateral native ACL width and length are measured at 3, 6, 12 months. Tendon graft width and length are measured at right after implantation, and 3, 6, 12 months. The surfaces of articular cartilage are observed rigorously (using india ink as contrast to identify scratches, and additionally using SEM if necessary) to exclude identify any abrasion caused by the implant.

Endpoints: General growth of tendon graft/native ACL. Characterization of graft elongation rate. Identification for risk of articular cartilage damage due to TCP particulate abrasion.

Biomechanical test

(n=6 at each time point)

Unnecessary soft tissues, including skin, muscles, fat, menisci, PCL, LCL, etc, except for tendon graft (or native ACL in control) are carefully removed. A special designed clamp system is used to fix the femur, and tibia, and ensure the tendon graft is vertically aligned, shown in Figure 6.5. The tests are applied a pre-conditioned loading of 5 N, and afterwards applied a force-controlled loading of 0.5 mm/second from 100 to 250 N over 250 cycles, which is to in consistency with our previous data. The force-displacement curve of each test is recorded. The dynamic creep is measured by the difference of displacement between the first cycle and the last cycle. The ultimate tensile strength is recorded at the first peak in the pull to failure test.

Endpoints: Pull to failure strength (UTS) and failure mode. Construct stiffness. Dynamic creep rate.

Histological evaluation

(n=4 at each time point)

Following samples on the right knee (experimental) will be taken: anchor part in femur tunnel, interference screw part in tibia tunnel, menisci around tendon graft, articular cartilage around bone tunnel at femur lateral condyle, synovium tissue in the joint. Following samples on the left knee (control) will be taken: menisci around CCL, articular cartilage, around ACL at femur condyle, synovium tissue in the joint. Following staining methods will be applied: HE, Goldner's trichrome, Toluidine blue, Saframin-O, Masson, Gomori, Picrosirius red, Immunochemistry(Col-I, Col-III).

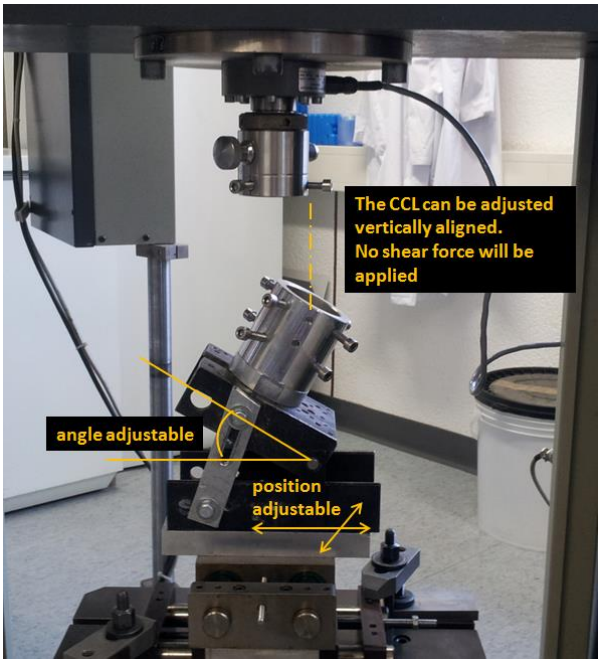

Figure 6.5 Photos of the specially designed clamp system for biomechanical test on canine CCL.

Paraffin embedded (PEEK removed, demineralized, n=2)

HE: for general assessment of bone, cartilage, tendon, transitional zone.

Toluidine blue, and Saframin-O: for cartilage observation

Masson, Gomori: for Sharpey's fiber observation

Picrosirius red, Immunochemistry(Col-I, Col-III): for special collagen fiber.

Resin Embedded (including PEEK, n=2)

Goldner's trichrome: for general assessment of bone, PEEK, newbone, TCP, cartilage, tendon, transitional zone.

Endpoints: Quality and nature of graft to bone attachment/healing in by TCP based device compared to the interference screw fixation (control in tibia side) at different time points.

REFERENCES

1. *Parkkari, J., et al., The risk for a cruciate ligament injury of the knee in adolescents and young adults: a population-based cohort study of 46,500 people with a 9 year follow-up. British Journal of Sports Medicine, 2008.* ***42****(6): p. 422-426.*
2. *freeman, J.W.K., A.L, Recent Advancements in Ligament Tissue Engineering: The Usw of Various Techniques and Materials for ACL Repair. Recent Pat. Biomed. Eng, 2008.* ***1****: p. 6.*
3. *Majewski, M., H. Susanne, and S. Klaus, Epidemiology of athletic knee injuries: A 10-year study. Knee, 2006.* ***13****(3): p. 184-188.*
4. *Junkin, D., et al., Knee ligament injuries. Orthopaedic knowledge update: sports medicine. Rosemont, IL: American Academy of Orthopaedic Surgeons. p, 2009.* ***136****.*
5. *Chen, K., et al., A hybrid silk/RADA-based fibrous scaffold with triple hierarchy for ligament regeneration. Tissue Eng Part A, 2012.* ***18****(13-14): p. 1399-409.*
6. *Murray, M.M., History of ACL Treatment and Current Gold Standard of Care, in The ACL Handbook. 2013, Springer. p. 19-28.*
7. *McIntosh, A.L., D.L. Dahm, and M.J. Stuart, Anterior cruciate ligament reconstruction in the skeletally immature patient. Arthroscopy-the Journal of Arthroscopic and Related Surgery, 2006.* ***22****(12): p. 1325-1330.*
8. *Lohmander, L.S., et al., High prevalence of knee osteoarthritis, pain, and functional limitations in female soccer players twelve years after anterior cruciate ligament injury. Arthritis and Rheumatism, 2004.* ***50****(10): p. 3145-3152.*
9. *Proffen, B.L. and M.M. Murray, In Vivo Models of ACL Injury (Central Defect, Porcine, Ovine, Canine), in The ACL Handbook. 2013, Springer. p. 139-166.*
10. *Hauser, R., et al., Ligament Injury and Healing: A Review of Current Clinical Diagnostics and Therapeutics. Open Rehabilitation Journal, 2013.* ***6****: p. 1-20.*
11. *Vavken, P., Tissue engineering of ligaments and tendons, in Fundamentals of Tissue Engineering and Regenerative Medicine. 2009, Springer. p. 317-327.*
12. *Murray, M.M., et al., Cell outgrowth from the human ACL in vitro: regional variation and response to TGF-beta 1. Journal of Orthopaedic Research, 2002.* ***20****(4): p. 875-880.*
13. *Murray, M.M. and M. Spector, The migration of cells from the ruptured human anterior cruciate ligament into collagen-glycosaminoglycan regeneration templates in vitro. Biomaterials, 2001.* ***22****(17): p. 2393-2402.*
14. *Gobbi, A., et al., Clinical Outcomes and Rehabilitation Program After ACL Primary Repair and Bone Marrow Stimulation, in Sports Injuries. 2012, Springer. p. 475-484.*
15. *Feagin, J.A., C.M. Pierce, and M.R. Geyer, ACL Primary Repair: What We Did, the Results, and How It Helps Today to Tailor Treatments to the Patient and the Pathology, in The ACL-Deficient Knee. 2013, Springer. p. 97-104.*
16. *Magarian, E.M., et al., Delay of 2 or 6 weeks adversely affects the functional outcome of augmented primary repair of the porcine anterior cruciate ligament. The American journal of sports medicine, 2010.* ***38****(12): p. 2528-2534.*
17. *Boykin, R.E. and W.G. Rodkey, Acute Anterior Cruciate Ligament Tear Surgery: Repair Versus Reconstruction–When?, in The ACL-Deficient Knee. 2013, Springer. p. 203-210.*
18. *Samuelsson, K., et al., Trends in surgeon preferences on anterior cruciate ligament reconstructive techniques. Clinics in Sports Medicine, 2013.* ***32****(1): p. 111-126.*
19. *Lin, T.W., L. Cardenas, and L.J. Soslowsky, Biomechanics of tendon injury and repair. Journal of Biomechanics, 2004.* ***37****(6): p. 865-77.*
20. *Sanchis-Alfonso, V., et al., Graft Healing in ACL Reconstruction: Can We Enhance It in Clinical Practice?, in The ACL-Deficient Knee. 2013, Springer. p. 113-129.*

21. *Nandra, R., et al., A review of anterior cruciate ligament injuries and reconstructive techniques. Part 1: Basic science. Trauma, 2013.*
22. *West, R.V. and C.D. Harner, Graft selection in anterior cruciate ligament reconstruction. Journal of the American Academy of Orthopaedic Surgeons, 2005.* ***13****(3): p. 197-207.*
23. *Mehran, N., et al., Contemporary Graft Options in Anterior Cruciate Ligament Reconstruction. Operative Techniques in Sports Medicine, 2013.* ***21****(1): p. 10-18.*
24. *Lipscomb, A.B., et al., Evaluation of hamstring strength following use of semitendinosus and gracilis tendons to reconstruct the anterior cruciate ligament. The American journal of sports medicine, 1982.* ***10****(6): p. 340-342.*
25. *Karlsson, J., et al., Anatomic single- and double-bundle anterior cruciate ligament reconstruction, part 2: clinical application of surgical technique. Am J Sports Med, 2011.* ***39****(9): p. 2016-26.*
26. *Magnussen, R.A., et al., Cross-cultural comparison of patients undergoing ACL reconstruction in the United States and Norway. Knee Surg Sports Traumatol Arthrosc, 2010.* ***18****(1): p. 98-105.*
27. *Zaffagnini, S., et al., ACL Reconstruction: Alternative Technique for Double-Bundle Reconstruction, in Sports Injuries. 2012, Springer. p. 395-400.*
28. *Hollis, R., et al., Autologous bone effects on femoral tunnel widening in hamstring anterior cruciate ligament reconstruction. Journal of Knee Surgery, 2010.* ***22****(02): p. 114-119.*
29. *Choi, N.-H., et al., Femoral tunnel widening after hamstring anterior cruciate ligament reconstruction with bioabsorbable transfix. The American journal of sports medicine, 2012.* ***40****(2): p. 383-387.*
30. *Nebelung, S., et al., High incidence of tunnel widening after anterior cruciate ligament reconstruction with transtibial femoral tunnel placement. Archives of Orthopaedic and Trauma Surgery, 2012.* ***132****(11): p. 1653-1663.*
31. *Iorio, R., et al., Bone tunnel enlargement after ACL reconstruction using autologous hamstring tendons: a CT study. International orthopaedics, 2007.* ***31****(1): p. 49-55.*
32. *Baumfeld, J.A., et al., Tunnel widening following anterior cruciate ligament reconstruction using hamstring autograft: a comparison between double cross-pin and suspensory graft fixation. Knee Surgery, Sports Traumatology, Arthroscopy, 2008.* ***16****(12): p. 1108-1113.*
33. *Hospodar, M.S.J. and M.D. Miller, Controversies in ACL reconstruction: bone-patellar tendon-bone anterior cruciate ligament reconstruction remains the gold standard. Sports Medicine and Arthroscopy Review, 2009.* ***17****(4): p. 242-246.*
34. *Sherman, O.H. and M.B. Banffy, Anterior cruciate ligament reconstruction: which graft is best? Arthroscopy: The Journal of Arthroscopic & Related Surgery, 2004.* ***20****(9): p. 974-980.*
35. *Chambat, P., et al., The evolution of ACL reconstruction over the last fifty years. International orthopaedics, 2013.* ***37****(2): p. 181-186.*
36. *Suzuki, T., et al., Early integration of a bone plug in the femoral tunnel in rectangular tunnel ACL reconstruction with a bone-patellar tendon-bone graft: a prospective computed tomography analysis. Knee Surgery, Sports Traumatology, Arthroscopy, 2011.* ***19****(1): p. 29-35.*
37. *Freedman, K.B., et al., Arthroscopic Anterior Cruciate Ligament Reconstruction A Metaanalysis Comparing Patellar Tendon and Hamstring Tendon Autografts. The American journal of sports medicine, 2003.* ***31****(1): p. 2-11.*
38. *Foster, T.E., et al., Does the graft source really matter in the outcome of patients undergoing anterior cruciate ligament reconstruction? An evaluation of autograft versus allograft reconstruction results: a systematic review. The American journal of sports medicine, 2010.* ***38****(1): p. 189-199.*
39. *Strickland, S.M., J.D. MacGillivray, and R.F. Warren, Anterior cruciate ligament reconstruction with allograft tendons. Orthopedic Clinics of North America, 2003.* ***34****(1): p. 41-+.*

40. *Badylak, S.F., et al., The Use of Xenogeneic Small-Intestinal Submucosa as a Biomaterial for Achilles-Tendon Repair in a Dog-Model. Journal of Biomedical Materials Research, 1995.* ***29****(8): p. 977-985.*
41. *Milthorpe, B.K., Xenografts for Tendon and Ligament Repair. Biomaterials, 1994.* ***15****(10): p. 745-752.*
42. *Lavoie, P., J. Fletcher, and N. Duval, Patient satisfaction needs as related to knee stability and objective findings after ACL reconstruction using the LARS artificial ligament. The Knee, 2000.* ***7****(3): p. 157-163.*
43. *Ye, J., et al., Arthroscopic reconstruction of the anterior cruciate ligament with the LARS artificial ligament: thirty-six to fifty-two months follow-up study. Eur Rev Med Pharmacol Sci, 2013.* ***17****(11): p. 1438-1446.*
44. *Ghalayini, S., et al., Arthroscopic anterior cruciate ligament surgery: Results of autogenous patellar tendon graft versus the Leeds-Keio synthetic graft: Five year follow-up of a prospective randomised controlled trial. The Knee, 2010.* ***17****(5): p. 334-339.*
45. *Murray, A.W. and M. Macnicol, 10–16 year results of Leeds-Keio anterior cruciate ligament reconstruction. The Knee, 2004.* ***11****(1): p. 9-14.*
46. *Legnani, C., et al., Anterior cruciate ligament reconstruction with synthetic grafts. A review of literature. International orthopaedics, 2010.* ***34****(4): p. 465-471.*
47. *Virk, S.S. and M.S. Kocher, Adoption of new technology in sports medicine: Case studies of the Gore-Tex prosthetic ligament and of thermal capsulorrhaphy. Arthroscopy: The Journal of Arthroscopic & Related Surgery, 2011.* ***27****(1): p. 113-121.*
48. *Li, H., et al., Biologic failure of a ligament advanced reinforcement system artificial ligament in anterior cruciate ligament reconstruction: a report of serious knee synovitis. Arthroscopy: The Journal of Arthroscopic & Related Surgery, 2012.* ***28****(4): p. 583-586.*
49. *Ventura, A., et al., Synthetic grafts for anterior cruciate ligament rupture: 19-year outcome study. The Knee, 2010.* ***17****(2): p. 108-113.*
50. *Laurencin, C.T. and J.W. Freeman, Ligament tissue engineering: An evolutionary materials science approach. Biomaterials, 2005.* ***26****(36): p. 7530-7536.*
51. *Liu, H.F., et al., A comparison of rabbit mesenchymal stem cells and anterior cruciate ligament fibroblasts responses on combined silk scaffolds. Biomaterials, 2008.* ***29****(10): p. 1443-1453.*
52. *Teh, T.K.H., S.L. Toh, and J.C.H. Goh, Aligned Hybrid Silk Scaffold for Enhanced Differentiation of Mesenchymal Stem Cells into Ligament Fibroblasts. Tissue Engineering Part C-Methods, 2011.* ***17****(6): p. 687-703.*
53. *Tovar, N., et al., ACL reconstruction using a novel hybrid scaffold composed of polyarylate fibers and collagen fibers. Journal of Biomedical Materials Research Part A, 2012.* ***100****(11): p. 2913-2920.*
54. *Lu, H.H., et al., Anterior cruciate ligament regeneration using braided biodegradable scaffolds: in vitro optimization studies. Biomaterials, 2005.* ***26****(23): p. 4805-4816.*
55. *Ge, Z., et al., Biomaterials and scaffolds for ligament tissue engineering. Journal of Biomedical Materials Research Part A, 2006.* ***77****(3): p. 639-652.*
56. *Altman, G.H., et al., Silk-based biomaterials. Biomaterials, 2003.* ***24****(3): p. 401-416.*
57. *Vunjak-Novakovic, G., et al., Tissue engineering of ligaments. Annual Review of Biomedical Engineering, 2004.* ***6****: p. 131-156.*
58. *Zhang, Q.A., S.Q. Yan, and M.Z. Li, Porous Materials Based on Bombyx mori Silk Fibroin. Textile Bioengineering and Informatics Symposium Proceedings, Vols 1-3, 2010: p. 254-261.*
59. *Ge, Z.G., et al., Biomaterials and scaffolds for ligament tissue engineering. Journal of Biomedical Materials Research Part A, 2006.* ***77A****(3): p. 639-652.*
60. *Sandmann, G.H. and T. Tischer, Tissue Engineering of the ACL - Efforts and Achievements. Anterior Cruciate Ligament (Acl): Causes of Injury, Adverse Effects and Treatment Options, 2010: p. 225-246.*

61. *Panas, E., C.J. Gatt, and M.G. Dunn, In Vitro Analysis of a Tissue-Engineered Anterior Cruciate Ligament Scaffold. 2009 35th Annual Northeast Bioengineering Conference, 2009: p. 286-287.*
62. *Weitzel, P.P., et al., Future direction of the treatment of ACL ruptures. Orthopedic Clinics of North America, 2002.* ***33****(4): p. 653-+.*
63. *Teh, T.K.H., S.L. Toh, and J.C.H. Goh, Optimization of the silk scaffold sericin removal process for retention of silk fibroin protein structure and mechanical properties. Biomedical Materials, 2010.* ***5****(3).*
64. *Wang, X., et al., Improved human tenocyte proliferation and differentiation in vitro by optimized silk degumming. Biomedical Materials, 2011.* ***6****(3).*
65. *Moy, R.L., A. Lee, and A. Zalka, Commonly Used Suture Materials in Skin Surgery. American Family Physician, 1991.* ***44****(6): p. 2123-2128.*
66. *Shen, W.L., et al., The effect of incorporation of exogenous stromal cell-derived factor-1 alpha within a knitted silk-collagen sponge scaffold on tendon regeneration. Biomaterials, 2010.* ***31****(28): p. 7239-7249.*
67. *Wang, Y.Z., et al., Stem cell-based tissue engineering with silk biomaterials. Biomaterials, 2006.* ***27****(36): p. 6064-6082.*
68. *Minoura, N., et al., Attachment and Growth of Cultured Fibroblast Cells on Silk Protein Matrices. Journal of Biomedical Materials Research, 1995.* ***29****(10): p. 1215-1221.*
69. *Inouye, K., et al., Use of Bombyx mori silk fibroin as a substratum for cultivation of animal cells. Journal of Biochemical and Biophysical Methods, 1998.* ***37****(3): p. 159-164.*
70. *Min, B.M., et al., Formation of silk fibroin matrices with different texture and its cellular response to normal human keratinocytes. International Journal of Biological Macromolecules, 2004.* ***34****(5): p. 281-288.*
71. *Min, B.M., et al., Electrospinning of silk fibroin nanofibers and its effect on the adhesion and spreading of normal human keratinocytes and fibroblasts in vitro. Biomaterials, 2004.* ***25****(7-8): p. 1289-1297.*
72. *Fang, Q., et al., In vitro and in vivo research on using Antheraea pernyi silk fibroin as tissue engineering tendon scaffolds. Materials Science & Engineering C-Biomimetic and Supramolecular Systems, 2009.* ***29****(5): p. 1527-1534.*
73. *Sahoo, S., S.L. Toh, and J.C.H. Goh, A bFGF-releasing silk/PLGA-based biohybrid scaffold for ligament/tendon tissue engineering using mesenchymal progenitor cells. Biomaterials, 2010.* ***31****(11): p. 2990-2998.*
74. *Lee, B.S., et al., Synthesis of metal ion-histidine complex functionalized mesoporous silica nanocatalysts for enhanced light-free tooth bleaching. Acta Biomaterialia, 2011.* ***7****(5): p. 2276-2284.*
75. *Ahn, S., et al., Chitosan microparticles incorporating gold as an enhanced contrast flow tracer in dynamic X-ray imaging. Acta Biomaterialia, 2011.* ***7****(5): p. 2139-2147.*
76. *Chen, X., et al., Synergic Combination of Collagen Matrix with Knitted Silk Scaffold Regenerated Ligament with More Native Microstructure in Rabbit Model. 13th International Conference on Biomedical Engineering, Vols 1-3, 2009.* ***23****(1-3): p. 1195-1198.*
77. *Fan, H.B., et al., Anterior cruciate ligament regeneration using mesenchymal stem cells and silk scaffold in large animal model. Biomaterials, 2009.* ***30****(28): p. 4967-4977.*
78. *Altman, G.H., et al., "The use of long-term bioresorbable scaffolds for anterior cruciate ligament repair" (vol 16, pg 177, 2008). Journal of the American Academy of Orthopaedic Surgeons, 2008.* ***16****(8): p. 22a-22a.*
79. *Panas-Perez, E., C. Gatt, and M. Dunn, Development of a silk and collagen fiber scaffold for anterior cruciate ligament reconstruction. Journal of materials science. Materials in medicine, 2013.* ***24****(1): p. 257-265.*

80. *Seo, Y.-K., et al., Wound healing effect of collagen-hyaluronic acid implanted in partially injured anterior cruciate ligament of dog. Biotechnology and Bioprocess Engineering, 2010.* ***15****(4): p. 552-558.*
81. *Sahoo, S., S.L. Toh, and J.C. Goh, A bFGF-releasing silk/PLGA-based biohybrid scaffold for ligament/tendon tissue engineering using mesenchymal progenitor cells. Biomaterials, 2010.* ***31****(11): p. 2990-2998.*
82. *Teh, T., J. Goh, and S. Toh. Characterization of electrospun substrates for ligament regeneration using bone marrow stromal cells. in 13th International Conference on Biomedical Engineering. 2009. Springer.*
83. *Horan, R.L., SeriACL™ Device (Gen IB) Trial for Anterior Cruciate Ligament (ACL) Repair, Serica Technologies, Inc. 2009(NCT00775892).*
84. *Bernardino, S., ACL prosthesis: any promise for the future? (Retracted Article. See vol 18, pg 1814, 2010). Knee Surgery Sports Traumatology Arthroscopy, 2010.* ***18****(6): p. 797-804.*
85. *Mascarenhas, R. and P.B. MacDonald, Anterior cruciate ligament reconstruction: a look at prosthetics--past, present and possible future. Mcgill J Med, 2008.* ***11****(1): p. 29-37.*
86. *Lei, J. and J.S. Temenoff, Engineering Fibrous Tissues and Their Interfaces with Bone, in Structural Interfaces and Attachments in Biology. 2013, Springer. p. 323-349.*
87. *He, P., et al., In Vitro Ligament–Bone Interface Regeneration Using a Trilineage Coculture System on a Hybrid Silk Scaffold. Biomacromolecules, 2012.* ***13****(9): p. 2692-2703.*
88. *Soon, M.Y.H., et al., An analysis of soft tissue allograft anterior cruciate ligament reconstruction in a rabbit model - A short-term study of the use of mesenchymal stem cells to enhance tendon osteointegration. American Journal of Sports Medicine, 2007.* ***35****(6): p. 962-971.*
89. *Lim, J.K., et al., Enhancement of tendon graft osteointegration using mesenchymal stem cells in a rabbit model of anterior cruciate ligament reconstruction. Arthroscopy-the Journal of Arthroscopic and Related Surgery, 2004.* ***20****(9): p. 899-910.*
90. *Wen, C.Y., et al., The Use of Brushite Calcium Phosphate Cement for Enhancement of Bone-Tendon Integration in an Anterior Cruciate Ligament Reconstruction Rabbit Model. Journal of Biomedical Materials Research Part B-Applied Biomaterials, 2009.* ***89B****(2): p. 466-474.*
91. *Huangfu, X.Q. and J.Z. Zhao, Tendon-bone healing enhancement using injectable tricalcium phosphate in a dog anterior cruciate ligament reconstruction model. Arthroscopy-the Journal of Arthroscopic and Related Surgery, 2007.* ***23****(5): p. 455-462.*
92. *Swetha, M., et al., Biocomposites containing natural polymers and hydroxyapatite for bone tissue engineering. International Journal of Biological Macromolecules, 2010.* ***47****(1): p. 1-4.*
93. *Dorozhkin, S.V., Bioceramics of calcium orthophosphates. Biomaterials, 2010.* ***31****(7): p. 1465-1485.*
94. *Farshad, M., et al., Embossing of a screw thread and TCP granules enhances the fixation strength of compressed ACL grafts with interference screws. Knee Surgery, Sports Traumatology, Arthroscopy, 2012.* ***20****(2): p. 268-274.*
95. *Shi, P., et al., Variation of the effect of calcium phosphate enhancement of implanted silk fibroin ligament bone integration. Biomaterials, 2013.*
96. *Yu, Y., et al., Bone morphogenetic proteins and Smad expression in ovine tendon-bone healing. Arthroscopy-the Journal of Arthroscopic and Related Surgery, 2007.* ***23****(2): p. 205-210.*
97. *Lee, J., et al., Enhanced regeneration of the ligament-bone interface using a poly(L-lactide-co-epsilon-caprolactone) scaffold with local delivery of cells/BMP-2 using a heparin-based hydrogel. Acta Biomaterialia, 2011.* ***7****(1): p. 244-257.*
98. *Kim, H.M., et al., The role of transforming growth factor beta isoforms in tendon-to-bone healing. Connective Tissue Research, 2011.* ***52****(2): p. 87-98.*
99. *Chan, K.M., et al., Expression of transforming growth factor beta isoforms and their roles in tendon healing. Wound Repair and Regeneration, 2008.* ***16****(3): p. 399-407.*

100. *Cooper, J.A., et al., Fiber-based tissue-engineered scaffold for ligament replacement: design considerations and in vitro evaluation. Biomaterials, 2005.* ***26****(13): p. 1523-1532.*
101. *Bach, B.R., et al., Arthroscopically assisted anterior cruciate ligament reconstruction using patellar tendon autograft - Five- to nine-year follow-up evaluation. American Journal of Sports Medicine, 1998.* ***26****(1): p. 20-29.*
102. *Bach, B.R., et al., Single-incision endoscopic anterior cruciate ligament reconstruction using patellar tendon autograft - Minimum two-year follow-up evaluation. American Journal of Sports Medicine, 1998.* ***26****(1): p. 30-40.*
103. *Maletius, W. and J. Gillquist, Long-term results of anterior cruciate ligament reconstruction with a dacron prosthesis - The frequency of osteoarthritis after seven to eleven years. American Journal of Sports Medicine, 1997.* ***25****(3): p. 288-293.*
104. *Miller, S.L. and J.N. Gladstone, Graft selection in anterior cruciate ligament reconstruction. Orthopedic Clinics of North America, 2002.* ***33****(4): p. 675-+.*
105. *D.I.Zeugolis, J.C.Y.C., and A. Pandit, Tendons: Engineering of Functional Tissues. Tissue Engineering, 2011: p. 36.*
106. *Dunkers, J.P., et al., Effect of surface modification on protein retention and cell proliferation under strain. Acta Biomaterialia, 2011.* ***7****(7): p. 2902-2909.*
107. *Junkin, M., D.D. Zhang, and P.K. Wong, Plasma lithography for control of cell morphology and proliferation. 2009 4th Ieee International Conference on Nano/Micro Engineered and Molecular Systems, Vols 1 and 2, 2009: p. 822-826.*
108. *Horan, R.L., et al., Yarn design for functional tissue engineering. Journal of Biomechanics, 2006.* ***39****(12): p. 2232-2240.*
109. *Altman, G.H., et al., Silk matrix for tissue engineered anterior cruciate ligaments. Biomaterials, 2002.* ***23****(20): p. 4131-4141.*
110. *Cartmell, S.R.S., Tissue Engineering of Ligaments. Tissue Engineering for Tissue and Organ Regeneration, 2011: p. 131-162.*
111. *Seo, Y.K., et al., The biocompatibility of silk scaffold for tissue engineered ligaments. ASBM7: Advanced Biomaterials VII, 2007.* ***342-343****: p. 73-76.*
112. *Liu, H., et al., Silk-Based Scaffold for Ligament Tissue Engineering. 14th Nordic-Baltic Conference on Biomedical Engineering and Medical Physics, 2008.* ***20****: p. 34-37.*
113. *Fessel, G., et al., Suitability of Thiel embalmed tendons for biomechanical investigation. Annals of anatomy = Anatomischer Anzeiger : official organ of the Anatomische Gesellschaft, 2011.* ***193****(3): p. 237-41.*
114. *Beynnon, B.D. and A.A. Amis, In vitro testing protocols for the cruciate ligaments and ligament reconstructions. Knee Surg Sports Traumatol Arthrosc, 1998: p. 7.*
115. *Nurmi, J., P. Kannus, and S. H, Interference Screw Fixation of Soft Tissue Grafts in Anterior Cruciate Ligament Reconstruction: Part 2. Am J Sports Med, 2004.* ***32****(2): p. 5.*
116. *Coleridge, S.D. and A.A. Amis, A comparison of five tibial-fixation systems in hamstring-graft anterior cruciate ligament reconstruction. Knee Surgery Sports Traumatology Arthroscopy, 2004.* ***12****(5): p. 391-397.*
117. *Huynh, C.T., M.K. Nguyen, and D.S. Lee, Biodegradable pH/temperature-sensitive oligo(beta-amino ester urethane) hydrogels for controlled release of doxorubicin. Acta Biomaterialia, 2011.* ***7****(8): p. 3123-3130.*
118. *Woo, S.L.Y., et al., Tensile Properties of the Human Femur-Anterior Cruciate Ligament-Tibia Complex - the Effects of Specimen Age and Orientation. American Journal of Sports Medicine, 1991.* ***19****(3): p. 217-225.*
119. *Guo, S., et al., Comparative study of human dental follicle cell sheets and periodontal ligament cell sheets for periodontal tissue regeneration. Cell Transplant, 2013.* ***22****(6): p. 1061-73.*
120. *Mascarenhas, R. and P.B. MacDonald, Anterior cruciate ligament reconstruction: a look at prosthetics - past, present and possible future. Mcgill J Med, 2008.* ***11****(1): p. 9.*

121. *Zamarripa, N., S. Farboodmanesh, and C.K. Kuo, Novel Biomimetic Scaffold for Tendon and Ligament Tissue Engineering. 2009 35th Annual Northeast Bioengineering Conference, 2009: p. 20-21.*
122. *Fan, H.B., et al., In vivo study of anterior cruciate ligament regeneration using mesenchymal stem cells and silk scaffold. Biomaterials, 2008.* ***29****(23): p. 3324-3337.*
123. *Mommersteeg, T.J.A., et al., The Fiber Bundle Anatomy of Human Cruciate Ligaments. Journal of Anatomy, 1995.* ***187****: p. 461-471.*
124. *Fuss, F.K., Anatomy and Function of the Cruciate Ligaments of the Domestic Pig (Sus-Scrofa-Domestica) - a Comparison with Human Cruciates. Journal of Anatomy, 1991.* ***178****: p. 11-20.*
125. *Kwansa, A.L., et al., Novel matrix based anterior cruciate ligament (ACL) regeneration. Soft Matter, 2010.* ***6****(20): p. 5016-5025.*
126. *Uppin, M.S., et al., Renal cortical necrosis at presentation in a patient with systemic lupus erythematosus: an autopsy case report. Clinical Rheumatology, 2010.* ***29****(7): p. 815-818.*
127. *Li, X., et al., Fabrication of porous beta-tricalcium phosphate with microchannel and customized geometry based on gel-casting and rapid prototyping. Proceedings of the Institution of Mechanical Engineers Part H-Journal of Engineering in Medicine, 2011.* ***225****(H3): p. 315-323.*
128. *Li, X. and J.G. Snedeker, Wired Silk Architectures Provide A Biomimetic Acl Tissue Engineering Scaffold. Journal of the Mechanical Behavior of Biomedical Materials, 2013.*
129. *Horan, R.L., et al., Biological and biomechanical assessment of a long-term bioresorbable silk-derived surgical mesh in an abdominal body wall defect model. Hernia, 2009.* ***13****(2): p. 189-199.*
130. *Altman, G.H., et al., The use of long-term bioresorbable scaffolds for anterior Cruciate ligament repair. Journal of the American Academy of Orthopaedic Surgeons, 2008.* ***16****(4): p. 177-187.*
131. *Dmitriev, I.A., S.I. Dorozhkin, and A.D. Mirlin, Photogalvanic effects originating from the violation of the Einstein relation in a 2D electron gas in high Landau levels. Physica E-Low-Dimensional Systems & Nanostructures, 2010.* ***42****(4): p. 1159-1162.*
132. *Schmitz, N., et al., Basic methods in histopathology of joint tissues. Osteoarthritis and Cartilage, 2010.* ***18****: p. S113-S116.*
133. *Li, X. and J. Snedeker, LONG TERM MECHANICAL BEHAVIOR OF SILK ACL SCAFFOLDS UNDER CYCLIC LOADING. Journal of Biomechanics, 2012.* ***45****: p. S325.*
134. *Fleming, B.C., et al., Collagen-platelet composites improve the biomechanical properties of healing anterior cruciate ligament grafts in a porcine model. Am J Sports Med, 2009.* ***37****(8): p. 1554-63.*
135. *Vavken, P., et al., Biomechanical outcomes after bioenhanced anterior cruciate ligament repair and anterior cruciate ligament reconstruction are equal in a porcine model. Arthroscopy-the Journal of Arthroscopic and Related Surgery, 2012.* ***28****(5): p. 672-80.*
136. *Milano, G., et al., Comparison of femoral fixation methods for anterior cruciate ligament reconstruction with patellar tendon graft: a mechanical analysis in porcine knees. Knee Surg Sports Traumatol Arthrosc, 2007.* ***15****(6): p. 733-8.*
137. *Liu, H.F., et al., In Vivo Study of ACL Regeneration Using Silk Scaffolds In a Pig Model. 13th International Conference on Biomedical Engineering, Vols 1-3, 2009.* ***23****(1-3): p. 1512-1514.*
138. *Chen, J.L., et al., Efficacy of hESC-MSCs in knitted silk-collagen scaffold for tendon tissue engineering and their roles. Biomaterials, 2010.* ***31****(36): p. 9438-9451.*
139. *Mayr, H.O., et al., Microporous calcium phosphate ceramics as tissue engineering scaffolds for the repair of osteochondral defects: Biomechanical results. Acta Biomaterialia, 2013.* ***9****(1): p. 4845-4855.*
140. *Fan, H., et al., Anterior cruciate ligament regeneration using mesenchymal stem cells and silk scaffold in large animal model. Biomaterials, 2009.* ***30****(28): p. 4967-4977.*

141. *Chen, X., et al., Synergic Combination of Collagen Matrix with Knitted Silk Scaffold Regenerated Ligament with More Native Microstructure in Rabbit Model. 13th International Conference on Biomedical Engineering, Vols 1-3, 2009.* ***23****(1-3): p. 1195-1198*

142. *Rodeo, S.A., et al., Use of recombinant human bone morphogenetic protein-2 to enhance tendon healing in a bone tunnel. Am J Sports Med, 1999.* ***27****(4): p. 476-88.*

143. *Noyes, F.R. and E.S. Grood, Strength of Anterior Cruciate Ligament in Humans and Rhesus-Monkeys. Journal of Bone and Joint Surgery-American Volume, 1976.* ***58****(8): p. 1074-1082.*

ACKNOWLEDGEMENTS

During my doctoral study in Switzerland, I have received numerous helps from many people in lots of institutes both in Switzerland and in China. It is impossible for me to finish such a doctoral project without their great supports. Here I would like to gratefully acknowledge them who have helped me, supported me and walked with me for the past four years.

I wish to express my sincere gratitude to **Prof. Dr. Jess G. Snedeker** for providing me a precious opportunity to join his group and carry out my doctoral study under his supervision. I gratefully appreciate him for giving me a large range of flexibility of carrying out research to realize my own ideas, and of course offering me lots of valuable resources, brilliant advices and great supports. Thank him so much for understanding and accepting my stubbornness during the research, which I believe do not always happen between professors and doctoral students. I am really thankful that I met such a really nice professor at the most important stage in my life.

I would like to give my special appreciation to my former supervisor of master study **Prof. Dr. Dichen Li** in Xi'an Jiaotong University for the collaboration on this project and providing me lots of valuable resources and constructive advices, particularly on the manufacturing techniques on TCP preparation and experiences on the animal tests. Thanks him very much for the great supports on my innovation grant application. I appreciate him as well for giving me lots of suggestions not just related on the research, but also for my career development.

I would like to express my sincere thanks to **Prof. Dr. Marc Bohner**, not only for being one of my co-examiners, but also for sharing his profound knowledge on TCP with me and providing me lots of TCP samples for my research.

And sincerely thank **Prof. Stephen J. Ferguson** for being one of my co-examiners for reviewing my dissertation and giving me lots of constructive comments.

I would also like to acknowledge **Prof. Dr. William R. Taylor** for representing the Department of Health Sciences and Technology at my doctoral examination.

I would like to express a big thank to our technician **Mr. Hansruedi Sommer** for the great supports on the prototype fabrication and bioreactor development.

I would like to give a special appreciation to **Dr. med. Roland Camenzind** for the kind help on translating the summary part of this dissertation into German, and also for the assistance on the in vitro biomechanical tests.

I would also like to specially thank **Dr. Nils Goedecke** for his great help and support on my fellowship application.

Many thanks to the medical doctors, doctoral students, master students, and semester students who helped me on the project. I am really grateful to **Dr. med. Weiguo Bian, Dr. med. Weijie Zhang,** and **Mr. Zheng Li** in First Hospital of Xi'an Jiaotong University, China for the great support on the animal experiments and further evaluation. Sincerely thank **Prof. Dr. Jiankang He, Prof. Dr. Qin Lian, Prof. Dr. Zhongmin Jin, Mr. Linzhong Zhu,** and **Mr. Wenyou Zhang** in State Key Lab for Manufacturing System Engineering, Xi'an Jiaotong University, China for the great assistance on the fabrication of TCP moulds and scaffolds as well as the in vitro biomechanical tests. Thanks very much to **Dr. Yufei Li, Dr. med. Arnd Viehöfer, Dr. med. Janosch Häberli, Mr. Bruno Jordan,** and in Unilinik Balgrist for the great help on the in vitro biomechanical tests, surgical tools development, and histological evaluation. Special thanks to my friends **Ms. Jingyi Rao** and **Dr. Xiaojun Wang** at ETH Hönggerberg for kind help on sample imaging and TCP sintering.

I take immense pleasure here to thank all my current and previous colleagues in the Biomechanik laboratory at Uniklinik Balgrist who helped me in any cases, and gave me a wonderful life and memorable experiences in Switzerland: **Dr. Philippe Favre, Dr. Yannick Loosli, Dr. Guido Bartalena, Mr. Gion Fessel, Dr. Jennifer Cadby, Mr. Marco Senteler, Dr. Unai Silvan, Ms. Maja Bollhalder, Mr. Tojo Razafiarison, Mr. Claude Holenstein, Ms. Stefania Wunderli, Mr. Aron Horvath, Mr. Enrico De Pieri, Mr. Stephan Reichmuth,** and **Mr. Andreas Ziegler.** And a special thank to **Ms. Helen Strebel** for the kind help on the administrative issues.

I also wish to thank Trudel Limited (Zurich, Switzerland) for providing raw silk for our research. And the following founding sources are sincerely acknowledged: Program of Leading Talent in Changshu of China, the National Natural Science Foundation of China, Research Fund for the Doctoral Program of Higher Education

of China, the Fundamental Research Funds for the Central Universities, the Chinese Scholarship Council, and the Bonizzi Theler Foundation.

Finally, yet importantly, I wish to express my deepest gratitude to my beloved family: **my grandmother, my parents, my wife and my son**, without their infinite support and unreserved contribution to the family for the past several years, it is impossible for me to finish this doctoral study.